Design of a High Speed Hydraulic On/Off Valve

A Thesis

Submitted to the Faculty of the

WORCESTER POLYTECHNIC INSTITUTE

In partial requirement for the

Degree of Master of Science

In

Mechanical Engineering

By:

_____

Allan Katz
May 28th, 2008

Approved:

_____

Professor James D. Van de Ven, Advisor

_____

Professor Allen Hoffman, Thesis Committee Member

_____

Professor Eben C. Cobb, Thesis Committee Member

_____

Professor John M. Sullivan, Graduate Committee Member

Abstract

On-off control of hydraulic circuits enables significant improvements in efficiency compared with throttling valve control. A key enabling technology to on-off control is an efficient high speed on-off valve. This project aims to design an on-off hydraulic valve that minimizes input power requirements and increases operating frequency over existing technology by utilizing a continuously rotating valve design. This is accomplished through use of spinning port discs which chop the flow into pulses, with the relative phase between these discs determining the pulse duration. A mathematical model for determining system efficiency is developed with a focus on the throttling, leakage, compressibility, and viscous friction power losses of the valve. Parameters affecting these losses were optimized to produce the most efficient design under the chosen disc-style architecture. Using these optimum parameter values, a first generation prototype valve was developed and experimental data collected. The experimental valve matched predicted output pressure and flows well, but suffered from larger than expected torque requirements and leakage, resulting in a maximum efficiency of 38% at 1.0 duty ratio. Also, due to motor limitations, the valve was only able to achieve a 64Hz switching frequency versus the designed 100Hz frequency. Future design iterations will need to focus on controlling leakage, hydrodynamically balancing the spinning port disc axially to reduce torque requirements, developing a computational fluid dynamics model to gain further insight into the workings of the valve, and creating a control methodology for single and multiple high speed valves.

Acknowledgements

First I would like to thank my advisor Jim Van de Ven for his ongoing support on this project over the past two years. His quick thinking, far ranging knowledge (both technical and practical), and professional yet friendly manner has truly been an inspiration for what it means to be a great engineer.

I would like to thank Professor Hoffman for being on my committee and for his guidance in the EPICS program, which has showed me the human aspect of engineering like nothing else. Also I would like to thank Professor Cobb and Professor Sullivan for being on my thesis committee.

Thank you to my lovely assistant Kushi, for letting me show her the ropes and for making me think I might actually know what I'm doing, the MEPS group for their critiques and camaraderie, the ladies of the Mechanical Engineering office for putting up with my shenanigans, Neil for his patient help in the shop, and all my friends for showing me that college is about so much more than homework.

Finally I'd like to thank my sister for her boundless enthusiasm and my parents for their endless support and encouragement, without which none of this would have been possible.

Table of Contents

Table of Figures

Table of Tables

Table of Symbols

α = phase angle[rad]
β_e = Effective bulk modulus[Pa]
β_{oil} = Bulk modulus of air free oil[Pa]
δ = Angle spanned by valve plate ports
γ = Angle spanned by Tier 1 and Tier 2 ports
μ = Viscosity [Pa-s]
ω = Angular velocity of valve plate [rad/s]
ρ = Density of oil[kg/m^3]
θ = Angular position of valve plate [rad]
θ_{trans} = Angle when leakage flow is assumed to transition from orifice to plate flow [rad]
A_1 = Orifice area created by the overlap of the valve plate and Tier 1[m^2]
A_2 = Orifice area created by the overlap of the valve plate and Tier 2[m^2]
c_{bore} = Radial clearance of valve plate to sleeve bore[m]
c_f = Clearance between valve plate and Tier 1[m]
c_b = Clearance between valve plate and Tier 2[m]
C_d = Orifice coefficient
Duty = Duty ratio
E = Young's modulus for steel[Pa]
$E_{leak,\ circum}$ = Circumferential leakage energy loss[J]
E_{comp} = Compressibility energy loss[J]
f = Pulse frequency [Hz]
K = Ratio of specific heats for air
L = Leakage pathway length[m]
N = Number of times porting is duplicated.
ΔP = Pressure differential, usually P_{High} - P_{Tank} [Pa]
ΔP_{check} = Pressure drop across check valve[Pa]
ΔP_{Tier1} = Pressure drop across Tier 1 orifice [Pa]
ΔP_{Tier2} = Pressure drop across Tier 2 orifice [Pa]
ΔP_{valve} = Pressure drop across valve [Pa]
Perimeter = Leakage perimeter [m]
P_{High} = Supply pressure [Pa]
P_{Tank} = Tank pressure [Pa]
$P_{throttling}$ = Instantaneous throttling power loss [W]
P_{floss} = Viscous friction power loss [W]
$P_{leak,\ rad}$ = Radial leakage power loss [W]
Q = flow rate [m^3/s]
Q_{check} = flow rate through check valve [m^3/s]
Q_{Leak} = Leakage flow rate [m^3/s]
$Q_{leak,rad,f}$ = Radial leakage between valve plate and Tier 1 [m^3/s]
$Q_{leak,rad,b}$ = Radial leakage between valve plate and Tier 2 [m^3/s]
$Q_{orifice}$ = Flow rate through orifice [m^3/s]
Q_{plate}= Parallel plate leakage flow [m^3/s]
$Q_{plate,\ const}$ = Parallel plate leakage flow with constant leakage length [m^3/s]
$Q_{plate,var}$ = Parallel plate leakage flow with variable leakage length [m^3/s]
Q_{valve} = Flow rate through valve [m^3/s]
R = Entrained air content by volume
R_{bore} = Radius to outer perimeter of valve plate [m]
R_i = Inner radius of ports [m]
R_o = Outer radius of ports [m]
$T_{journal}$ = Journal bearing torque [Nm]
$T_{plate,\ f,\ o}$ = $T_{plate,\ b,\ o}$ =Viscous torque outside of switching area between valve plate and Tier 1 & 2 [Nm]
$T_{plate,f,\ switch}$ = $T_{plate,b,\ switch}$ = Viscous torque of switching area between valve plate and Tier 1 & 2 [Nm]
t_{vp} = Valve plate thickness[m]
ΔV = Change in volume from switching[m^3]
$V_{circum,\ f}$ = $V_{circum,\ b}$ = Circumferential leakage volume between valve plate and Tier 1 & Tier 2 [m^3]
V_{switch} = Switching volume[m^3]

Chapter 1: Introduction & Background

This chapter introduces the concept of switch-mode hydraulic control and its uses. Then a literature review of one of the key components of switch-mode control, the high speed valve, is discussed. Lastly, a preview of the remaining chapters is outlined.

The world of hydraulic systems is dominated by two methods for controlling the speed and torque or force of a hydraulic rotary or linear actuator. The first method throttles the fluid flow until the desired output pressure is reached; however this throttling converts excess power into heat and is very wasteful. The second method uses a variable displacement pump or motor to achieve the desired output flow rate, but these systems are often bulky, expensive, and relatively complicated. Additionally, these systems often exhibit limited operational bandwidth and are not capable of positive and negative displacement, though some can go "over-center", which is necessary for regenerative braking.

An emerging technology is hydraulic switch-mode control. This method rapidly opens and closes a valve to effectively create a virtually variable displacement pump or motor. By varying the ratio of the on-time to the total cycle time, or duty ratio, a variable output pressure is produced. Switch-mode control has efficient on and off states and promises to convert any fixed displacement pump or motor into a virtually variable displacement component. For these reasons, a switch-mode hydraulic circuit is proposed.

The switch-mode hydraulic circuit of Figure 1 is analogous to a switch-mode power supply in electrical circuits [1]. In the electrical system, the capacitor is used to store energy, while in the hydraulic system the accumulator and flywheel store energy. In the electrical system, the inductor is used to maintain a continuous current, while in the hydraulic system the inertia of the fluid and the inertia of the flywheel maintain a continuous flow. The resistor is the load for electrical systems, while the desired power output of the pump/motor is the load for the hydraulic system. The diode prevents a backflow of current, and though not shown, the hydraulic system will utilize check valves to prevent a back flow of fluid. Lastly, the state of the high speed switch and valve will determine whether their respective systems are in "On" or "Off" mode. Currently there are no high speed switching valves commercially available.

When the high speed switching valve is in the "On" state, as shown in Figure 1, the pump/motor is connected to supply pressure. When the high speed switching valve changes to the "Off" state the pump/motor is connected to tank pressure and is allowed to freewheel. By switching between the "On" and "Off" states, pressure pulses are generated and the pump/motor will see an average pressure. By remaining in the "On" state longer than the "Off" state, the average pressure will approach supply pressure. Conversely, by remaining in the "Off" state longer than the "On" state, the average pressure will be closer to tank.

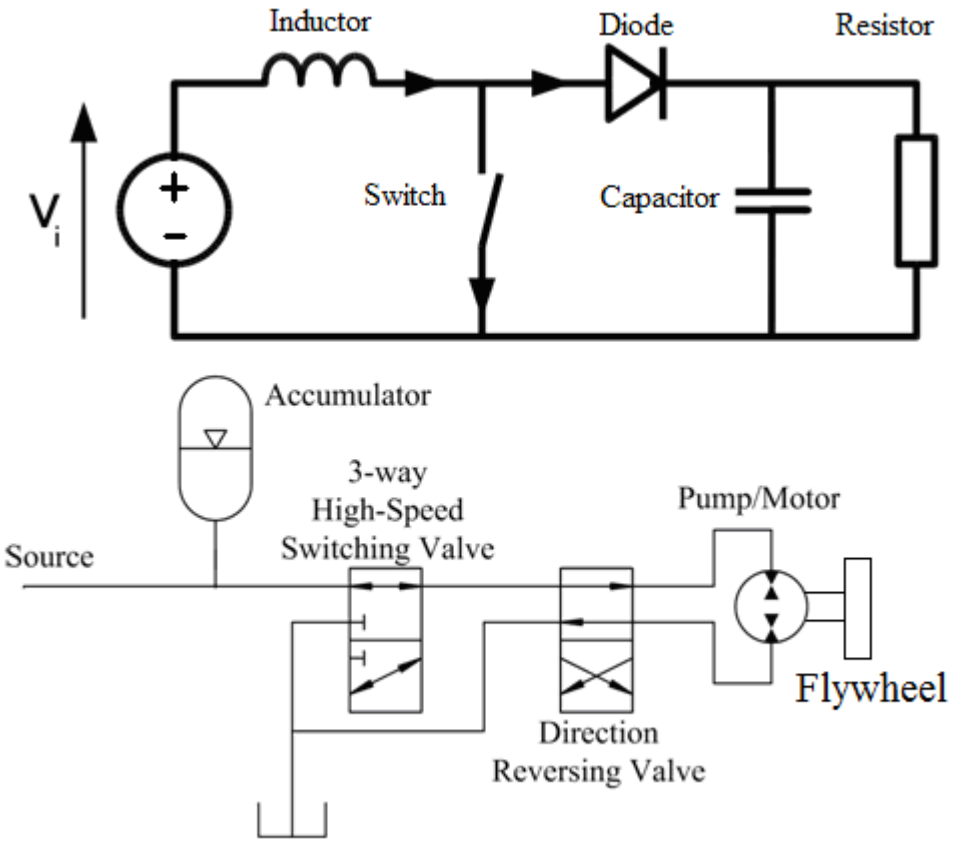

Figure 1: Electrical and fluidic circuit comparison

One promising use for a switch-mode hydraulic circuit is for use with hydraulic hybrid vehicles. Currently there is a need for an efficient pump/motor with a wide displacement range that is capable of operating as a pump or motor in forward or reverse, known as 4-quadrant control [2]. These features are necessary if regenerative braking is desired. Different configurations for hydro-mechanical hybrid systems are shown in Figure 2, Figure 3, and Figure 4 [2]. Configuration A replaces the clutch, transmission, and drive shaft of a typical vehicle with variable displacement pump/motors, accumulators, and hydraulic lines. In Configuration B, each wheel is independently controlled by its own variable displacement pump/motor. This allows for independent wheel-torque control, delivering power precisely when and where it is needed. Lastly, Configuration C uses a standard internal combustion engine drive train and a hydraulic system in parallel to power the wheels. This setup is beneficial because it allows IC engine to operate at its peak efficiency by diverting excess power to charge the accumulator. When the accumulator is full, the IC engine shuts off and the vehicle is powered by the hydraulic system. Once the accumulator empties, the IC engine turns back on and the process repeats. Also, if additional power is needed then the hydraulic system can provide assistance. Each of these systems utilize a variable displacement pump/motor, but all of these can be replaced with the fluidic switch-mode circuit described above and fixed displacement pump/motors.

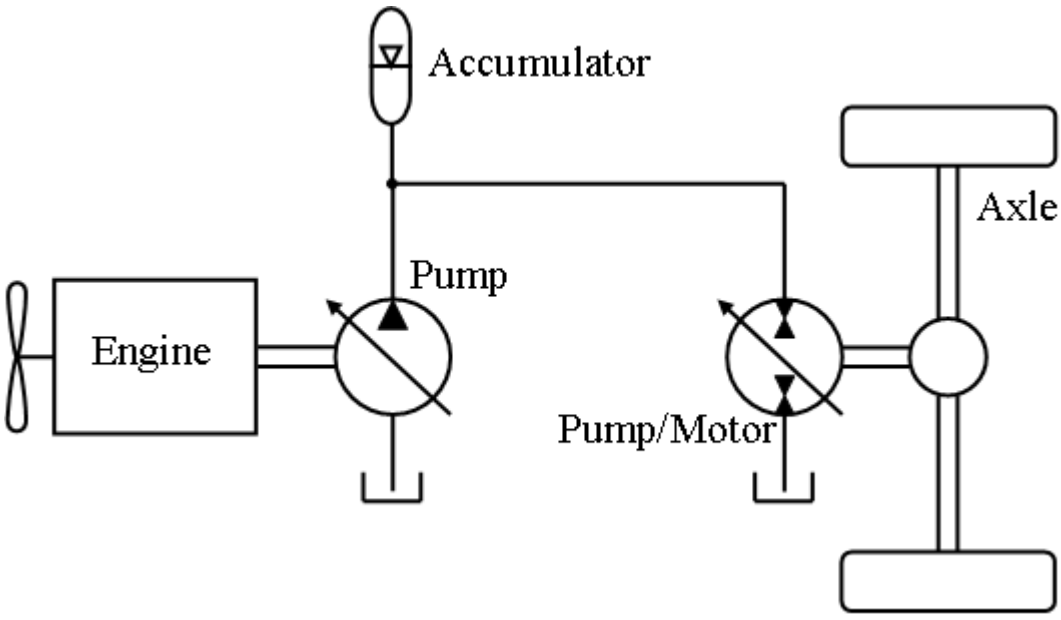

Figure 2: Hydro-mechanical hybrid vehicle configuration A. In this setup, the clutch, transmission, and drive shaft of a typical internal combustion engine vehicle are replaced by variable displacement pump/motors, an accumulator, and hydraulic lines.

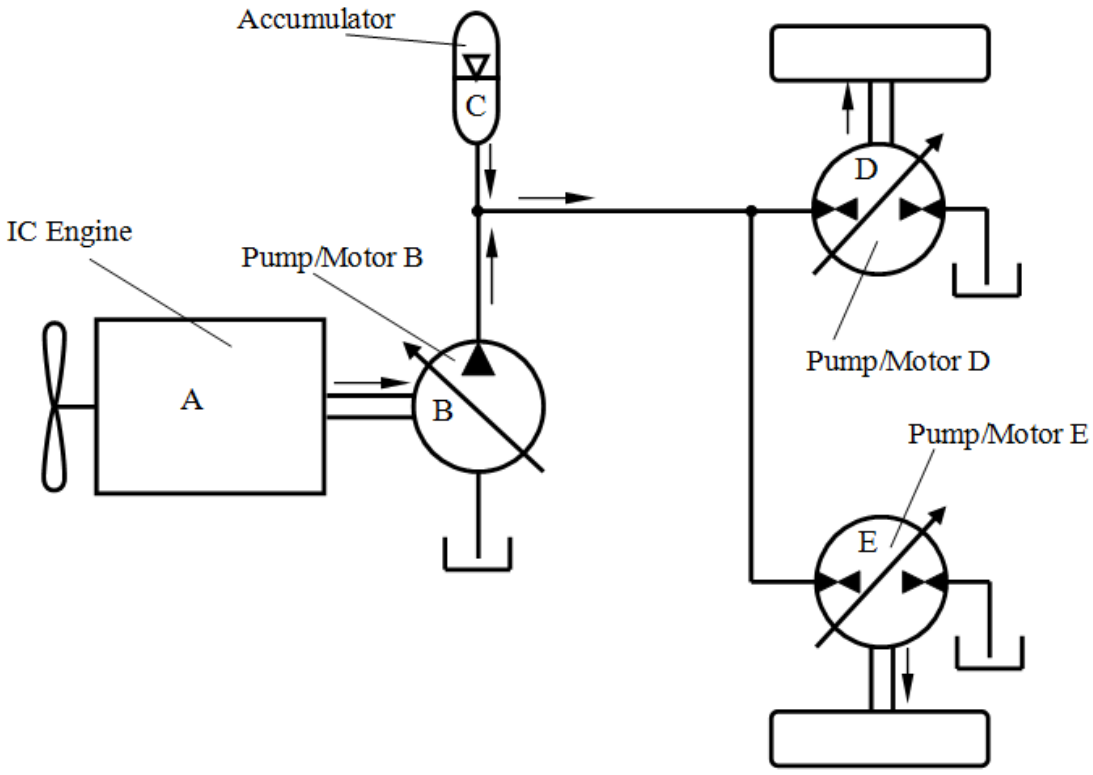

Figure 3: Hydro-mechanical hybrid vehicle configuration B. In this setup, each wheel is independently controlled by a variable displacement pump/motor

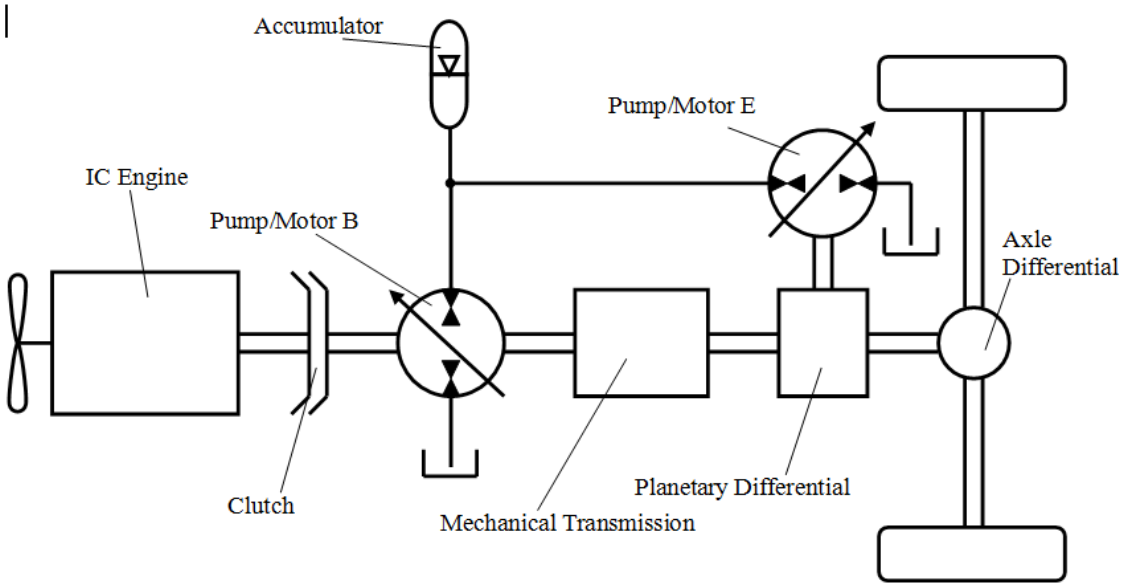

Figure 4: Hydro-mechanical hybrid vehicle configuration C. In this setup, the wheels can receive power from a traditional mechanical drive train, a hydraulic system, or both

1.1 Literature Review

High speed switching valves have been in development since at least the late 1970s when the electrical control circuits for electric actuators, such as solenoids, became readily available. However, several challenges not experienced in traditional valve design have prevented high speed hydraulic switch mode circuits from becoming common place. The energy required to drive conventional valves at high frequencies creates excessive heating, so the thermal characteristics of the actuator need to be well understood to prevent overheating [4]. Also, because of the pulsing nature of the system, an output pressure ripple is generated. This pressure ripple and the mean output pressure is dependent upon the frequency and the duty ratio[5]. In order to have a small pressure ripple the valve must operate at high frequencies, but because of the high switching frequencies, compressibility losses, which are primarily derived from the effective bulk modulus, become a significant source of energy loss[6]. Thus, the challenge is to maximize the switching frequency while minimizing the compressibility losses and power requirements.

A review of the current technologies shows a wide array of methodologies for creating a high speed on/off valve. These different approaches can be sorted into two general categories, oscillatory and continuous rotation valves. Oscillatory valves rapidly oscillate some component, usually a spool or poppet, to switch between on and off modes while continuously rotating valves utilize a continuously rotating component, usually a spool, to switch between on and off states.

Oscillatory type valves suffer from repeated and rapid accelerations which lead to large power losses at high operating frequencies. The most common oscillatory type valves use a solenoid or servomotor to actuate the switching member. In order to keep acceleration

forces low, high speed solenoid valves tend to be small[7], resulting in low flow rates, have minimal spool mass[8], and/or oscillate the control component small distances[9]. The minimized spool mass described in [8] is shown in Figure 5. Typically the spool is required to be solid or have thick walls to resist the large pressure forces acting on it, but in this interesting design the internal and external surfaces of the spool are hydrostatically balanced, allowing for an extremely thin walled annular spool. The shape of the spool is also designed so the required axial travel is at a minimum. These two features allow the valve to operate at ultra high frequencies on the order of a few hundred to a few thousand Hertz, though details on the exact size of the valve, working fluid, efficiency, and energy requirements are not given.

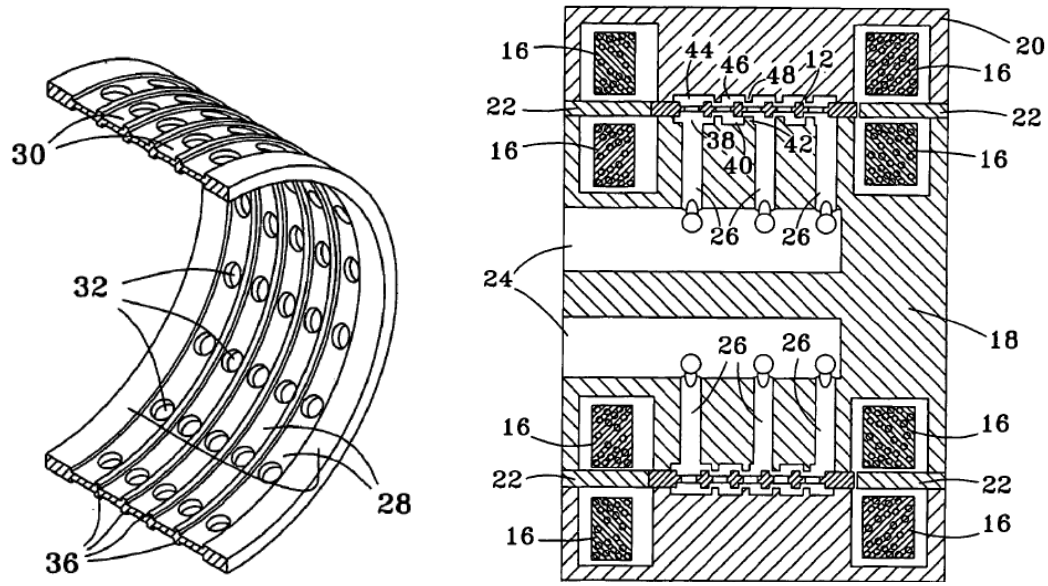

Figure 5: The minimal spool shown above is #12 on the cutaway view shown at the right [8].

Other systems simply use solenoids to control a gate valve[10] or an unloading valve[11] to create a switch mode hydraulic circuit. Solenoid valves are limited in the amount of force that they can generate. In order to address this, one design uses a rotary actuator [12] to move the internal porting of the valve. This creates a pressure differential on the spool, providing large hydrostatic forces to rapidly accelerate the spool.

Another novel design uses a system of 3-way check valves [13] to control a hydraulic actuator, shown in Figure 6. The two solenoids at the top of the figure create two control inputs of either high or low pressure. When a solenoid changes state the resultant pressure differential causes the downstream check valves to move, creating a new flow pathway. Depending on the state of the two input solenoids an attached hydraulic actuator can move forward, in reverse, move freely, or be prevented from moving. A benefit of the design is that it is very easy to implement, but the operating frequency of the system is limited by the solenoids and by the check valves which begin to experience valve float beyond 50Hz[13]. An interesting aspect of the design is that complex functionality is built upon simple modular components.

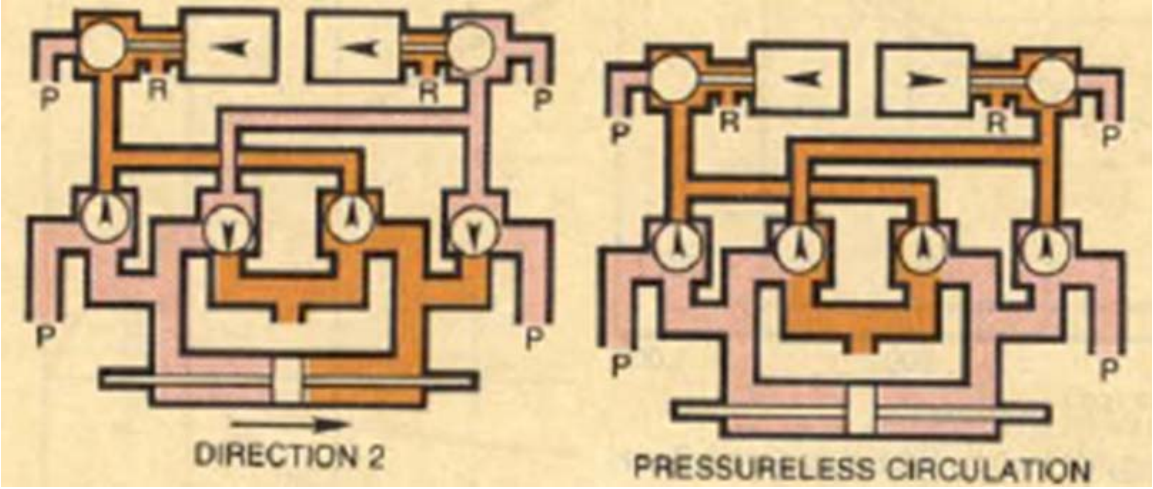

Figure 6: Solenoids at the top create a high or low control input which determines whether the actuator moves forward, reversed, can move freely, or if it is locked [13].

For some designs the solenoids can be replaced with piezoelectric actuators. Piezoelectric materials change their shape when a voltage is applied across them. The displacement is typically very small, but it has a fast response time and can generate large forces. To generate larger displacements piezoelectric actuators have been attached to a gear train amplifier [14] or stacked into a pile [15] to produce a cumulative displacement, shown in Figure 7, but this reduces the output force. In the figure, the piezoelectric actuators control a poppet valve to direct flow supply to load A or load B.

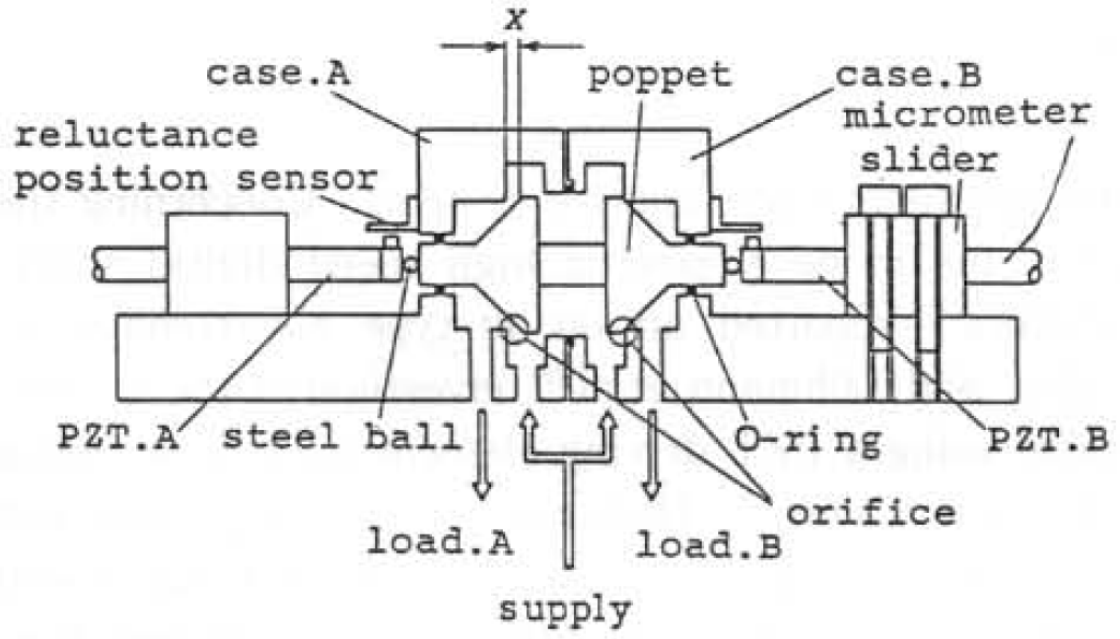

Figure 7: Piezoelectric actuated high speed valve [15].

The other category of high speed valves uses a continuously rotating spool to generate the switching events. Continuously rotating valves are promising because they no longer suffer from the debilitating power losses associated with accelerating and decelerating the spool mass at high frequencies. Designs for continuously rotating spools also go back to

at least the late 1970s. These designs consisted of a rotating spool with cross drilled ports and an outer sleeve with accompanying ports[13]. As the spool rotates, different flow pathways through the valve would be opened and closed.

The design of a continuously rotating valve and control scheme is described by researchers at the University of Minnesota [17-19]. Shown in Figure 8, the valve consists of a spool with a raised helical section. When the inlet flow is open to the top helix, the flow is sent to the application, and when the flow is open to the bottom helix, the flow is sent to tank. By adjusting the axial position of the valve the ratio of time that the inlet flow is sent to the application versus tank can be varied. The valve also incorporates turbines so the rotation of the valve does not need to be powered from an external source. However these very turbines and the rhomboid shape of the inlet port, along with tight manufacturing tolerances make the valve difficult to manufacture. This valve is also prone to seizing from thermal expansion, and because of the radial inlets, generates a centrifugal pumping action. This valve was estimated to run at 84Hz with a majority of the energy loss created from throttling. A similar valve design[20] utilizes miniature accumulators to smooth large pressure swings when the valve is transitioning from one state to the next.

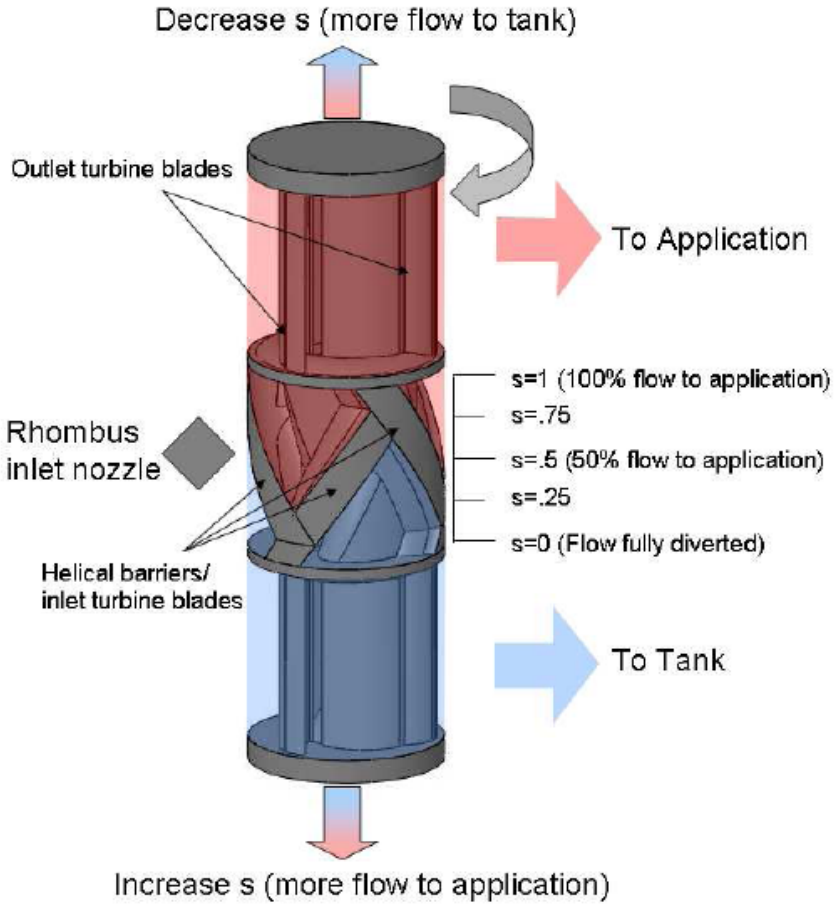

Figure 8: Continuously rotating high speed valve. Flow entering the top helix is sent to the application while flow entering the lower helix is sent to tank. The ratio of high to low is controlled by the axial position of the spool[19].

The last type of high speed rotary valve uses a relative angle difference between valve components to create the pulsing flow. This method has been used to create a flow divider[21] and a pulse width modulated pneumatic rotary valve[22] shown in Figure 9. In this design the relative angle of the actuator port with respect to the fixed stator can be varied. This will change the amount of time the actuator port is connected to the supply port and the return port for each revolution of the inner shaft. The design is simple and compact, however the discontinuous outer sleeve, while appropriate for low pressure pneumatics would not work well for high pressure hydraulic applications.

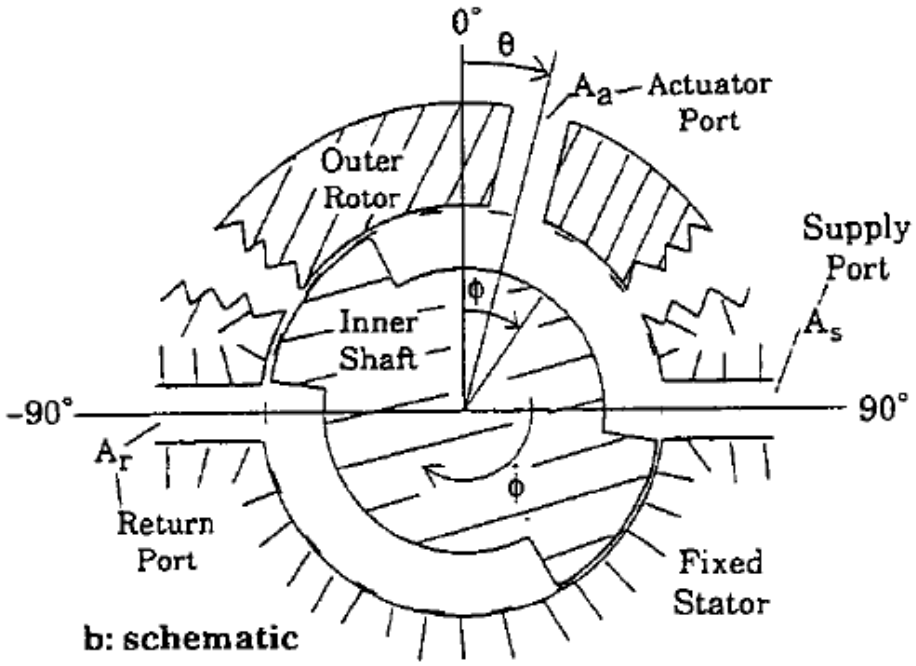

Figure 9: Pneumatic rotary valve. The relative angle of the actuator port with respect to the fixed stator can be varied, thus changing the duty ratio.

Much research has been done towards properly controlling these high speed hydraulic systems. A method for controlling an actuator was developed for use with 2 solenoids [23] and eight solenoids using a Modified PWM algorithm with feedback control [24]. Lastly, a method using adaptive control techniques has also been developed [25]. These control methods are necessary if precise positioning of the hydraulic actuator is required.

Lastly, the Artemis Digital Hydraulic Pump[26] is a combination of a radial piston pump and high speed switching valves. There are two solenoid activated poppet valves on each cylinder of the pump. Each one connects to tank or the application and can be controlled independently. By timing the opening and closing of each valve any duty ratio can be achieved. Artemis benefits from high efficiencies at all duty ratios and each cylinder can independently actuate a hydraulic unit. Note that Artemis is an entire pump and control system whereas the valve proposed would be used to create virtually variable displacement pump/motors out of existing fixed displacement pump/motors.

After searching through the literature, several concepts were developed which must be kept in mind when designing the high speed hydraulic valve.

1) The major energy losses of the valve will likely be from throttling losses and compressibility losses. Therefore transitions times and the switching volume will try to be minimized.
2) The high speed valve will need to be hydrostatically balanced to prevent large misalignment forces. If possible, completely hydrodynamically balancing the valve could save significant weight and allow for faster frequencies, as in [8].
3) Continuously rotating valves will tend to be more efficient than oscillatory type valves because they do not have to rapidly accelerate and decelerate the control mass. These also tend to be easier to analyze since many of the forces are constant.
4) If the valve experiences transition events, then accumulators or check valves may be necessary to buffer large pressure fluctuations.
5) While many of the pneumatic valves sported switching frequencies in the several hundred Hertz range, a fast switching frequency for hydraulic systems will be around 100 Hertz.
6) Systems of small simple components can generate complex functionality.

This paper presents the concept of a phase-shift high speed hydraulic valve for switch-mode hydraulic circuit control. Chapter 2 introduces the concept and architectural options of a high speed valve. Chapter 3 presents an analysis of the disc style architecture with focus on the forms of energy loss, including: throttling, leakage, compressibility, and viscous friction energy losses. Chapter 4 presents the results of the energy loss analysis. Design of the prototype is discussed in Chapter 5. The experimental setup, procedure, and results are discussed in Chapter 6, and concluding remarks in Chapter 7.

Chapter 2: Method of Approach

The following is a discussion of how the final concept for the high speed valve was derived. The two primary methods to control hydraulic actuators are to use throttling valves or variable displacement pump/motors. Another method which has not seen wide acceptance in the hydraulic industry is switch mode control. This method rapidly opens and closes a valve to produce a series of pressure pulses. This creates an average pressure and flow rate determined by the ratio of time that the pressure remains high compared to the time that it remains low for each switching cycle. By varying this ratio, known as the duty ratio, the effective pressure and flow can be modulated. Therefore, the primary goal for this research is to create a hydraulic valve capable of producing a pulsed flow with a variable duty ratio. Other tasks specifications include:

1) Fast switching times from on to off states to reduce throttling losses
2) High switching frequency, on the order of 100Hz, to reduce system pressure fluctuations and to allow for greater precision when controlling hydraulic actuators
3) Small switched volume to reduce compressibility losses
4) Large usable bandwidth, operates from 0 to 1 duty ratio
5) Usable in a four-quadrant control system
6) Hydrodynamically balanced to reduce side loading
7) Fast response time to change from 0 to 1 duty ratio.
8) High efficiency, greater than 50% at 0.3 duty ratio and greater than 90% at 1.0 duty ratio
9) Easy to implement control schemes
10) Duty ratio is uncoupled from valve speed.
11) Few parts to reduce manufacturing costs and simplify assembly
12) Few moving parts to increase valve life cycle and to reduce viscous friction losses
13) Loose manufacturing tolerances to reduce cost, while maintaining low leakage losses
14) Minimal additional accessory equipment required, such as check valves and accumulators
15) Desirable to have continuous rotation to reduce oscillatory power requirements
16) Flexible, can be used with different pump/motor architectures and rotary or linear hydraulic actuators.
17) Low noise level

Of these design goals, high efficiency, wide bandwidth, integrable with 4-quandrant control, and fast pulsing cycles were deemed the most important. With these design goals several preliminary designs were evaluated.

2.1 Preliminary Concepts

Before the final valve design was selected, numerous designs and iterations were conceived. These concepts utilized unique geometry, cams, or networks of sub-valves to produce a variable duty ratio. This section documents the primary concepts.

One of the earliest design ideas, shown in Figure 10, was a modification to the high speed valve by [19]. This design mirrored the raised helical section to allow for flow reversal or the control of two separate hydraulic actuators. However, this design still suffered from the faults of the design from which it was based, including tight manufacturing tolerances, large throttling losses, seizing due to thermal expansion, and centrifugal pumping.

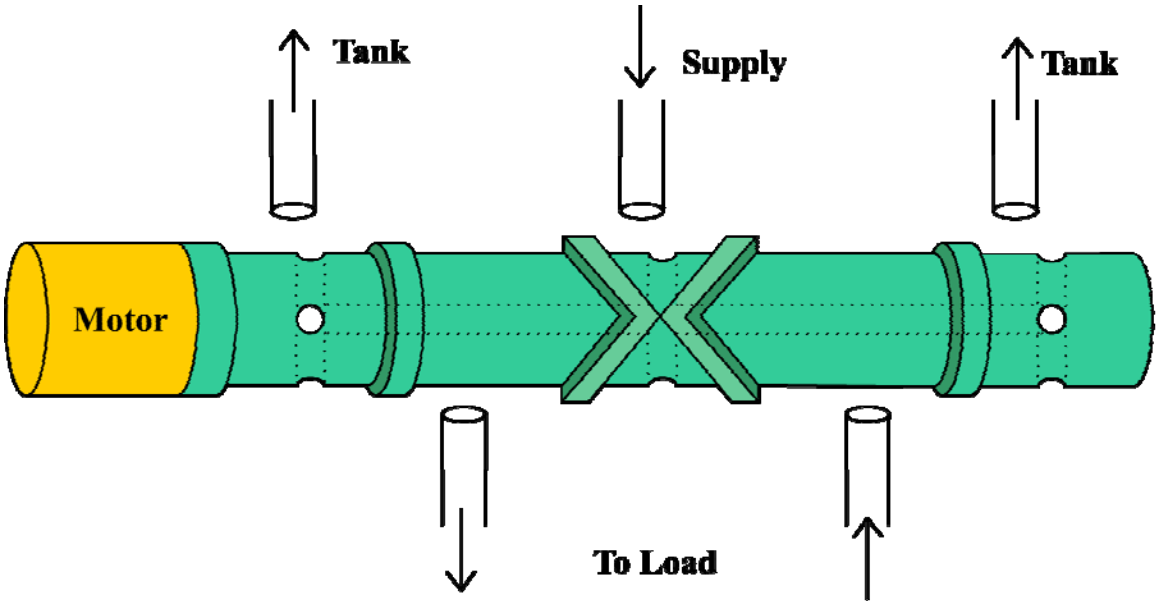

Figure 10: Valve concept with geometry similar to [19], but capable of pulsing flow between two different loads.

Continuing with the idea of geometric shapes used to control the duty ratio, several ideas were generated, some of which are shown in Figure 11. In the first concept, a rotating disc has internal passages for high pressure flow and axial outlet ports. A plate with a specific geometry is placed on the top of the disc and can translate radially. Depending on the position of the plate, the amount of time that the port on the disc is blocked by the plate can be varied, thus changing the duty ratio. This design would be difficult to implement because of the sliding seal around the plate. Also, it was difficult to find a geometric shape which would allow for the full range of duty ratios. The second concept is similar to the first, but this time the geometric shape takes the form of a cutout on the rotating disc. By moving the inlet ports radially the amount of time that they are connected to the outlet ports can be varied, thus changing the duty ratio. The primary disadvantage of this design is that it would be difficult to implement the motion of the input ports. Other designs were investigated to see if a more elegant solution could be found.

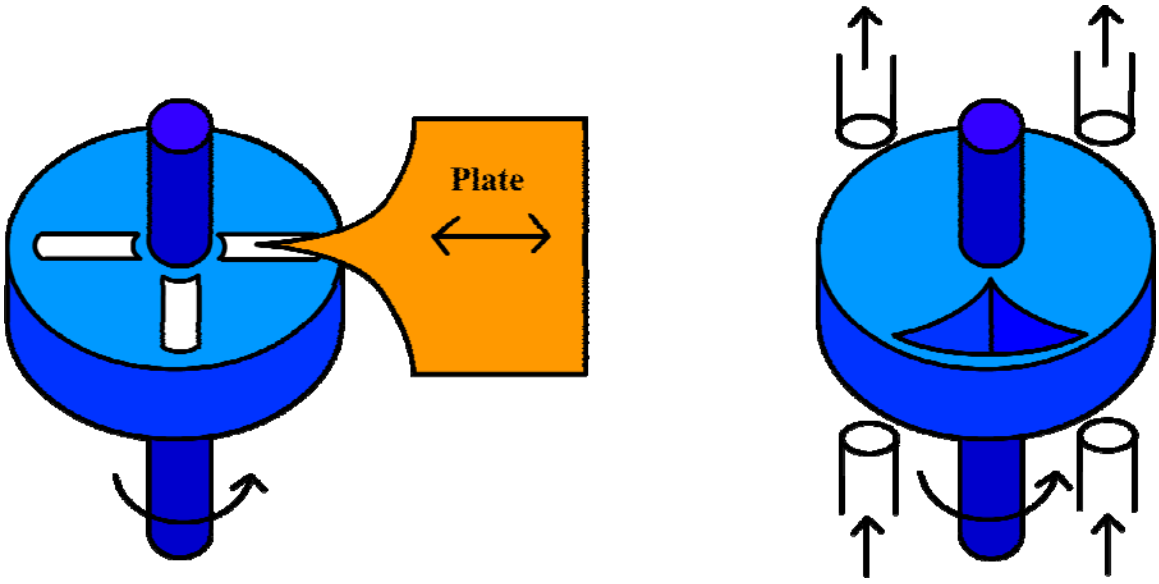

Figure 11: Valve concept utilizing discs and geometric shapes to achieve a variable duty ratio.

The next concept, shown in Figure 12, utilizes an eccentric cam to drive two gates which are attached to the cam followers. The load and tank side gate alternate between open and closed, creating the pulse. The linear position of the cam pivot determines the duty ratio. This design is undesirable because of the oscillating masses and sliding seals.

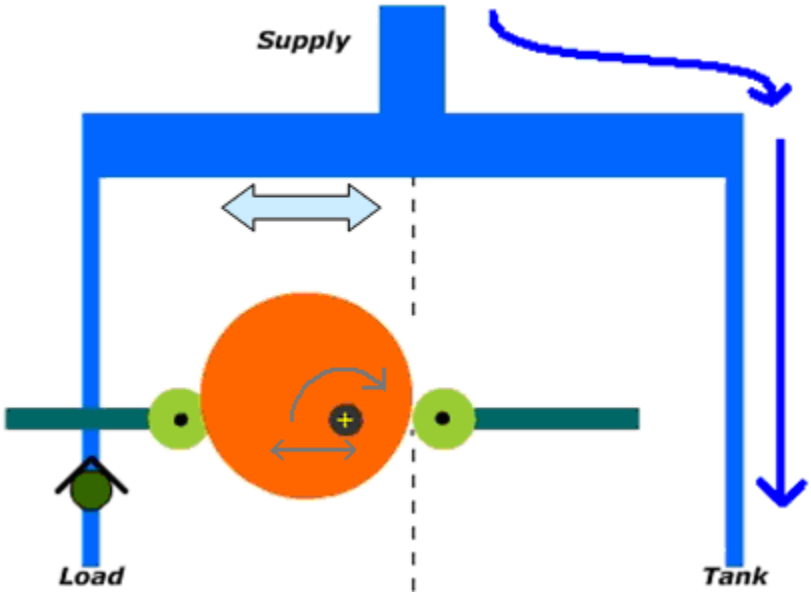

Figure 12: Valve concept utilizing an eccentric cam with an axis of rotation capable of translation to change the duty ratio.

The next concept shown in Figure 13 uses a bottom up approach to create a switch mode valve. Three sub-valves each consist of a half cylinder spool with one radial supply inlet and two radial outlets. These sub-valves each rotate at the same angular velocity, but the phase between them can be varied to change the duty ratio. In the example shown a snapshot of each quarter cycle is displayed. The flow is connected to tank for half the

cycle, then is blocked, and is then connected to the load for the last quarter cycle. The primary disadvantage of this concept and other variations is that the duty ratio could not exceed 0.5 and the valve typically spent at least a quarter cycle completely blocked. The main advantage of the design is that it is simple and easy to implement.

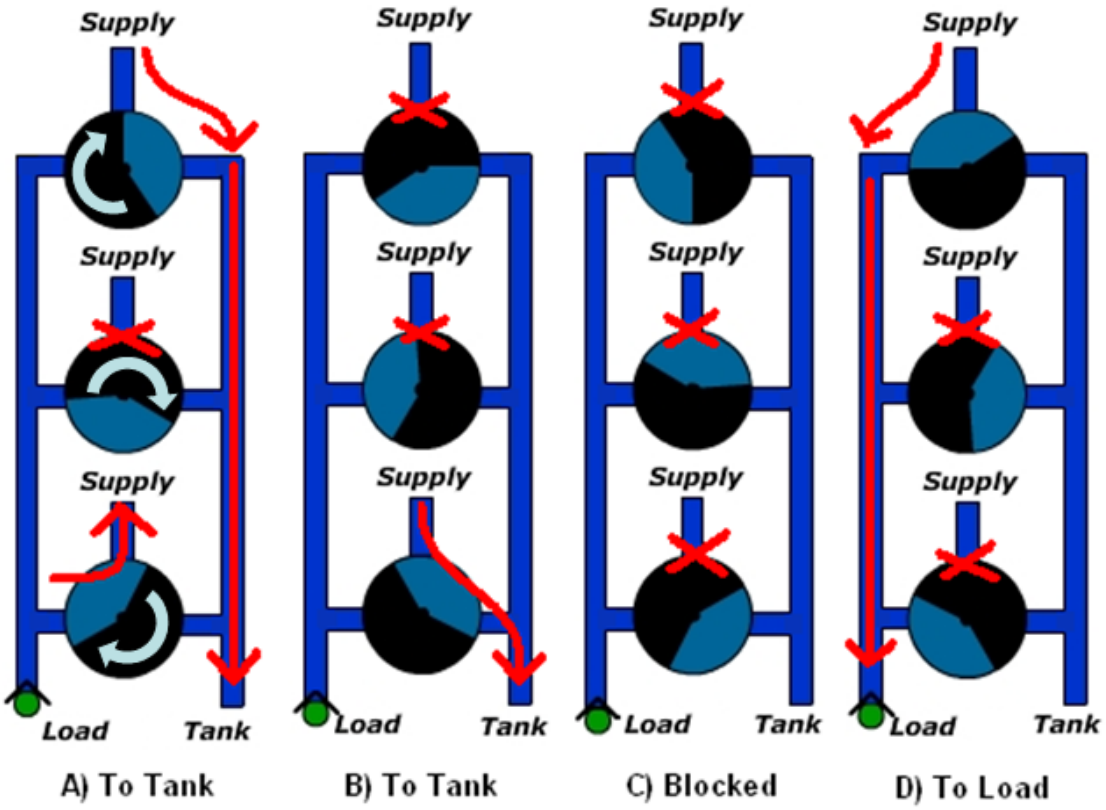

Figure 13: Valve concept utilizing three interconnected sub-valves, each with one radial inlet port and two outlet ports. Four different snapshots are depicted to show how the supply flow can be diverted to tank, blocked, or diverted to the load.

By changing one of the ports to be an axial connection the system of sub-valves can achieve a 0 to 1 duty ratio by changing the phase of the sub-valves with respect to each other. In Figure 14 the arrow heads denote the axial inlet port which ideally is always connected to one of the radial ports. The sub-valves were connected to each other in various ways to determine the least number of sub-valves needed to produce a modulated pulsed flow. Realizing that it is not necessary to pulse the return flow from the motor, the minimum number of sub-valves required is three.

It was also desirable that the system of sub-valves allow for direction reversal and a locked mode in which the hydraulic unit would not be able to move. The reversal feature in particular significantly increased the number of sub-valves required so it was decided to use a standard 2-position, 4-way flow reversing valve. The primary disadvantages of this concept are:

1) It is difficult to keep a relative phase between the spinning valves
2) A relatively large number of moving parts

3) All the porting between sub-valves could create a large switched volume, increasing the compressibility loss.

The primary advantages of the design are that it is relatively simple, does not oscillate, and operates over the full duty cycle range.

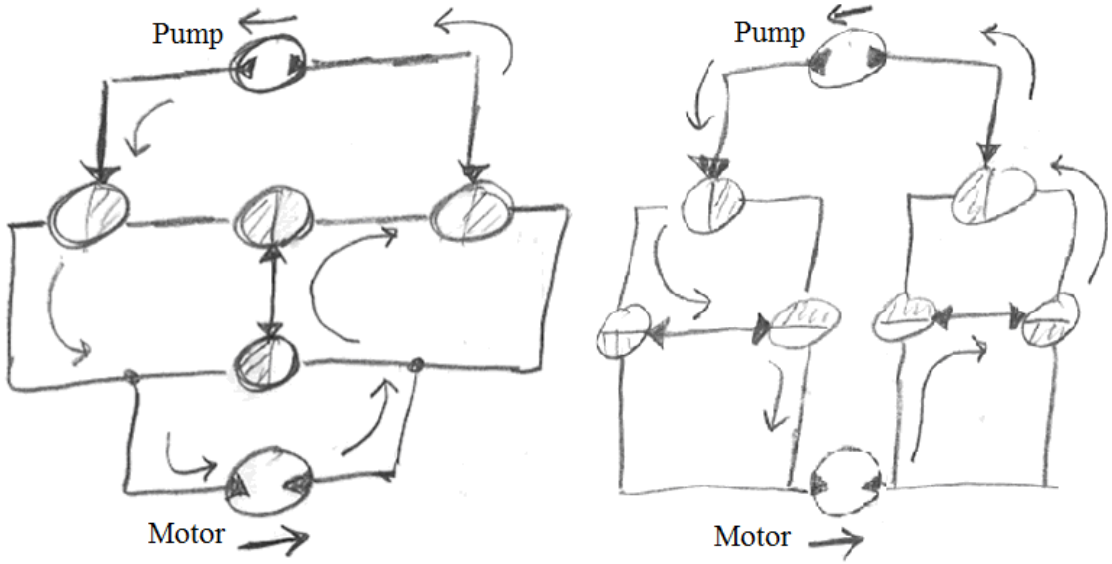

Figure 14: Testing different interconnections to see what combination will allow for forward, reverse, blocked, and free wheeling modes by only changing the phase between sub-valves. Arrowheads denote the axial inlet port to each sub-valve, other lines denote radial outlet ports.

After considering each design, it was decided that the two most promising are the system of sub-valves and the second shaped disc from Figure 11. As will be seen in the next section, a combination of these two designs along with a few other changes eliminates many of the disadvantages from both while retaining their benefits.

2.2 Final Concept

A conceptual schematic of a high speed valve capable of producing a pulsed flow with variable duty ratio is presented in Figure 15. The valve consists of three sub-valves labeled Section 1A, 1B, and 2 which rotate at the same constant angular velocity. Each sub-valve is composed of a half cylinder spool inside a sleeve with two radial inlet ports and one axial outlet port. The outlet port of each sub-valve is connected to each inlet port for half of a revolution. Looking at snapshot a) the only open flow path is from Port P (supply pressure) to inlet port 1a, to the outlet port of section 1A, then to inlet port 2a and finally exiting section 2 to Port A (to a hydraulic actuator). Snapshot b) shows the same system after a $\pi/2$ rotation. The previous flow path is now blocked at inlet port 2a, but the flow path from Port T (tank) to Port A is now open. By varying the relative phase between the top Tier 1 sub-valves with respect to the bottom Tier 2 sub-valve the ratio of time Port A is connected to Port P versus Port T, defined as the duty ratio, can be continuously varied from 0 to 1.

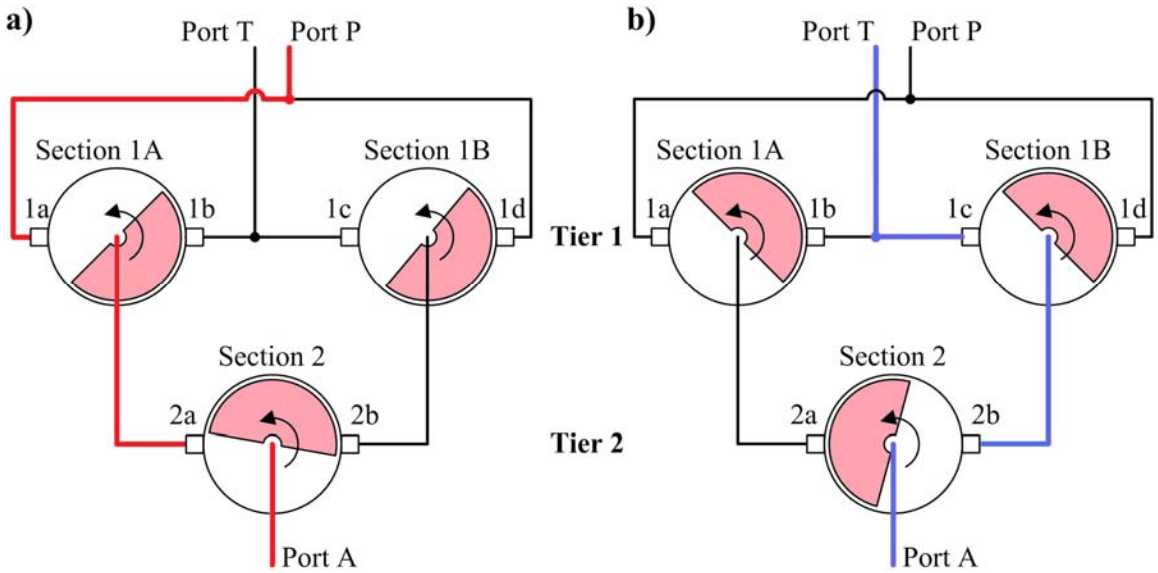

Figure 15: Schematic of the phase shift valve for two different positions. The spool, semi-circle, is a half cylinder with two radial inlet ports and a central outlet port. In snapshot a) the only open flow path is from Port P to Port A. After a 90 degree rotation shown in b) the previous path is blocked but a new flow pathway is opened from Port T to Port A.

The flow diversion of the valve during a single cycle is shown in Figure 16. Note that Section 1A and 1B remain synchronized at π phase with respect to each other, while section 2 can vary from 0 to π phase with respect to section 1. This creates a continuously variable duty ratio from 0 to 1, where zero is defined as full flow from/to tank, Port T, and a duty ratio of 1 is defined as full flow from/to supply pressure, Port P. A negative phase shift or a phase shift beyond π will also result in a duty ratio between 0 and 1

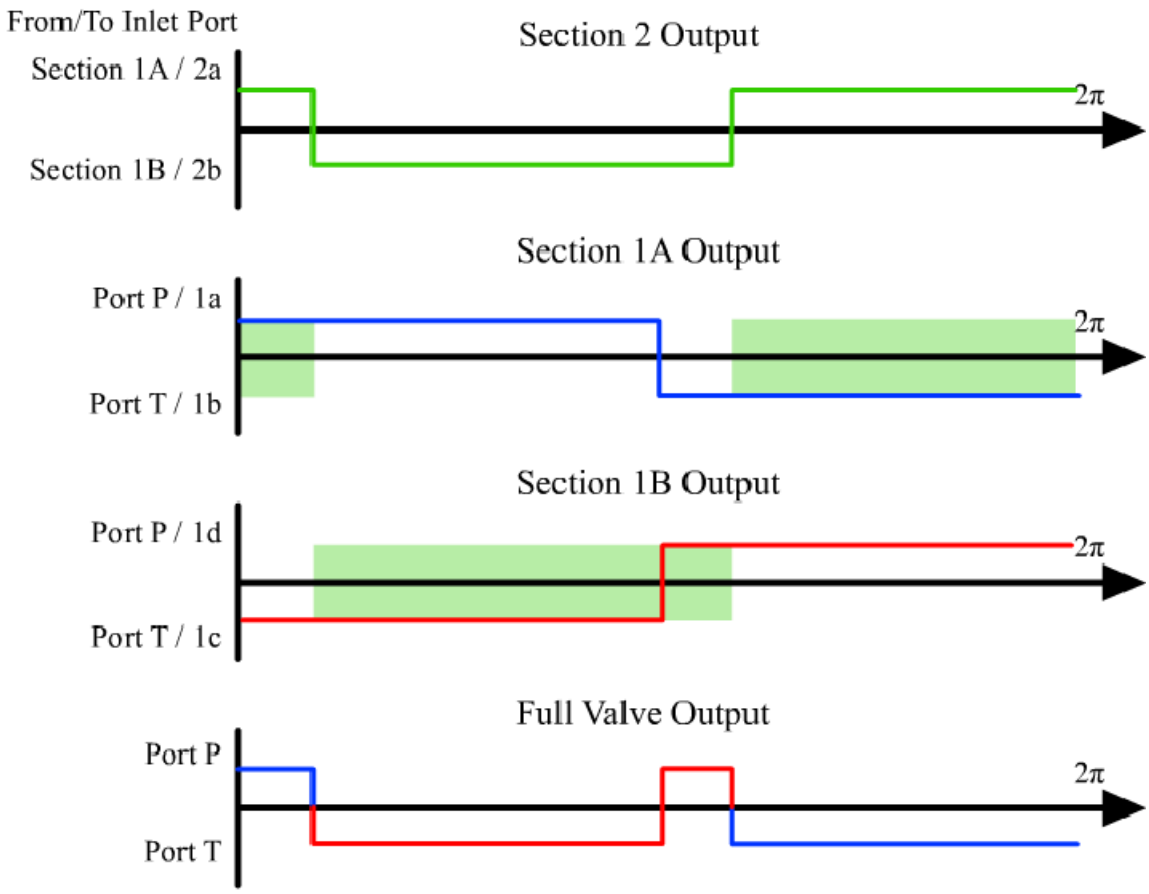

Figure 16: Plot of the flow diversion in the valve for a given phase shift. Shaded regions denote when Section 2 is receiving flow from Section 1. Labeling is consistent with Figure 15.

A beneficial characteristic of the phase-shift architecture is that 2 pulsed segments are generated for every rotation of the valve. This creates a switching frequency which is 2X the operating frequency of the valve, an advantage compared to other continuously rotating valve methods.

Initially the high speed valve was going to utilize spool type sub-valves like those shown in Figure 17. The supply pressure port and the tank port are radial and centered to the Tier 1 valve, but at 90° to each other. Note that the Tier 1 sub-valves have been combined into the Tier 1 spool. The inlet ports are long slits in order to minimize the transitioning time and throttling losses. As the Tier 1 sub-valve rotates the raised square- wave pattern directs high pressure to one end of the spool and tank pressure to the other end. After a 90° rotation these pressures will be directed to opposite ends of the spool. The ends of the Tier 1 spool are connected to radial inlet ports on the Tier 2 spool. One of these inlets will always be blocked so the Tier 2 spool will only allow the supply pressure or tank pressure to connect to the load.

The spool style architecture suffered from several disadvantages.

1) On the Tier 1 sub-valve, the pressure distribution switches sides four times per revolution, incurring large vibrations.

2) The spool and sleeve have to be made to tight tolerances in order to maintain small radial clearances. These clearances are sensitive to the temperature and the elastic deformation of the spool from pressure fluctuations.
3) The relative phase between the two spools must be maintained while they are both rotating, which is difficult to do.
4) The porting to connect the sub-valves together creates a large inlet volume leading to large compressibility losses.
5) The shape of the valve can create a centrifugal pumping action, lowering the effectiveness of the valve. For these reasons it was decided to develop a disc style architecture.

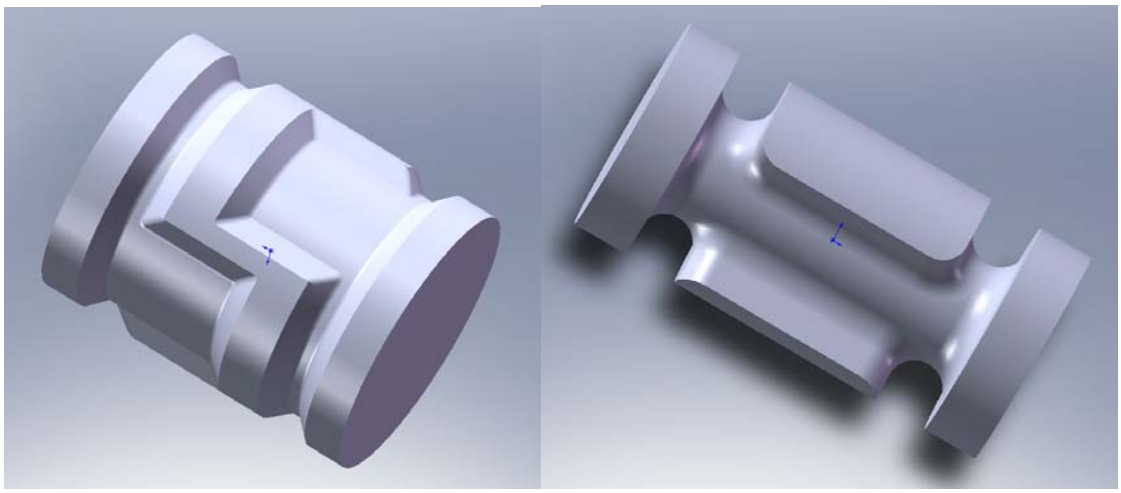

Figure 17: Tier 1 and Tier 2 sub-valves for the spool architecture

In Figure 18, the three discs are stacked on top of each other. Note that section 1A and 1B have been combined into Tier 1. In this setup, varying the duty ratio is achieved by changing the phase of Tier 1 relative to Tier 2, which is fixed. A continuously rotating valve plate is used to produce the switching cycles.

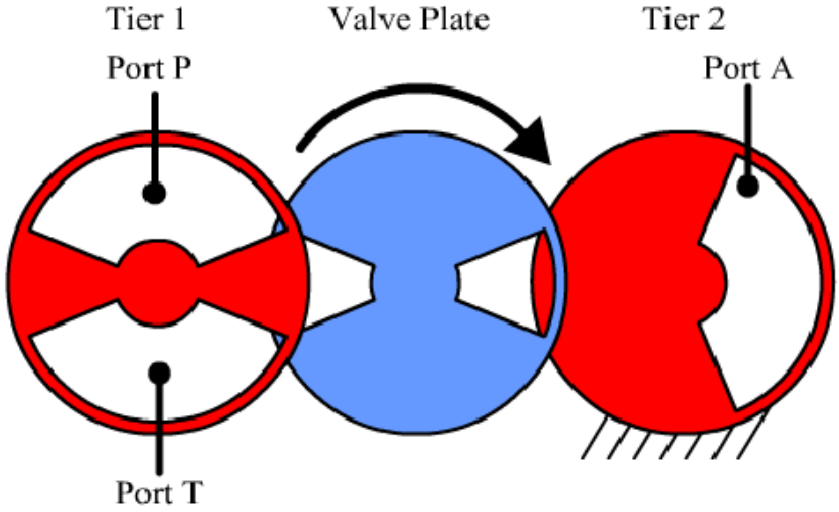

Figure 18: Disc architecture with Section 1 sub-valves combined into Tier 1. Tier 1 can change phase relative to Tier 2, which is fixed, to change the duty ratio. A new component, the continuously rotating valve plate generates the switching pulses.

The disc style valve is shown schematically in Figure 19. The Tier 1 sub-valve, valve plate, and Tier 2 sub-valve are layered on top of each other and enclosed by an extension of the Tier 2 sub-valve. Bearings support the valve plate and allow the Tier 1 and Tier 2 sub-valve to change phase relative to each other through use of the phase servomotor. A valve plate motor continuously spins the valve plate at a constant speed while a directional control motor actuates the flow reversing valve. Tie rods, not shown, would hold the entire assembly together.

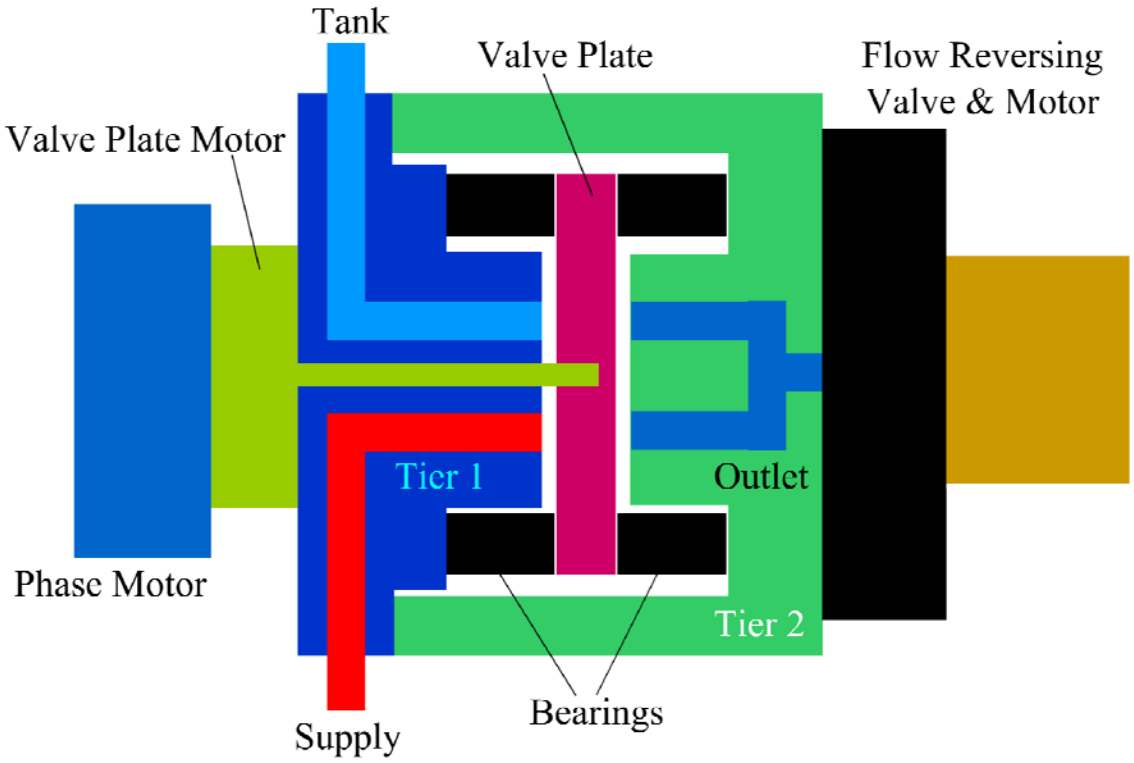

Figure 19: Schematic of disc style valve detailing all major components, radial view

The disc style architecture offers several advantages over the spool style.

1) The pressure fluctuations can be easily balanced or made to be unidirectional.
2) Manufacturing tolerances can be looser, particularly if hydrodynamic thrust bearings are used to maintain clearances between the Tier 1, valve plate, and Tier 2 sub-valve. This is because the thrust bearings can be used to maintain clearances, instead of manufacturing tolerances.
3) In this configuration the phase only needs to be maintained between two stationary components.
4) The large porting volume of the spool design is reduced to the volume of the valve plate slots.
5) Because the flow travels axially through the valve, the centrifugal pumping is no longer an issue.

6) The disc style valve allows the use of hydrodynamic thrust bearings to maintain clearances between valve surfaces, minimizing wear and allowing the valve to adapt to internal dynamic forces. The disc style valve is a promising and unexplored area of valve design and for these reasons it was decided to develop a disc-style model for analysis.

Chapter 3: Modeling and Analysis

To better understand the pressure drops and flow rates of the high-speed phase shift valve a mathematical model is developed. The energy losses of the valve are of primary interest and include the throttling losses of the fully open and transitioning phases, the internal leakage losses of the valve, the compressibility losses due to compliance in the fluid, and the viscous friction losses between relative rotating components. Losses which will not be analyzed include hysteresis losses in the accumulator, inefficiencies in the pump/motor, compressibility losses due to compliance in the valve and pump/motor structure, and viscous pipe flow losses.

Once the equations for energy loss are developed, the model can be optimized in Matlab for the highest efficiency. The valve will also be designed to achieve a wide operating range, minimum pressure ripple, and fast response time.

For modeling purposes, a simplified system is analyzed. Referring back to Figure 1, it is noted that the 4-way 2-position direction control valve only controls the direction of torque on the pump/motor and has no effect on the operation of the valve besides the added volume for compressibility losses. For this reason, the direction control valve will be removed from the analysis.

Also, referring to Figure 18, it can be seen that for the instant shown, the flow path from Tier 1 to Tier 2 is momentarily blocked. This occurs whenever the valve transitions from one state to the next, which is twice per cycle. A typical application for the valve would be the control of a fixed displacement pump/motor on a hydraulic hybrid vehicle. As the valve transitions, fluid flow will be blocked. The motor will continue to rotate and draw a constant flow, causing the motor inlet to vacuum and cavitate. If the hydraulic unit was acting as a pump, then this momentary blockage would create a large pressure spike at the outlet of the pump. To alleviate these issues, two check valves are placed in the simplified hydraulic circuit shown in Figure 20. The right check valve prevents cavitation during motoring, and the top check valve prevents pressure spikes during pumping.

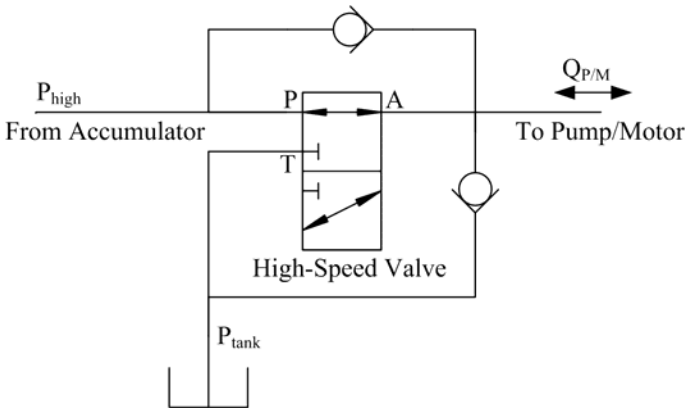

Figure 20: Simplified high-speed valve circuit used for analysis purposes. The two check valves have been added to avoid extreme pressure fluctuations occurring when flow is completely blocked during valve transitions.

The key geometry features of the valve are shown in Figure 21. First, we can define the number of replications of ports on the valve components by the variable N (Figure 21 shows N = 1). The ports of the valve are defined by the inner radius R_i and the outer radius R_o. The ports on the valve plate span an angle of δ while the larger ports of Tier 1 and 2 span an angle of γ. Note that $\delta+\gamma = \pi/N$, thus the valve will be completely blocked twice each switching cycle. Keeping Tier 1 fixed, the angular position of the valve plate θ is defined as zero degrees when the valve plate ports are completely blocked. Looking axially at the valve, the phase angle α is referenced as zero degrees when Port A is aligned with Port T. The phase can vary from 0 to π/N for a 0 to 1 duty ratio, respectively. A_1 is the variable orifice created by the overlap of Tier 1 with the valve plate, while A_2 is the variable orifice created by the overlap of Tier 2 with the valve plate.

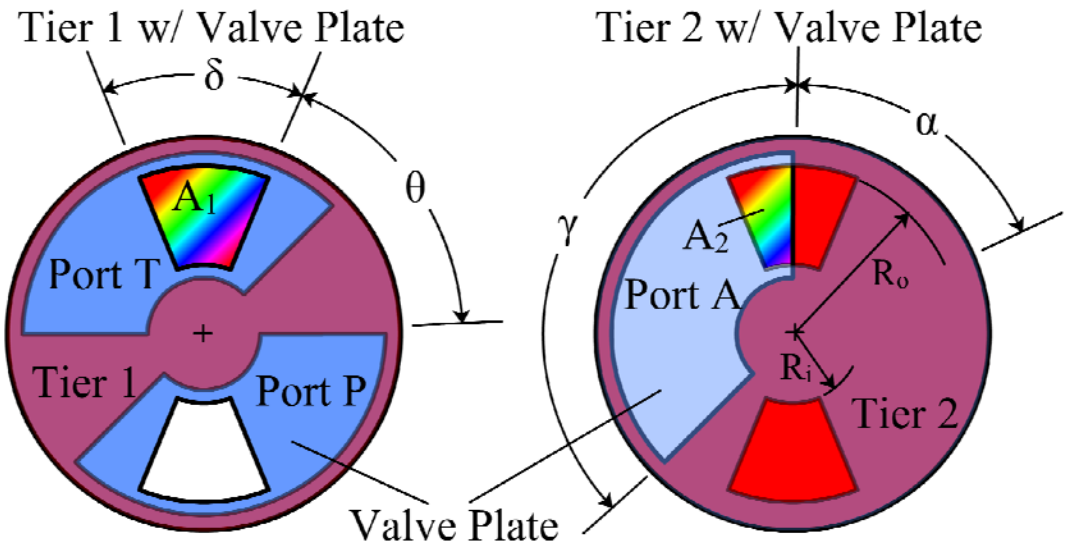

Figure 21: Schematic of disc style valve with key features defined

3.1 Throttling Analysis

Despite the fact that a switch-mode valve was chosen to avoid the inefficient throttling loss of common valves, a significant source of power loss is actually from throttling within the high speed valve. This is because large throttling losses are incurred when the valve transitions from one state to another. Since there are two full on-off periods for each switching cycle of the valve, there are 4*N switches per revolution. For each of these switches, the area of one of the internal valve ports changes from fully open to fully closed or vice versa, creating throttling across a variable area orifice. At low or high duty ratios, throttling across two variable area orifices can occur.

Before calculating the energy loss due to throttling, expressions for the internal port areas of the valve must be developed. Referring back to Figure 21, the first variable orifice area A_1 is defined as the port area created by the overlap of Tier 1 and the valve plate. Again, defining the valve plate angle θ as zero degrees when the valve plate ports are fully blocked and about to transition to Port T, A_1 is given by:

$$A_1(\theta) = \frac{\theta \cdot N}{2}\left(R_o^{\,2} - R_i^{\,2}\right) \quad \text{for } 0 \le \theta \bmod \frac{\pi}{N} < \delta \qquad \text{Equation 1}$$

$$A_1(\theta) = \frac{\delta \cdot N}{2}\left(R_o^{\,2} - R_i^{\,2}\right) \quad \text{for } \delta \le \theta \bmod \frac{\pi}{N} < \gamma \qquad \text{Equation 2}$$

$$A_1(\theta) = \frac{(\pi/N - \theta)\cdot N}{2}\left(R_o^{\,2} - R_i^{\,2}\right) \quad \text{for } \gamma \le \theta \bmod \frac{\pi}{N} < \frac{\pi}{N} \qquad \text{Equation 3}$$

where θ modulo π/N maintains the evaluated angle between 0 and π/N for multiple rotations. Similarly, the second variable orifice area A_2 is defined as the port area created by the overlap of the valve plate and Section 2. Creating a new variable $\theta^* = \theta - \alpha$, A_2 is given by:

$$A_2(\theta^*) = \frac{\theta^* \cdot N}{2}\left(R_o^{\,2} - R_i^{\,2}\right) \quad \text{for } 0 \le \theta^* \bmod \frac{\pi}{N} < \delta \qquad \text{Equation 4}$$

$$A_2(\theta^*) = \frac{\delta \cdot N}{2}\left(R_o^{\,2} - R_i^{\,2}\right) \quad \text{for } \delta \le \theta^* \bmod \frac{\pi}{N} < \gamma \qquad \text{Equation 5}$$

$$A_2(\theta^*) = \frac{(\pi/N - \theta^*)\cdot N}{2}\left(R_o^{\,2} - R_i^{\,2}\right) \quad \text{for } \gamma \le \theta^* \bmod \frac{\pi}{N} < \frac{\pi}{N} \qquad \text{Equation 6}$$

The symmetry of the valve allows the use of π/N instead of 2π/N. Note that the valve plate has 2*N ports, but only N ports have flow. Also, besides the instantaneous moment when the valve is completely blocked, N ports on the valve plate will always have flow. The internal port areas as a function of rotation angle for a phase shift of 30º are shown in Figure 22.

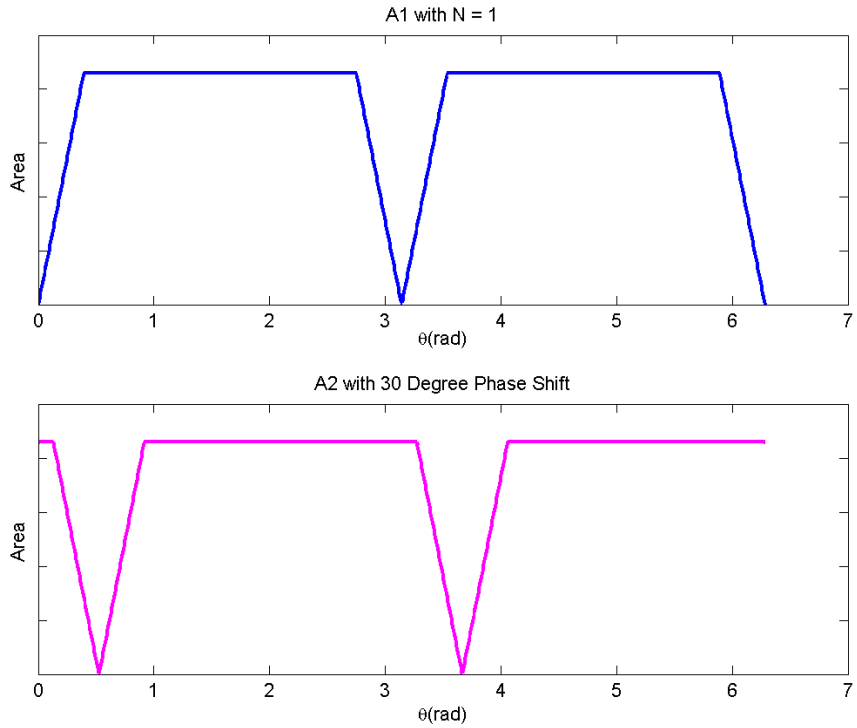

Figure 22: Open areas of the internal ports of the valve as a function of rotation angle

The addition of check valves to the system means that for a portion of time during each transition, flow will be split between the valve and check valve pathways. For instance, referencing Figure 20, when the high speed valve is in motoring mode and switching from Port P to Port T, the internal variable orifices begin to close, causing a large pressure drop. Eventually the pressure at the output of the valve reaches the cracking pressure of the tank side check valve, which causes it to open. Flow thru the check valve increases until all flow passes thru the check valve when the high speed valve passageways become completely blocked. As valve plate continues to rotate, the internal variable orifices begin to open to Port T. The check valve will hold the output pressure steady as it begins to close. Eventually, the output pressure of the valve reaches the cracking pressure of the check valve and it closes. Full flow from Port T to the hydraulic motor is now going through the valve.

To begin the throttling loss analysis it is necessary to first develop an expression for the full flow pressure drop across the high speed valve. By assuming the valve as two orifices[30] in series the pressure drop is given by:

$$\Delta P_{valve} = \Delta P_{Tier1} + \Delta P_{Tier2} = \frac{\rho}{2}\left(\frac{Q}{C_d A_1}\right)^2 + \frac{\rho}{2}\left(\frac{Q}{C_d A_2}\right)^2$$

$$= \frac{\rho Q^2\left(A_1^{\,2} + A_2^{\,2}\right)}{2C_d^{\,2} A_1^{\,2} A_2^{\,2}} \qquad \text{Equation 7}$$

where ΔP_{valve}, ΔP_{Tier1}, and ΔP_{Tier2} are the pressure drop due to full flow through the high-speed valve, Tier 1 of the valve, and Tier 2 of the valve respectively, ρ is the mass density of the fluid, Q is the flow rate, C_d is the discharge coefficient of the orifice, and A_1 and A_2 are the current area of the first and second Tier orifices respectively.

Next it is necessary to determine when flow will be split between the high speed valve and the check valves. It is assumed that the pressure drop across the check valve is always P_{check}. When the hydraulic unit is in motoring mode, the low pressure check valve will have flow when:

$$\Delta P_{valve} > P_i - P_{\tan k} + \Delta P_{check} \qquad \text{Equation 8}$$

Where P_i is the input pressure of the valve, either P_{High} or P_{Tank} and ΔP_{check} is the cracking pressure of the check valve. If this condition is met, then the pressure drop across the valve is held constant by the check valve and is given by:

$$\Delta P_{valve} = P_i - P_{\tan k} + \Delta P_{check} \qquad \text{Equation 9}$$

When the hydraulic unit is in pumping mode, the high pressure check valve will have flow once:

$$\Delta P_{valve} > P_{High} - P_i + \Delta P_{check} \qquad \text{Equation 10}$$

If this condition is met, then the pressure drop across the valve is held constant by the check valve and is given by:

$$\Delta P_{valve} = P_{High} - P_i + \Delta P_{check} \qquad \text{Equation 11}$$

If these conditions are not met, then the pressure drop across the high speed valve is given by Equation 7. However, if these conditions are met, note that the pressure drop across the high speed valve remains constant while the flow rate thru the valve becomes variable. The calculation of the flow through the high-speed valve is attained simply by rearranging Eqn 7, which gives:

$$Q_{valve} = C_d A_1 A_2 \sqrt{\frac{2\Delta P_{valve}}{\rho\left(A_1^{\,2} + A_2^{\,2}\right)}} \qquad \text{Equation 12}$$

By assuming a constant flow through the external hydraulic unit, the flow through the check valve is always described by:

$$Q_{check} = Q - Q_{valve}\,. \qquad \text{Equation 13}$$

The pressure drop across and flow through the high speed valve when the hydraulic unit is acting as a motor are shown in Figure 23. Parameter values used to generate these plots are shown in Table 1. Notice the four large pressure drop spikes corresponding to the four transition events, along with the decrease in flow as a result of the check valves opening. Looking at the middle plot, the effect of the check valve can be seen when the valve transitions to Tank pressure around 0.4 radians. The output pressure is held constant until the threat of cavitation is averted.

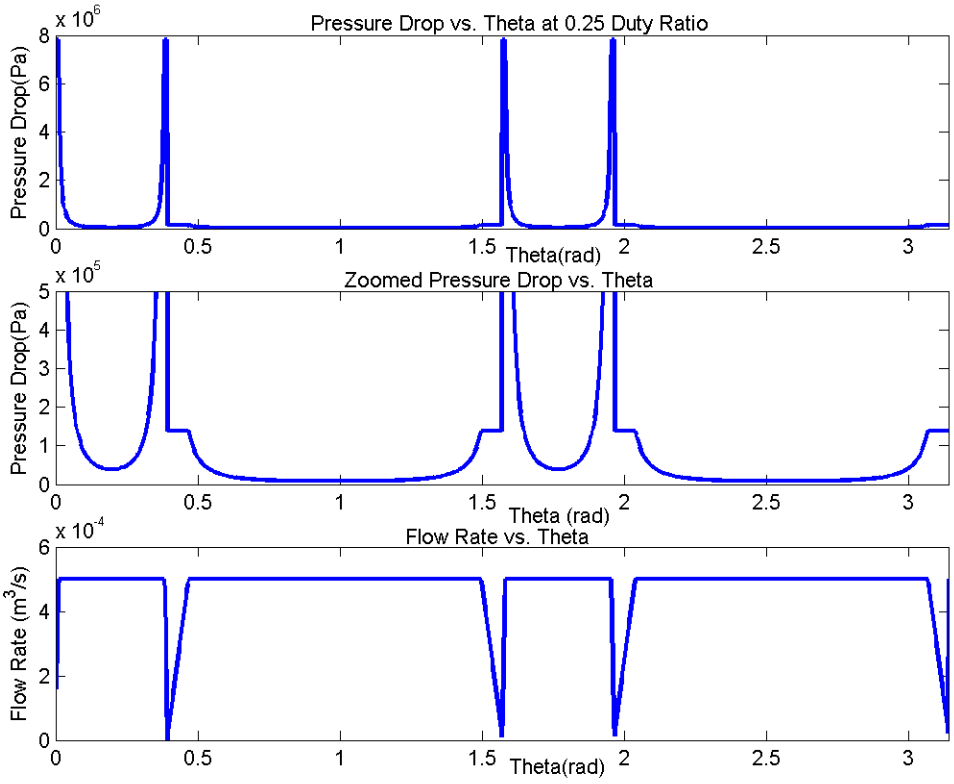

Figure 23: Pressure drop and flow rate thru valve vs. angular position

Table 1: Values used to generate throttling pressure drop and flow plots

Variable	Value

R_i	0.0025m
R_o	0.015m
δ	22.5 deg
N	2
Q	$5*10^{-4}$ m^3/s
P_s	7.77MPa
P_{check}	0.2MPa
P_{tank}	0.1MPa

Once the pressure drop and flow rate thru the valve is determined, the instantaneous power loss due to throttling can be calculated from:

$$P_{throttling} = \Delta P_{valve} Q_{valve} + \Delta P_{check} Q_{check} . \quad \text{Equation 14}$$

3.2 Leakage Analysis

Another form of energy loss is from the internal leakage of the valve. Starting from the high pressure port of Tier 1, the two primary leakage paths are radially outward to the bore, which is held at tank pressure, and circumferentially to the tank pressure ports. These leakage paths exist between two parallel surfaces, so parallel plate leakage is assumed[30].

$$Q_{leak} = \frac{Perimeter \cdot c^3 \cdot \Delta P}{12 \cdot \mu \cdot L} \quad \text{Equation 15}$$

where *Perimeter* is the perimeter of the leakage path given by the average arc length $\gamma \cdot (R_{bore} + R_o)/2$, c is the clearance between the plates, ΔP is the pressure differential, μ is the fluid viscosity, and L is the length of the leakage path given by $(R_{bore} - R_o)$. The radial leakage on the front side of the valve plate, the region between the valve plate and Tier 1, is given by:

$$Q_{leak,f} = \frac{N \cdot \gamma \cdot c_f^{\,3} \cdot \Delta P \cdot (R_{bore} + R_o)}{24 \cdot \mu \cdot (R_{bore} - R_o)} \quad \text{Equation 16}$$

where R_{bore} is the radius to the bore of the valve, and c_f is the clearance between the front face of the valve plate and the Tier 1 sub-valve. The rear side of the valve plate, the region between the valve plate and Tier 2, will also experience leakage losses, but this loss is affected by the duty ratio. When the high pressure ports are blocked the perimeter of the rear side of the valve plate will be determined by the valve plate port angle δ, but when the ports are unblocked the perimeter will be determined by the Tier 2 port angle γ. This gives:

$$Duty = \frac{\alpha \cdot N}{\pi} \quad \text{Equation 17}$$

$$Q_{leak,b} = \frac{N \cdot c_b^{\,3} \cdot \Delta P \cdot (R_{bore} + R_o)}{24 \cdot \mu \cdot (R_{bore} - R_o)} \cdot \left(\gamma \cdot Duty + \delta \cdot (1 - Duty)\right) \quad \text{Equation 18}$$

where *Duty* is the duty ratio and c_b is the clearance between the back face of the valve plate and the Tier 2 sub-valve. Once the leakage flow rate is calculated, the power loss due to radial leakage is simply:

$$P_{Leak,rad} = \left(Q_{leak,f} + Q_{leak,b}\right) \cdot \Delta P \quad \text{Equation 19}$$

The circumferential leakage analysis is complicated by the fact that the rotating valve plate creates variable leakage lengths. Furthermore, at the start of the cycle when the ports are completely blocked, the leakage length L from Equation 15 is zero, predicting infinite flow. To simplify the analysis, orifice flow will be assumed around transition events and parallel plate flow once the leakage path length increases. The cycle of leakage modes is shown in Figure 24. Initially the leakage length is near zero and orifice flow is assumed. As the valve plate advances the leakage path length L becomes sufficiently long for parallel plate flow to be used, but L is dependent upon the valve plate position θ. Once the valve plate port advances beyond the Tier 1 land at an angle of δ, the leakage length remains constant until the start of the next transition event. During the next transition event the process is reversed (Constant Parallel Plate→Variable Length Parallel Plate→Orifice).

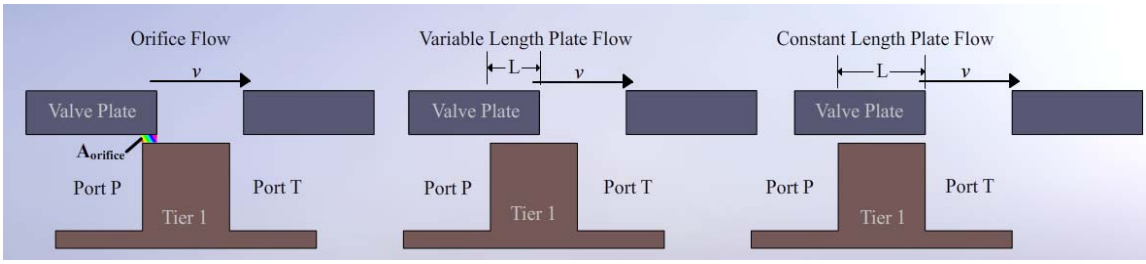

Figure 24: Circumferential leakage pathways for three moments in time

In order to determine the circumferential leakage it is first necessary to determine the leakage length that corresponds to when the parallel plate equation can be used. By setting the orifice equation equal to the parallel plate equation we can get an expression for the minimum leakage length and thus the angle at which to assume parallel plate flow.

$$Q_{orifice} = Q_{plate}$$

$$C_d \cdot A\sqrt{\frac{2}{\rho}\cdot\Delta P} = \frac{b\cdot c^3\cdot\Delta P}{12\cdot\mu\cdot L} \qquad \text{Equation 20}$$

where $Q_{orifice}$ and Q_{plate} are the orifice flow and parallel plate flow respectively, b is the width, c is the distance between the plates, $\Delta P = P_{high}-P_{tank}$, and L is the flow length. By recognizing through geometry that $A = bc$, $b = R_o - R_i$, and $L = \theta\cdot(R_i + R_o)/2$, and rearranging Eqn 19:

$$\theta_{trans} = \frac{c^2}{6\cdot\mu\cdot C_d\cdot(R_i+R_o)}\sqrt{\frac{\rho\cdot(P_{high}-P_{\tan k})}{2}} \qquad \text{Equation 21}$$

where θ_{trans} is the rotation angle where the flow transitions from orifice flow to parallel plate flow. Further recognizing that the leakage cycle described above happens 2N times per revolution per leakage path, that there are 2N leakage paths, and using the definition of $\omega = d\theta/dt$, the volume of leakage flow per revolution is:

$$V_{circum,f} = 4\cdot N^2\cdot\int_{t=o}^{t=\frac{\pi}{N\cdot\omega}} Q(\theta)dt$$

$$= \frac{4 \cdot N^2}{\omega} \int_{\theta=0}^{\theta=\frac{\pi}{N}} Q(\theta) d\theta$$

$$= \frac{4 \cdot N^2}{\omega} \left[\begin{array}{l} 2 \int_{\theta=0}^{\theta=\theta_{trans}} Q_{orifice} d\theta + 2 \int_{\theta=\theta_{trans}}^{\theta=\delta} Q_{plate,\mathrm{var}}(\theta) d\theta \\ \qquad + \int_{\theta=\delta}^{\theta=\gamma} Q_{plate,const} d\theta \end{array} \right] \qquad \text{Equation 22}$$

where $Q_{orifice}$ is given by the left side of Equation 20 and:

$$Q_{plate,\mathrm{var}}(\theta) = \frac{(R_o - R_i) \cdot c_f^3 \cdot \Delta P}{6 \cdot \mu \cdot (R_o + R_i) \cdot \theta} \qquad \text{Equation 23}$$

$$Q_{plate,const} = \frac{(R_o - R_i) \cdot c_f^3 \cdot \Delta P}{6 \cdot \mu \cdot (R_o + R_i) \cdot \delta} \qquad \text{Equation 24}$$

Substituting Eqn 23 and Eqn 24 into Eqn 22 and integrating yields Equation 25, the circumferential leakage volume per revolution:

$$V_{circum,f} = \frac{4 \cdot N^2}{\omega} \left[\begin{array}{l} 2 \cdot C_d \cdot A \cdot \theta_{trans} \sqrt{\frac{2}{\rho} \cdot \Delta P} \\ \qquad + \frac{(R_o - R_i) \cdot c_f^3 \cdot \Delta P}{6 \cdot (R_o + R_i) \cdot \mu} \left(2 \cdot \ln\left(\frac{\delta}{\theta_{trans}} \right) + \frac{\gamma - \delta}{\delta} \right) \end{array} \right] \qquad \text{Equation 25}$$

Equation 25 only constitutes the circumferential volume on the front side of the valve plate. The rear side circumferential leakage is the flow from the high pressure valve plate port to the low pressure valve plate port. Like the rear side radial leakage, the rear side circumferential leakage is further complicated by the duty ratio of the valve. One other complication is that the leakage paths pass thru variable area orifices so the pressure differential is not constant anymore. However, as seen from the throttling loss analysis the pressure drop remains fairly constant and only varies greatly for brief instants of time. Thus it will be assumed that the pressure differential on the rear side of the valve remains constant at $\Delta P = P_{high} - P_{tank}$.

The derivation of the rear side circumferential leakage is similar to the front side leakage with the addition of conditions dependent upon the phase angle α. For the range

$$\delta \le \alpha \le \frac{\pi}{N} - \delta$$

$$V_{circum,b} = \frac{4 \cdot N^2}{\omega} \left[\begin{array}{l} \int_{\theta=\alpha-\theta_{trans}}^{\theta=\alpha+\theta_{trans}} Q_{orifice} d\theta + \int_{\theta=0}^{\theta=\alpha-\theta_{trans}} Q_{plate,\mathrm{var}1}(\theta) d\theta \\ \qquad + \int_{\theta=\alpha+\theta_{trans}}^{\theta=\pi/N} Q_{plate,\mathrm{var}2}(\theta) d\theta \end{array} \right] \qquad \text{Equation 26}$$

where $Q_{plate,\mathrm{var}1}(\theta)d\theta$ and $Q_{plate,\mathrm{var}2}(\theta)d\theta$ are the same as Equation 23, but with θ replaced by $\alpha-\theta$ and $\theta-\alpha$, respectively. For the range $0 \le \alpha \le \delta$

$$V_{circum,b} = \frac{4 \cdot N^2}{\omega}\left[\begin{array}{l}\int_{\theta=\alpha-\theta_{trans}}^{\theta=\alpha+\theta_{trans}} Q_{orifice}d\theta + \int_{\theta=0}^{\theta=\alpha-\theta_{trans}} Q_{plate,\mathrm{var}1}(\theta)d\theta \\ + \int_{\theta=\alpha+\theta_{trans}}^{\theta=\alpha+\gamma} Q_{plate,\mathrm{var}2}(\theta)d\theta + \int_{\theta=\alpha+\gamma}^{\theta=\pi/N} Q_{plate,const}d\theta\end{array}\right] \qquad \text{Equation 27}$$

Where $Q_{plate,\mathrm{var}1}(\theta)d\theta$ and $Q_{plate,\mathrm{var}2}(\theta)d\theta$ are the same as Equation 23, but with θ replaced by $\alpha-\theta$ and $\theta-\alpha$, respectively and $Q_{plate,const}d\theta$ is the same as Equation 24 but with δ replaced by γ. Due to symmetry, Equation 27 can also be used for the range $\frac{\pi}{N}-\delta \le \alpha \le \frac{\pi}{N}$ with the simple conversion $\alpha = \frac{\pi}{N} - \alpha$. Note that Equations 26 and 27 will use the back side clearance c_b instead of c_f. Finally the energy loss from circumferential leakage is:

$$E_{Leak,circum} = \left(V_{circum,f} + V_{circum,b}\right) \cdot \Delta P \qquad \text{Equation 28}$$

3.3 Compressibility Analysis

The next major form of energy loss of the high speed valve is due to the compressibility of the fluid subjected to a fluctuating pressure. Every time the valve switches from low to high pressure the fluid is compressed, increasing its density. As the valve switches to the tank port the energy put into compressing the fluid is lost as it decompresses to tank pressure. The volume of fluid subjected to this fluctuating pressure includes the internal volume of the pump/motor, the internal volume of one path of the directional control valve, the output porting of the high speed valve, the port volume of the valve plate and Tier 2 of the high speed valve, and the volume of any passages leading to the check valves.

The bulk modulus β is defined as the pressure increase needed to cause a given relative decrease in volume, $\beta = -\frac{\Delta P}{\Delta V} \cdot V$. The effective bulk modulus strongly depends on the entrained air content of the fluid, the fluid pressure, the fluid temperature, and the flexibility of the fluid's container. Merritt [31] gives a simple expression for the effective bulk modulus as:

$$\frac{1}{\beta_e} = \frac{1-R}{\beta_{oil}} + \frac{R}{P_{high} \cdot k} \qquad \text{Equation 29}$$

where β_e is the effective bulk modulus, β_{oil} is the bulk modulus of air free oil, R is the entrained air content by volume at atmospheric pressure, and k is the ratio of specific heats for air. From the definition of bulk modulus, the change in volume due to every switch from the tank branch to the pressure branch can be described by:

$$\Delta V = \frac{\left(P_{high} - P_{\tan k}\right)\cdot V_{switch}}{\beta_e} \qquad E_{comp} = \frac{\left(P_{high} - P_{\tan k}\right)^2 \cdot V_{switch}}{\beta_e}$$

Equation 30

where ΔV is the change in volume and V_{switch} is the switching volume. Finally, the energy loss during each switch due to fluid compression is:

$$E_{comp} = \left(P_{high} - P_{\tan k}\right)\cdot \Delta V \qquad \text{Equation 31}$$

3.4 Viscous Friction Analysis

The last form of energy loss to be considered is caused by viscous friction, which is the friction caused by the shearing of fluid. Viscous friction primarily takes effect in the area between the outer surface of the valve plate and the bore of the valve and between the face of the valve plate and the Tier 1 & Tier 2 sub-valve. Furthermore, the area on the face of the valve plate can be divided into two sections: the annular region outside the port switching area and the annular region within the port switching area. For the viscous friction between the valve plate and the bore, Petroff's equation gives the required torque of a journal bearing under no load [29].

$$T_{journal} = \frac{2\cdot\pi\cdot\omega\cdot\mu\cdot t_{vp}\cdot R_{bore}^{\ 3}}{c_{bore}} \qquad \text{Equation 32}$$

where $T_{journal}$ is the torque applied to the circumference, t_{vp} is the axial thickness of the valve disc, R_{bore} is the outer diameter of the valve disc, ω is the angular velocity in rad/s and c_{bore} is the radial clearance between the valve plate and the bore. Because the valve plate is thin and has large radial clearances this Torque will be small compared to the viscous face torques.

The other viscous friction forces are developed on the front and rear face of the valve plate. From Newton's postulate, the frictional torque on the valve plate outside the switching area between the valve plate and Tier 1 is:

$$T_{plate,f,o} = Fr = \frac{\mu\cdot A\cdot u}{c_f} r = \int_{\theta=0}^{\theta=2\pi}\int_{r=R_o}^{r=R_b} \frac{\mu\left(r\cdot dr\cdot d\theta\right)\left(\omega r\right)}{c_f} r = \frac{\pi\omega\mu}{2c_f}\left(R_{bore}^{\ 4} - R_o^{\ 4}\right) \qquad \text{Equation 33}$$

The outer friction face torque on the rear side of the valve plate, between the valve plate and Tier 2, $T_{plate,b,o}$, is of the same form of Equation 31, but with c_f replaced by c_b. The viscous friction within the switching area is complicated by transition events. As a simplification Equation 33 will be used with the limits of integration from $\theta=0$ *to* $2N\delta$ for the front face switching torque, $T_{f,switch}$, and $\theta=0$ *to* π for the rear face switching torque, $T_{b,switch}$. These new limits of integration are because the ports prevent a full annular region between the valve plate and the Tier 1 & 2 sections in which viscous losses can have a significant effect. The power loss from these frictional torques is then:

$$P_{fLoss} = \omega\cdot\left(T_{journal} + T_{plate,f,o} + T_{plate,b,o} + T_{f,switch} + T_{b,switch}\right) \qquad \text{Equation 34}$$

3.5 Optimization Procedure

Once the equations for the various energy losses were determined, a Matlab script was written to determine what the energy loss of the high speed valve would be for a set of given parameters. Because the throttling, leakage, and viscous friction losses are heavily coupled and nonlinear it would normally be difficult to find optimum parameter values. Thus the Matlab function *fmincon* was used to find the valve parameters which minimize the energy loss. The function *fmincon* uses a sequential quadratic programming (SQP) method to perform a constrained nonlinear optimization. This function takes in arrays that hold the starting guess values, lower bound, and upper bound of the variables you would like to optimize. The function then iterates these parameters until a minimum value is found.

The variables that were optimized were the inner radius R_i and outer radius R_o of the valve ports, the valve plate port angle δ, the radial clearance of the bore c_{bore}, the clearance of the front c_f and back c_b face of the valve plate, the valve plate outer radius R_b, the flow rate Q, and the supply pressure P_s. When using *fmincon* it is important to realize that the function can get stuck at local minima therefore it is necessary to try different starting values and see if the same optimum values are reached. One should also be cautious because *fmincon* may derive parameters which cause the system to behave abnormally. A case in point is if the upper bound of R_i is too close to the lower bound of R_o then *fmincon* will optimize for zero slot area, causing the check valves to remain open at all times. The Matlab code that determines energy loss is Disc_Energy_Loss.m and the code that minimizes the energy loss is Opt2.m. These files can be found in Appendix E: Matlab Files.

In summary, throttling, leakage, compressibility and viscous friction losses for the high speed valve were derived. Many of these losses are dependent on the duty ratio and each other which complicates the analysis further. By using Matlab, these complex equations can be solved, and valve parameters optimized for minimum energy loss.

Chapter 4: Analytic Results

In this chapter, the given model properties and the resultant optimized model property values are displayed. The results of the throttling, leakage, compressibility, viscous and overall power losses are also presented.

The optimization was performed with the goal of creating the most efficient high speed valve. The model was optimized at a 0.25 duty ratio based on the fact that the peak power requirements of a hybrid vehicle drive train are often a fraction of the peak power[2]. Table 2 shows the given parameters and the resultant optimized values. For these parameters the model predicts 58.7% efficiency at a 0.25 duty ratio. The predicted efficiency at 1.0 duty ratio is over 90%. The total hydraulic power which could be transferred thru the valve at a 0.25 duty ratio is 2520 Watts.

Table 2: Model properties

Given Property Description	**Symbol**	**Value**
Number of cycles on valve plate	N	2
Inlet volume exposed to fluctuating pressure	V_{switch}	$1.0x10^{-5}$ m^3
Switching frequency	f_{switch}	100 Hz
Rotating angular velocity	ω	1500rpm
Duty ratio	Duty	0.25
Pressure of the tank	P_{tank}	101 kPa
Pressure drop across check valve	ΔP_{check}	138 kPa
Orifice coefficient	C_d	0.61
Density of the hydraulic fluid	ρ	850 kg/m^3
Absolute viscosity of fluid, DTE28@60°C	μ	0.0875 Pa*s
Bulk modulus of air free hydraulic fluid	β_{oil}	1.8 GPa
Entrained air by volume at atmospheric pressure	R	2%
Axial thickness of valve disc	t_{vp}	5mm

Table 3: Optimized parameters and calculated values

Optimized Property Description	**Symbol**	**Value**
Inner radius of valve ports	R_i	5mm
Outer radius of valve ports	R_o	17.6mm
Angular port width	δ	$\pi/8$
Angular width of open sector of valve disc	γ	$7\pi/8$
Clearance of front face of valve plate	c_f	25.4μm
Clearance of back face of valve plate	c_b	25.4μm
Radial clearance of valve disc	c_{bore}	1mm
Outer radius of valve disc	R_{bore}	24.7mm
Flow rate to/from the pump/motor	Q	6.3e-4 m^3/s
Pressure of the source/accumulator	P_{high}	16MPa

4.1 Throttling Loss Results

The high speed valve will throttle the fluid flow at all times; this is usually in the form of the fully open pressure drop, but during transition events large throttling losses are incurred. Throttling of the valve is the major source of energy loss in the system accounting for 38.7% or 399 Watts of the total losses. Figure 25 shows the throttling power loss for the high speed valve and check valves. Notice that the average power loss of the check valve is an order of magnitude smaller than the average power loss of the valve. The fully open throttling power loss only accounted for 2% of the total throttling loss.

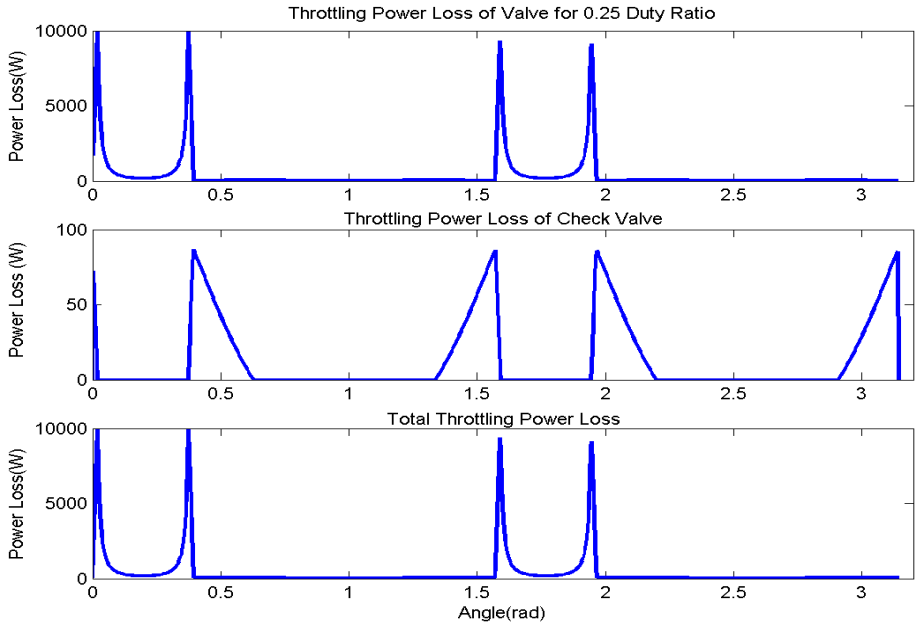

Figure 25: Instantaneous throttling power loss of the high speed valve, check valves, and total for 1 cycle

Remember that the throttling power loss is also a function of the duty ratio. This can be seen in Figure 26. At zero duty ratio the high speed valve has no flow and thus does not have any throttling losses. As the duty ratio increases the high speed valve will start to experience simultaneous variable orifices from the Tier 1 and Tier 2 sections creating a rapid increase in throttling losses. As the duty ratio increases further the Tier 1 and Tier 2 orifices will experience transition events separately which creates a constant throttling power loss over the mid range of duty ratios. Starting at 0.65 duty ratio, a slight dip in the throttling power loss curve is seen. This is from the tank-side check valve opening and increasingly supplying more flow. Increasing the duty ratio further will cause the valve to experience simultaneous variable orifices again. At these higher duty ratios, flow is throttled from P_{high}-P_{tank} for longer periods of time compared to when the valve experienced simultaneous variable orifices at low duty ratios. This causes another large increase in throttling power loss. The ratio of the throttling power loss to the output power is shown in Figure 27. At low duty ratios, the throttling power loss saps a significant portion of the output power, but this rapidly decreases as the duty ratio is increased.

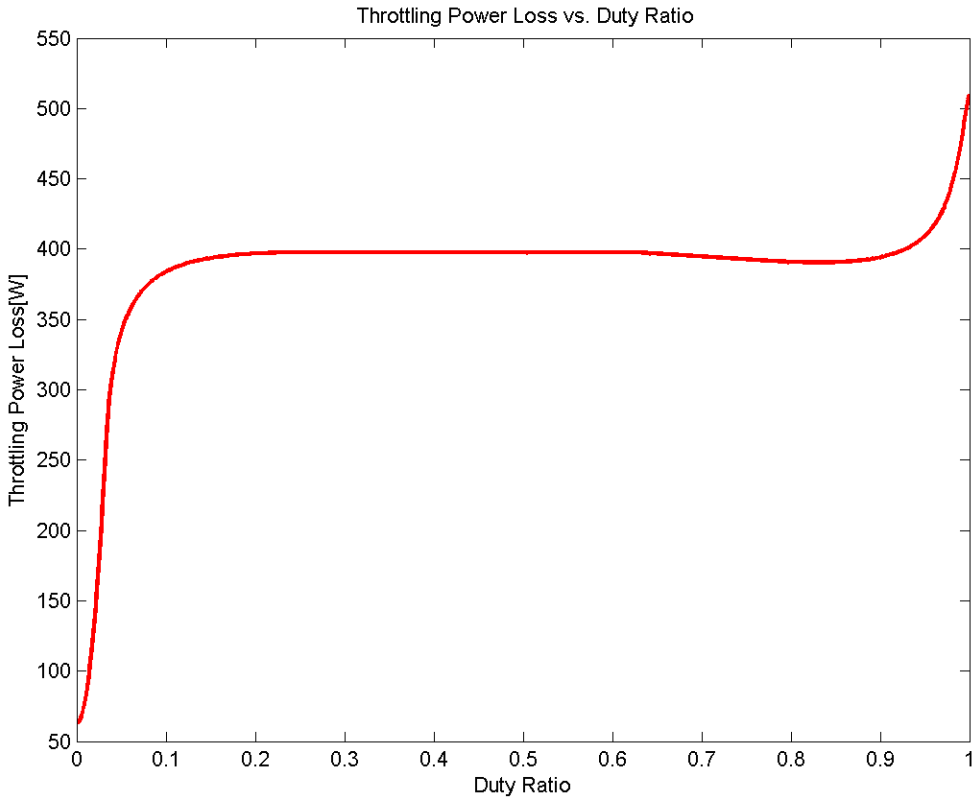

Figure 26: Throttling power loss vs. duty ratio

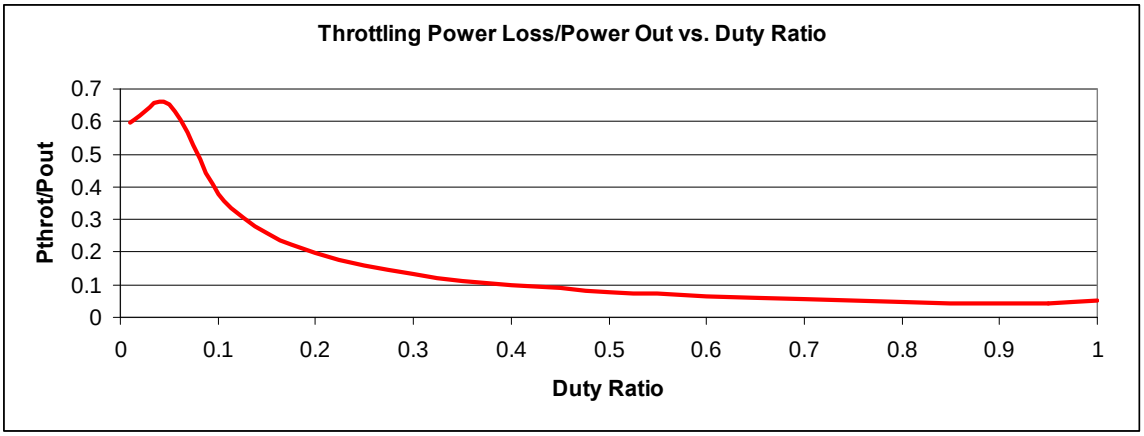

Figure 27: Throttling power loss/power out vs. duty ratio

4.2 Leakage Loss Results

Leakage losses directly reduce the output flow of the high speed valve causing a power loss. Leakage losses accounted for 34.4% or 354W of the total losses. The largest contributor to this loss was the circumferential leakage at 258 Watts. The radial leakage was the other 98 Watts worth of power loss. An optimization was also performed with the viscosity as a variable. In contrast to typical pump/motor and valve design, the system experienced optimum efficiency at high viscosities. For this reason, Mobil DTE28, a higher viscosity oil is used for the simulation.

As with throttling losses, the leakage losses also depend on the duty ratio. Figure 28 shows how the leakage losses vary over the range of duty ratios. The front side of the valve plate will always experience a constant leakage flow which determines the minimum leakage power loss. As the duty ratio is increased the rear side leakage paths of the valve plate begin to operate, causing a sharp increase in power loss. Increasing the duty ratio further maintains these leakage paths for longer periods of time, resulting in a steady increase of power loss. Increasing the duty ratio also causes the rear leakage path to effectively decrease in length. Eventually as the duty ratio is further increased, the symmetry of the valve causes the rear side leakage pathways to effectively extend in length, reducing the power loss.

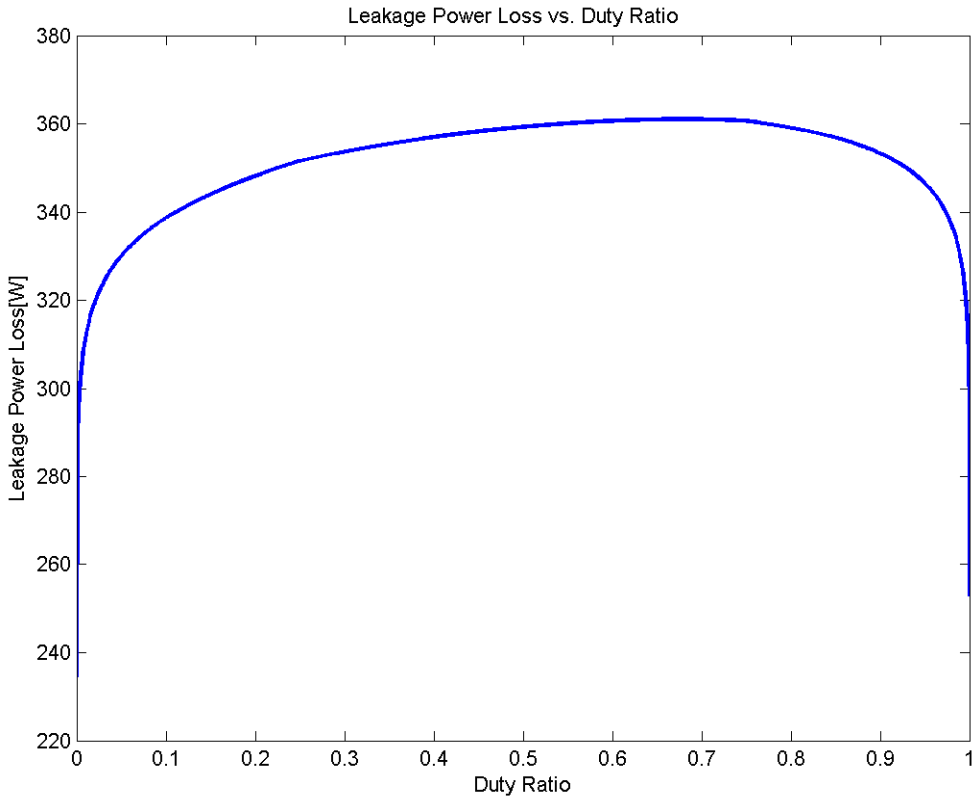

Figure 28: Leakage power losses vs. duty ratio

4.3 Compressibility Loss Results

The pressure fluctuations caused by the switching of the high speed valve within the inlet volume of the pump/motor leads to compressibility energy loss. The total inlet volume was estimated at 10.3cm^3, with 4.1cm^3 from the internal passages of the valve, 2.1cm^3 from the four-way directional control valve, and 4.1cm^3 from the hydraulic motor. In order to reduce the inlet volume, it is assumed that the high speed valve, check valves, and four-way directional valve are mounted in a manifold which is directly mounted to the hydraulic unit. This also eliminates any flexible hydraulic lines which are a major contributor to compressibility losses [31]

For the optimized model, compressibility losses accounted for 11.9% or 121 Watts, of the total power loss. This loss is heavily dependent upon the volume of fluid that experiences pressure fluctuations, the switching frequency, and the percent air entrainment as shown in Figure 29. Higher pressure values cause the effective bulk modulus to approach the bulk modulus of air free oil. Notice that at the optimized pressure of 16MPa the effective bulk modulus for oil with 2% entrained air will be 1/3rd that of oil without any air.

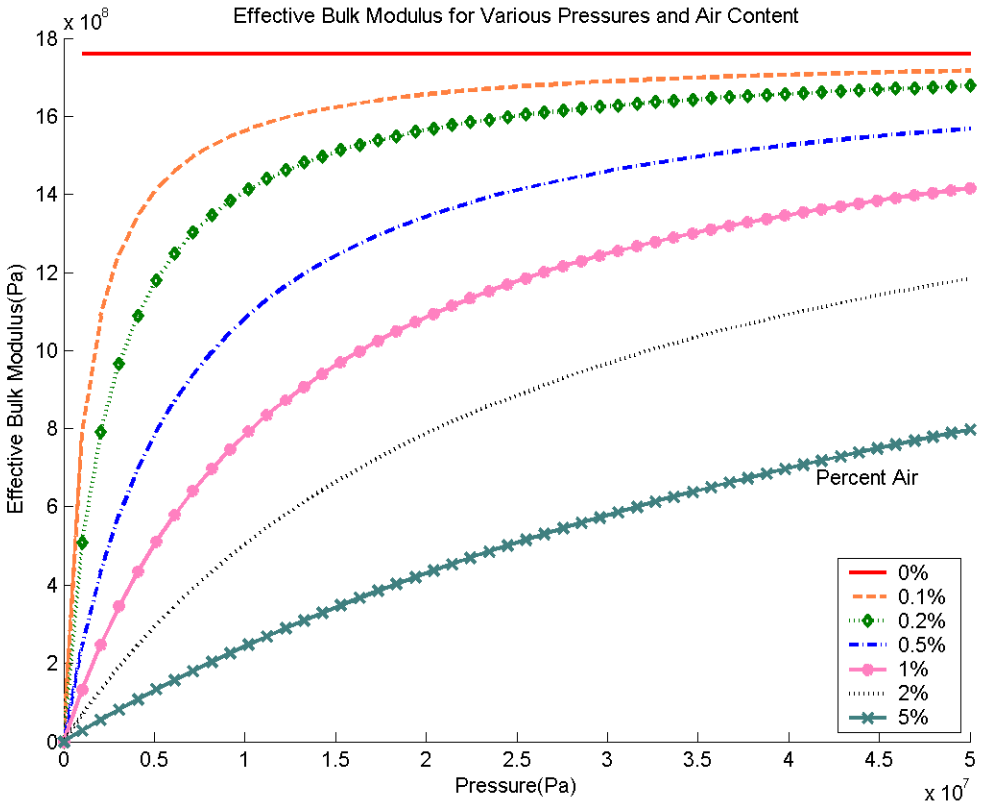

Figure 29: Effective bulk modulus for various pressures and air content

4.4 Viscous Friction Loss Results

The final form of energy loss is from the shearing of the fluid as the valve rotates. This power loss was 15.3% or 158 Watts of the total power loss of the valve. The viscous friction on face of the valve plate outside of the porting region contributed the most to this loss with 147 Watts. The next largest contributor was the viscous friction within the porting region at 9.5 Watts and finally the viscous friction losses of the bore were only 1 Watt.

4.5 Power Loss Summary

The contributions of each form of power loss are shown in Table 4. Remember that these results are for a 0.25 duty ratio and that the throttling and leakage losses are dependent upon the duty ratio. The total power loss as function of duty ratio is shown in Figure 30. The viscous and compressibility losses are independent of the duty ratio so the variability of the total power loss is due to the throttling and leakage power losses. The sharp increase in power loss at low duty ratios from these two cause almost a doubling of the total power loss. From about 0.1 to 0.95 duty ratio the power loss remains fairly constant. Finally, at very high duty ratios there is a final increase in total power loss due to the throttling losses.

Table 4: Power loss summary depicting each form of power loss

Power Loss Summary		
Throttling	38.7%	399 Watts
Leakage	34.4%	354 Watts
Compressibility	11.9%	121 Watts
Viscous	15.3%	158 Watts
Total		**1032 Watts**

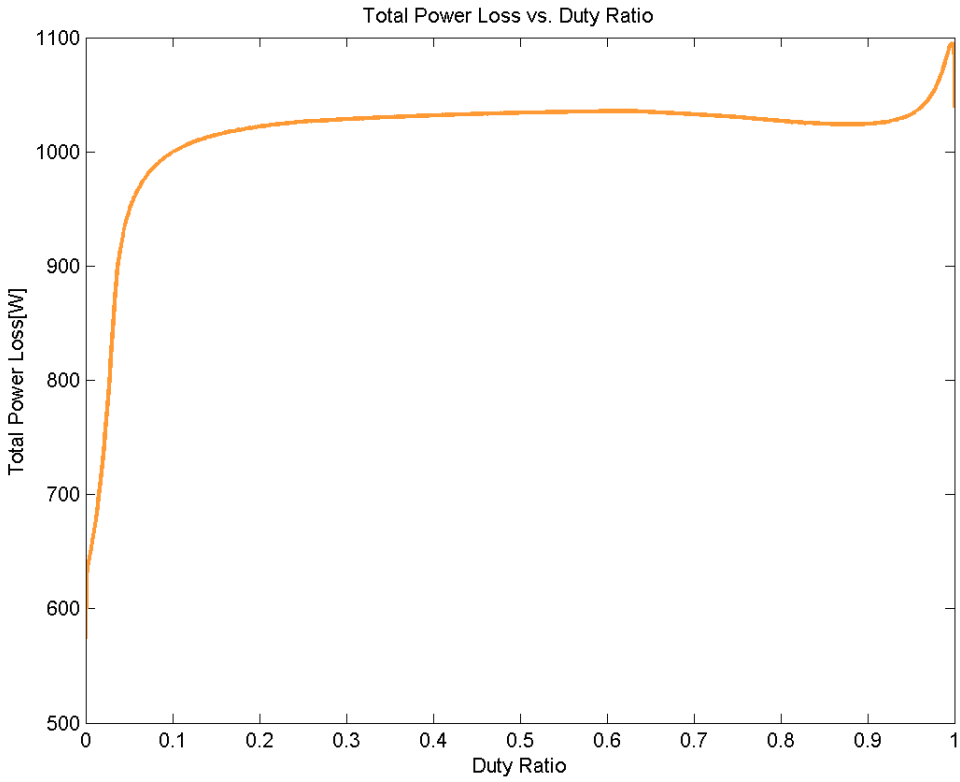

Figure 30: Total power loss vs. duty ratio

The high speed valve's efficiency for all duty ratios is shown in Figure 31. In order to detail the hydraulic performance of the high speed valve, the plot shows the efficiency with and without viscous friction losses. Viscous friction does not affect the hydraulic output power of the valve, i.e. the viscous losses are drawn from an external power source. Two points of interest can be seen. First, there is a dead band region until 0.08 duty ratio. At these small duty ratios, the throttling, leakage, and compressibility losses effectively drain all power from the output flow. It is desirable to reduce this dead band region as much as possible. Secondly, after 0.35 duty ratio the high speed valve is estimated to operate at over 75% efficiency, with a maximum efficiency near 90% at a duty ratio of one. This is comparable to the efficiency of a variable displacement pump/motor and better than a throttling valve, Figure 32.

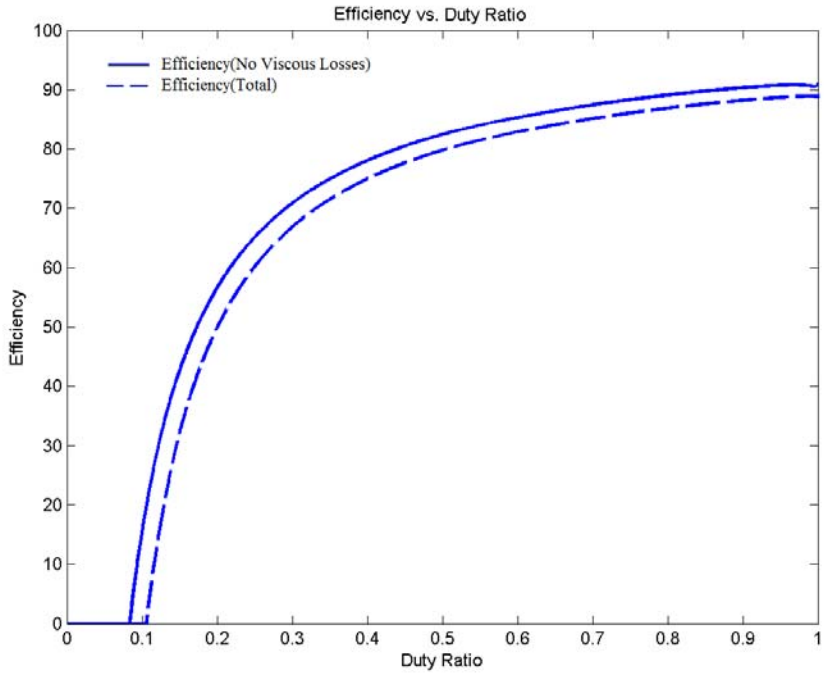

Figure 31: System efficiency vs. duty ratio

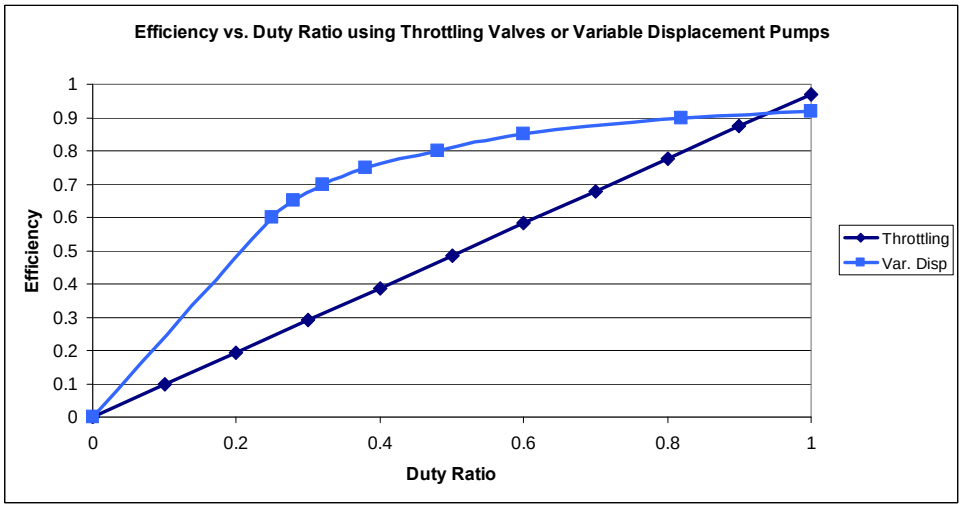

Figure 32: Efficiency vs. duty ratio for typical throttling valves or variable displacement pumps[32]

The above analysis has shown that an efficient 100Hz high speed hydraulic valve is possible. From the above optimization procedure some of the system parameter preferences were noticed. Firstly, though the leakage losses were not the largest form of loss in the system, it drove many of the optimization parameters to their upper or lower bounds. The front and rear face clearances were always driven to their lower bound to reduce leakage despite the fact that this would increase viscous friction. Also, the valve plate port angle δ was always driven to its upper bound to minimize the leakage pathway lengths despite the fact that this would increase throttling losses. Leakage is also the reason why the system prefers highly viscous hydraulic fluids.

Chapter 5: Prototype Design

The optimization procedure determined the sizes of all the key geometric features, however real world availability caused the optimized values to be recalculated. In particular, the hydraulic pump in the lab is only capable of 2gpm at 1000psi. This is a $1/5^{th}$ of the desired flow rate and ½ of the desired pressure. Also, Mobil DTE28 hydraulic oil was not readily available so Mobil 15M was used. This oil has a viscosity roughly a third of what was desired. Optimizing with these new properties changed the inner slot radius R_i and R_o to 4mm and 8mm, respectively. These changes had the following detrimental effect on the valve performance. As can be seen in Table 5 the new valve will perform worse overall, especially at lower duty ratios.

Table 5: Performance values for new optimized valve parameters

Duty Ratio	Efficiency
0.25	11.80%
0.50	55.30%
0.75	70.30%
1.00	79%

After the critical parameters of the high speed valve were optimized in Matlab, SolidWorks was used to model the physical valve. The CAD software was used to determine the relative size of the valve, how the valve would be actuated, how the valve would be assembled, and if any components would interfere with each other. When available, off the shelf parts were used in the valve to decrease manufacturing costs, though some components such as the Tier 1 and Tier 2 sub-valve needed to be custom made. Once a preliminary layout of the high speed valve was determined an in-depth design and analysis process followed. This included the selection of components such as thrust bearings and bushings for support, leakage control via O-rings and shaft seals, and hydraulic accessories such as connectors, hoses, and check valves. The valve also needed to be balanced, capable of withstanding high pressures, and have tolerable deflections. Finally, actuators and sensors needed to be properly sized and positioned.

5.1 Preliminary Prototype Designs

The original disc style design shown in Figure 33 kept all functional parts separate. The Tier 1, valve plate, and Tier 2 sub-valve are stacked together as shown in the drawing. The schematic shown in Figure 18 is hydrodynamically unbalanced because the high pressure port of the Tier 1 sub-valve does not have a high pressure counterpart on the other side. This will create a large moment on the valve plate and will cause other components to misalign. In order to maintain balance, the ports are replicated (N=2), such that the high pressure port has an opposing high pressure port. A collector plate is added to recombine the two flow paths created from the port replication. The collector plate also contains a check valve and a connection to tank. A reversing plate is added so the hydraulic actuator can change direction. The end caps and outer sleeve enclose the entire assembly and offer locations to attach hydraulic tubing.

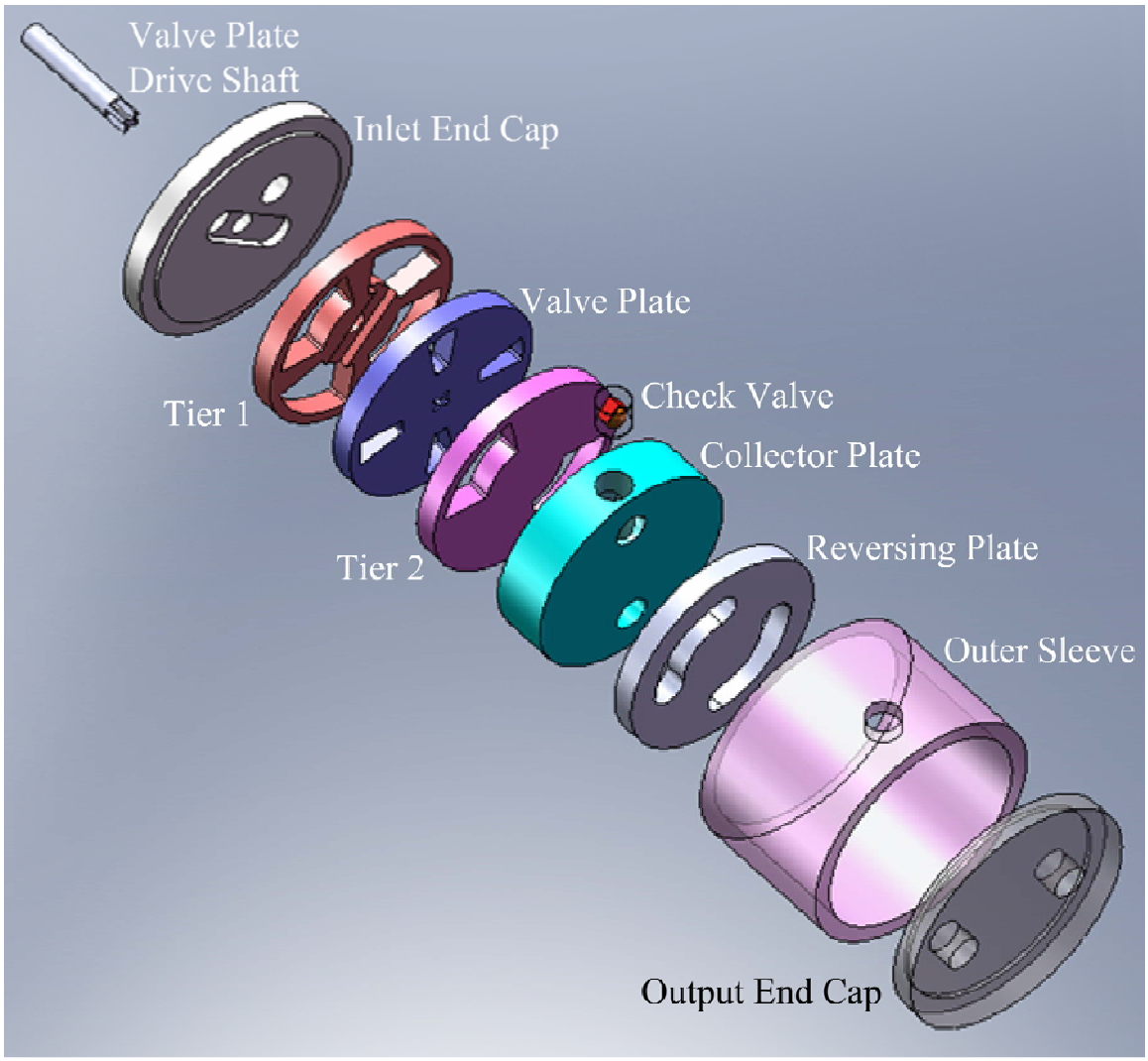

Figure 33: Disc style architecture version 1

In the next iteration of the design, shown in Figure 34, a few components have been merged together. The Tier 1 sub-valve has been merged with the end cap. In addition, hydrodynamic thrust bearings were experimented with during this period and were added around the outside of the switching area. Though not shown, the Tier 2 sub-valve would also have an integrated hydrodynamic thrust bearing. The collector plate and directional control plate have also been merged. At this point it was decided to power the valve plate and directional plate by the shafts shown. The Tier 2 sub-valve would be attached to the outer sleeve and then the sleeve could be rotated to change the phase angle.

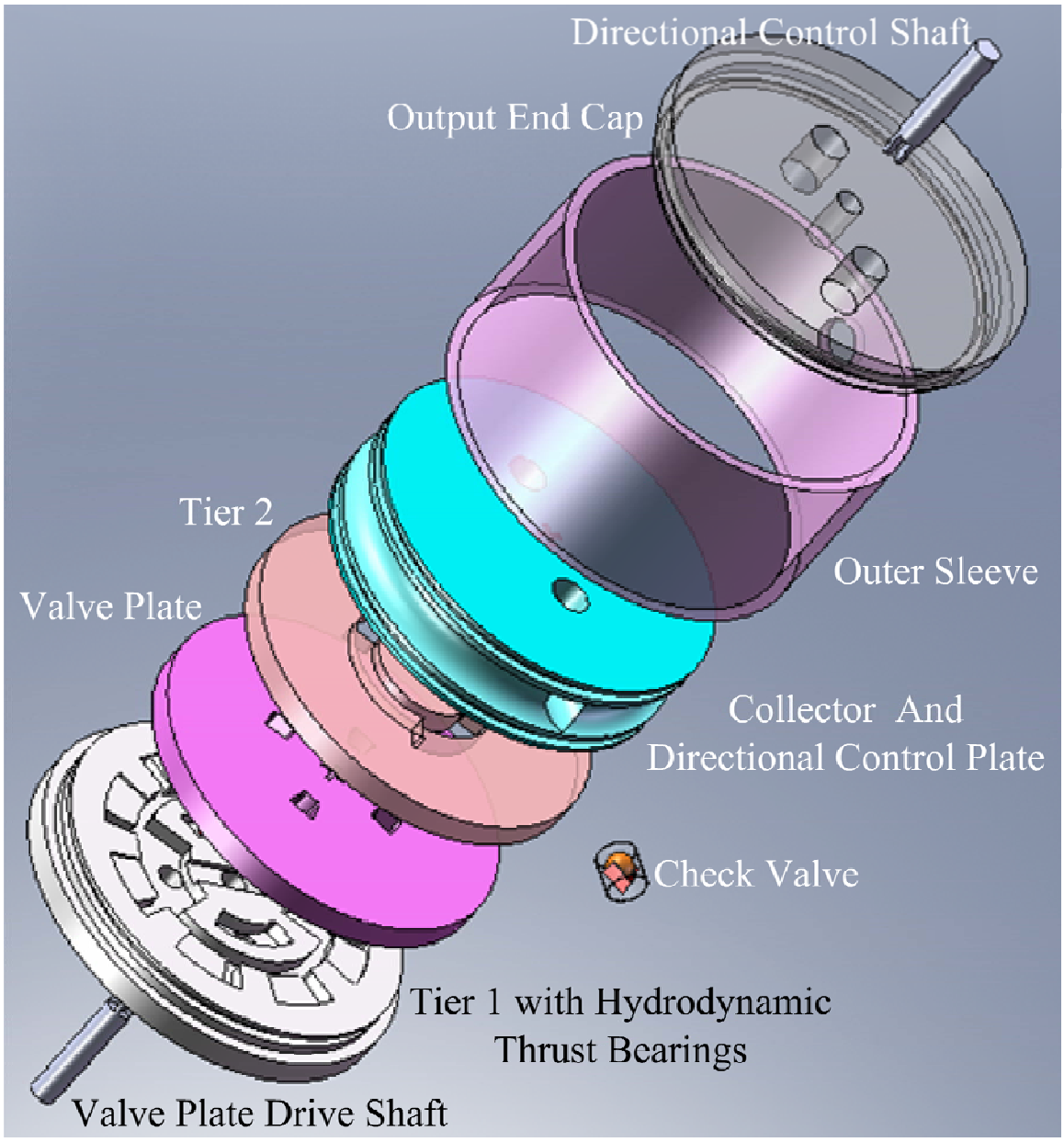

Figure 34: Disc style architecture version 2

In the last iteration of the disc style design before detailed analysis took place, it was decided to leave out the directional control plate in order to simplify the model. This allowed for the Tier 2 sub-valve, end cap, and outer sleeve to be merged into one piece. Tie rods, springs, and a thrust bearing are used to apply a clamping force to the valve and keep it together. This also allows the Tier 2 sub-valve to rotate within the assembly to control the duty ratio of the valve. This final merging of components created a very compact design.

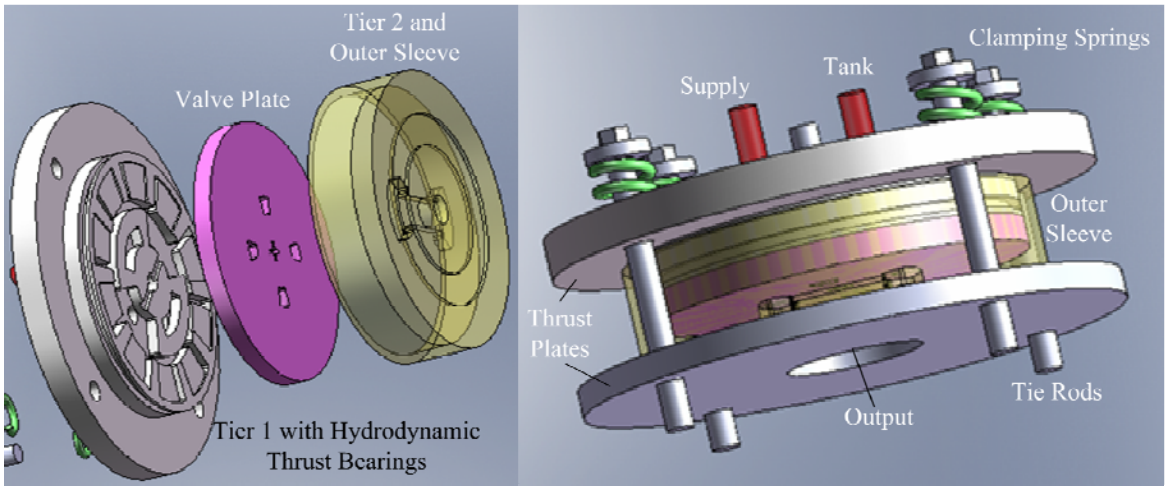

Figure 35: Disc style architecture, version 3

5.2 Detailed Design

Once the layout for the high speed valve assembly was determined, it was necessary to size the components and choose appropriate accessory parts. This includes choosing adequate motors and their connections, calculating minimum wall thickness to prevent bursting, sealing the valve, and determining the hydrodynamic forces acting on the valve so correct bearings could be chosen. The final prototype design is shown in Figure 36 with cut-away views showing the tank flow pathways in Figure 37 and the supply pressure pathways in Figure 38. Note that the cut-away views are perpendicular to each other.

One issue with the high speed valve that was never satisfactorily solved was how to effectively actuate the valve. For the original schematic shown in Figure 19 three actuators would be necessary: a continuously rotating motor to drive the valve plate, thus determining the frequency, an intermittent motor to change the phase of the Tier 1 sub-valve, changing the duty ratio, and another intermittent actuator to change the 4-way directional control valve. Because these three actuators are essentially rotary actuators, ideally they would be mounted concentrically with the axis of the valve to reduce side loads and accessory hardware.

Several novel methods have been proposed on how to actuate a rotary valve without mechanically connecting a drive shaft. These include turning the spool into the core of an electric motor [28] or adding small hydraulic turbines which use the flow through the valve to spin the valve[19]. While interesting, these methods are bulky or lead to large energy losses, so it was decided to mechanically connect the valve plate to an electric motor. The methods considered for doing this include:

1) Press fit the shaft into the valve plate.
2) Use a set screw or collar to attach the shaft to the valve plate.
3) Use a wobble connection like the ball end to an Allen wrench.

Because of the small thin size of the valve plate, it was difficult to find space for setscrews or a collar. A press fit would be simple, but it would also be difficult to align properly. A wobble connection would allow the valve plate to align itself, though it would require an additional custom component. For simplicity it was decided to use a press fit.

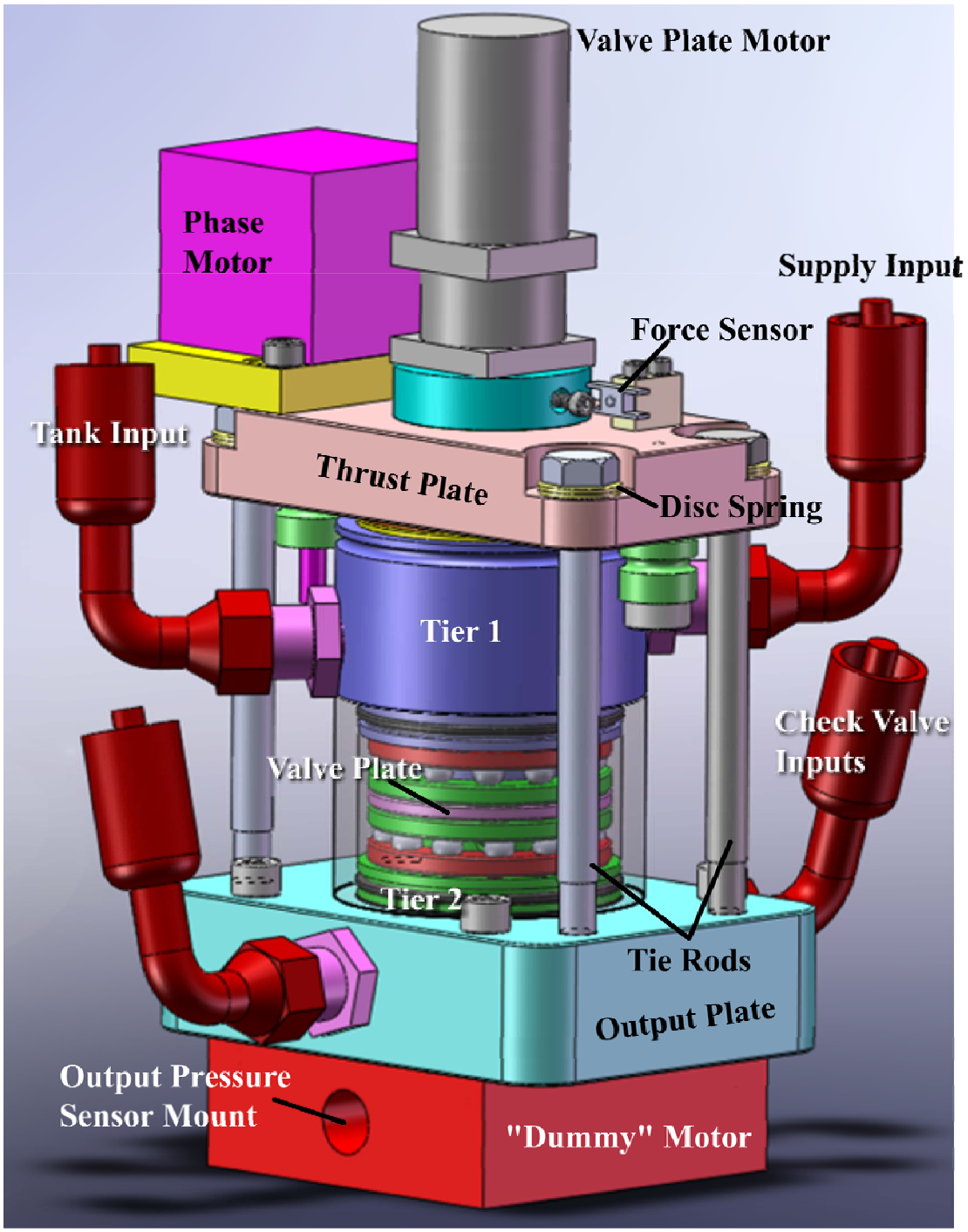

Figure 36: The final disc type model assembly

The high speed valve is bolted directly to the hydraulic motor, “dummy” motor in the figure, to reduce the inlet volume. To further reduce the inlet volume, the valve is mounted with it’s axis of rotation normal to the mounting surface of the hydraulic motor, as opposed to parallel to the mounting surface, which would require an additional cross port. This configuration leaves only one position for an actuator to be easily mounted concentrically with the axis of the valve. Because the valve plate motor is always on and because a slight misalignment could ruin the small clearances of the valve, it was decided to place the valve plate motor concentrically with the axis of the valve. The valve plate motor will need to overcome viscous friction torque and the friction torque of the thrust bearings. The MP-28005-385 Banebots motor met the torque requirement and is capable of running at the 1500rpm speed needed to generate a 100Hz pulse.

The phase control motor operates intermittently, but needs to have precise position control. This is a situation well suited for a servomotor or stepper motor. Since in this setup the larger Tier 1 sub-valve is what actually changes phase, a larger motor or a geared down motor would be necessary to provide the larger torque requirements to move this larger mass and overcome the friction of the large diameter O-ring. Also, the hydraulic hoses attached to the Tier 1 sub-valve increase the torque requirements. A stepper motor has continuous rotation and exact positioning. For these benefits and because one was available on hand, it was decided to use a stepper motor to control the duty ratio of the valve. The stepper motor used was a ROB-08420 from www.sparkfun.com. A limit switch or light sensor would need to be used to determine the zero phase angle of the high speed valve during startup.

It would be difficult to mount the phase control motor concentrically with the axis of the valve, so the motor is mounted off axis next to the valve plate motor. This can cause a problem because the belt drive of the off axis phase control motor will apply a radial force to the axis of the Tier 1 valve section, which is itself essentially floating. This force could compromise the small clearances of the valve and cause it to seize. Therefore an additional idler pulley is added to the other side of the valve so only a moment about the axis is experienced by the valve. Figure 39 shows a top section view of the phase control belt.

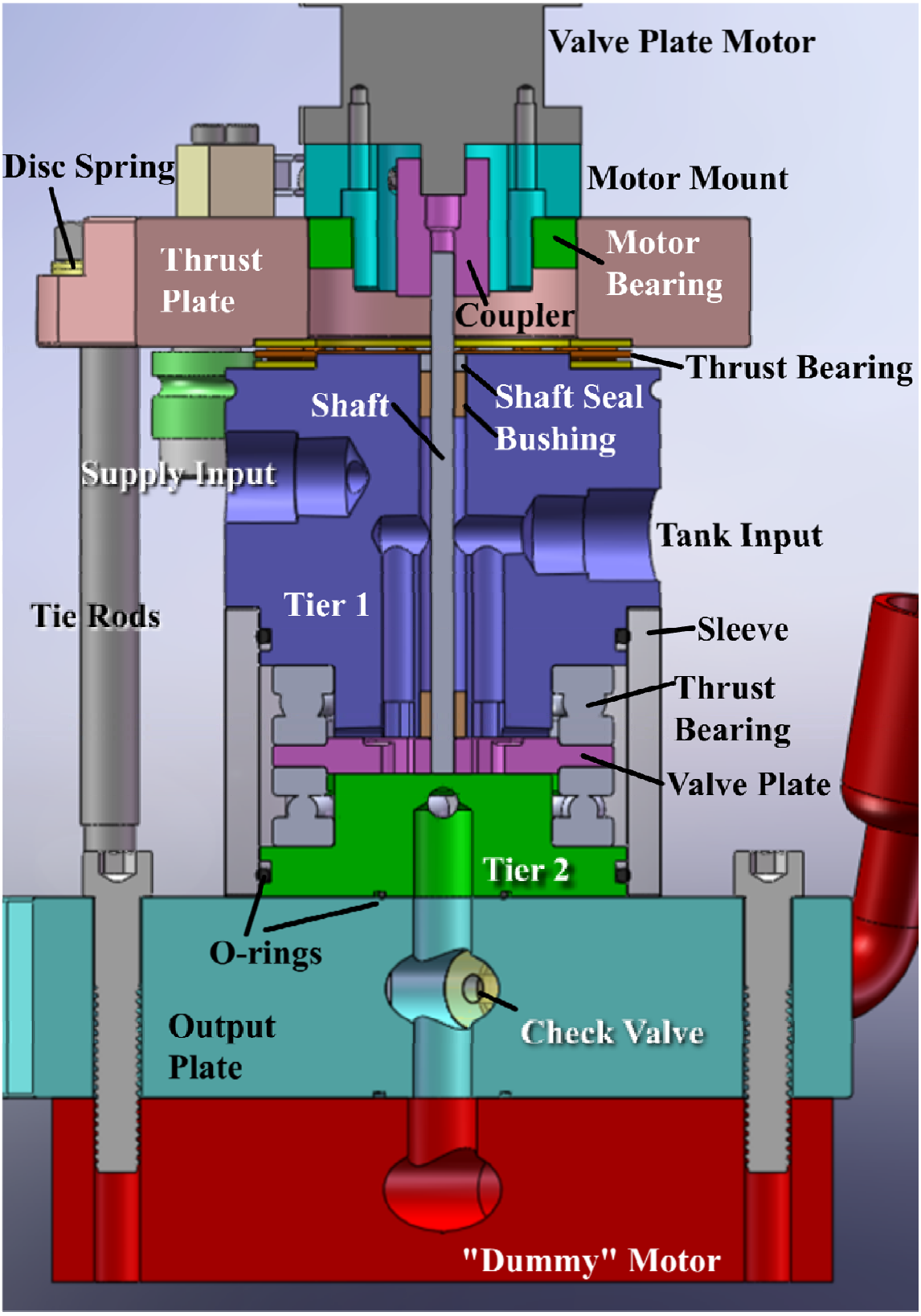

Figure 37: Section view detailing tank flow pathways.

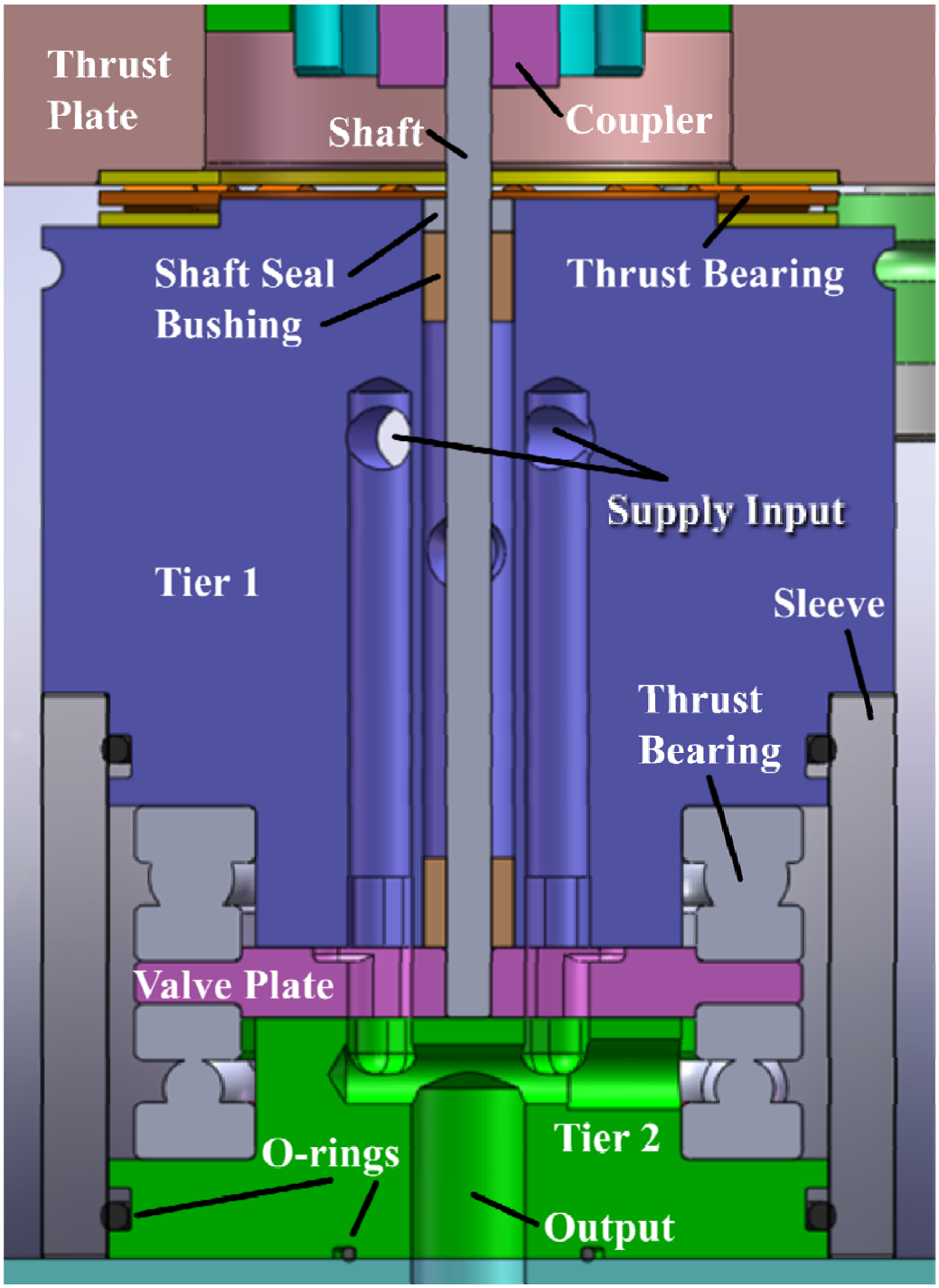

Figure 38: Section view of valve detailing supply pressure pathways. This figure is a perpendicular cut to Figure 37

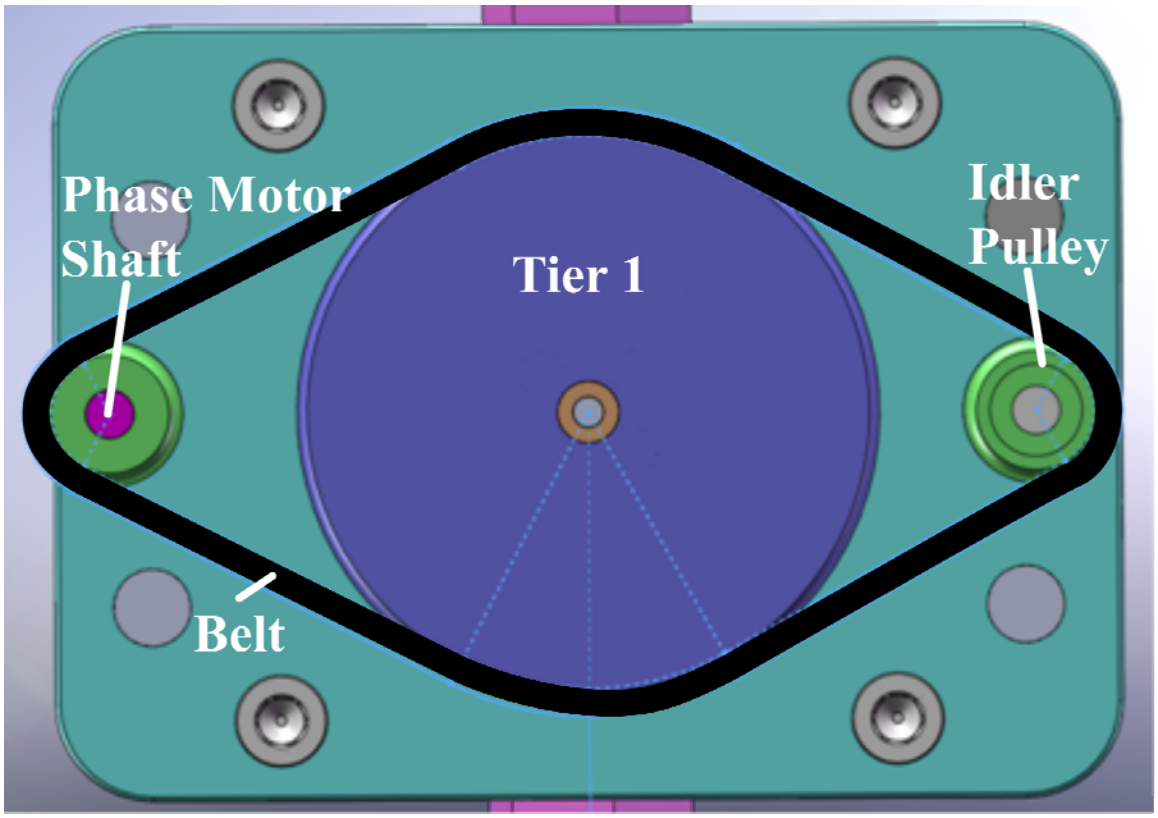

Figure 39: Phase control belt

Since the high speed valve will be operating under high pressures, large forces are generated. It is necessary to ensure that the internal ports of the valve have sufficient wall thickness to prevent bursting. Also, one downside of the disc-style architecture is that it needs to have end caps capable of holding the valve pieces together against these large forces, whereas a spool style valve is simply contained by a sleeve.

Several off the shelf parts were chosen for use with the valve. Since it was decided not to use hydrodynamic thrust bearings, the valve plate will be supported by mechanical ball bearing thrust bearings. In order to choose an appropriate thrust bearing the maximum load must be determined. Figure 40 shows the forces on the valve plate for one ½ cycle. Despite the small cross-sectional area of the valve plate, several hundred Newtons of force are developed by the fluid pressure. The free body diagram used to calculate the maximum forces on the thrust bearings is shown in Figure 41. Nachi offers bearings of the appropriate size which could handle these thrust loads. In order to maintain the proper clearance between the valve plate and the Tier 1 and Tier 2 sections, shims will be used under the thrust bearings to increase the clearance until the desired clearance is reached. Finally, conical disc springs rated at 1000N at full deflection are used on the tie rods, in a series configuration, to create the necessary clamping force to counteract the large fluid forces that are trying to force the valve apart.

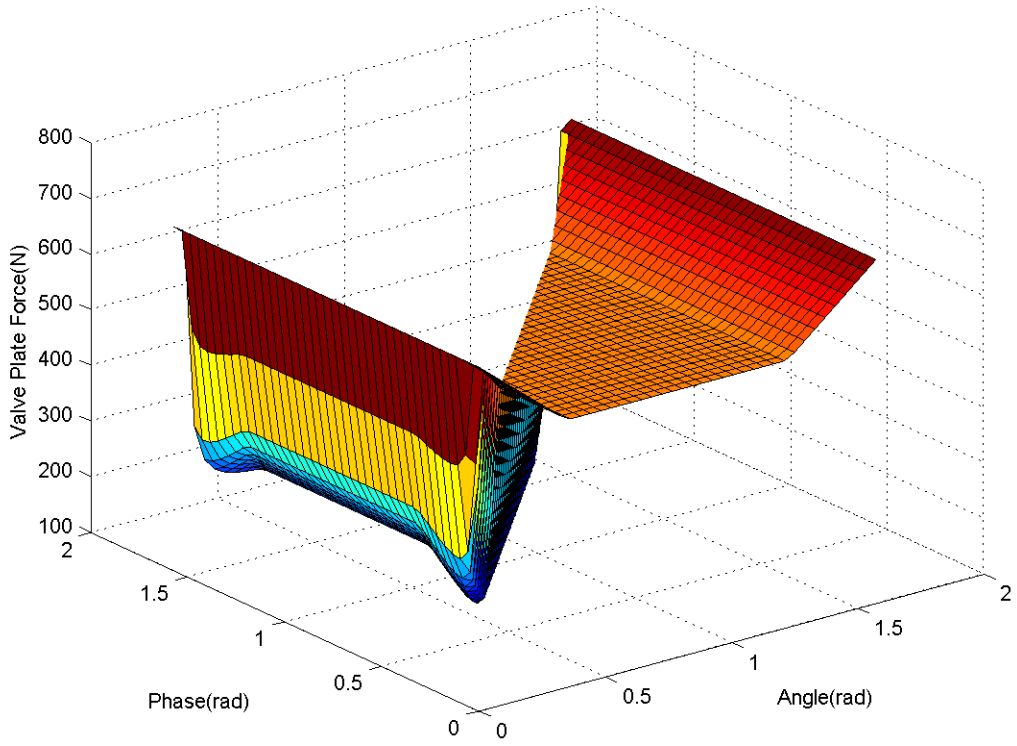

Figure 40: Forces on valve plate for various angles and phases for one half cycle

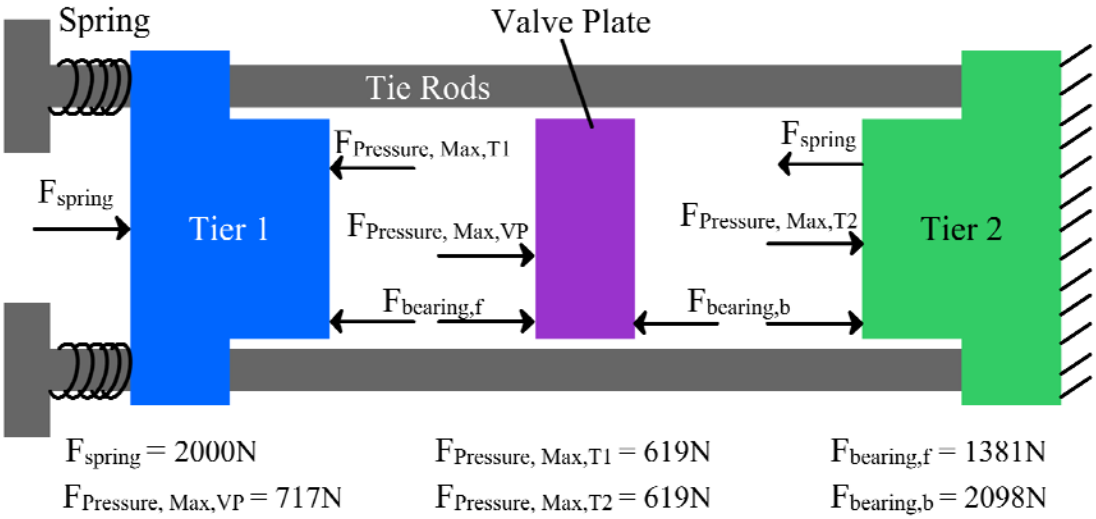

Figure 41: Free body diagram of valve components used to calculate thrust bearing loads. The valve experiences dynamic loads, but for this calculation only the maximum is needed.

These large fluid forces also require the use of balancing techniques to ensure smooth running and minimal vibration. For the high speed valve the ports were replicated so there are two complete cycles per revolution, N=2, for a total of 4 pulses/rev. Increasing the number of cycles per revolution has the benefit of increasing the switching frequency for the same angular velocity, but it also creates more leakage paths. For the small size of

the valve, increasing N above 2 had no benefit. Also, recalling Figure 40, it can be seen that the force on the valve plate is only in one direction. Originally, the force on the valve plate would change direction twice per cycle. This large and rapidly changing oscillatory force would quickly degrade the high speed valve and create excessive noise. In order to create a unidirectional force, pockets were added to the front face of the valve plate, shown in Figure 42. This generates a larger force on the thrust bearing, but only creates a unidirectional force on the valve plate.

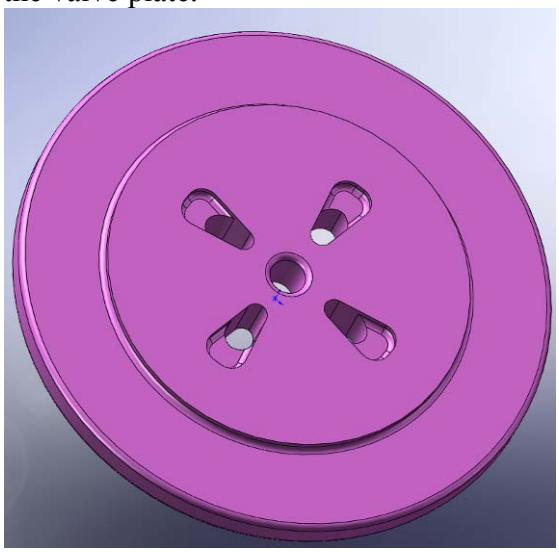

Figure 42: Valve plate showing hydrostatic balancing pockets around ports

In order to seal the valve, O-rings are used between adjoining surfaces that are exposed to the hydraulic fluid. Looking at Figure 38, O-rings are located between the Tier 2 sub-valve and the output plate, between the output plate and the motor housing, and between the outer sleeve and the two sub-valves. Also, a spring loaded shaft seal is used around the drive shaft of the valve plate to prevent leakage. Looking at Figure 37, notice that the valve plate drive shaft is connected to tank, so the shaft seal is not under high pressure.

In hydraulic systems it is necessary to have the proper hydraulic connections and seals to prevent leakage. The hydraulic workbench in the lab utilizes quick disconnect connections. In order to interface with the valve it was necessary to make adaptors to go from the quick disconnect to a ¼ NPT pipe fitting. From the pipe fitting the valve is connected to hydraulic lines via -06 JIC 37º flare fittings. The flare fittings are advantageous because they have a swivel end until tightened.

The other parts of the valve were custom made. Mark at L&M Machine was commissioned to manufacture the higher precision valve plate, Tier 1, and Tier 2 sections. The rest of the parts, including the top and bottom thrust plates, motor mounts, sensor mount, and outer sleeve were manually machined in Higgins shops. The part drawings for these components are shown in Appendix D: Drawings. Finally, the Bill of Materials and component costs are shown in Appendix C: Bill of Materials. The total cost for the project was $2,031.77.

Chapter 6: Experimental Setup

In this chapter the electrical circuitry and sensors used to collect data are detailed. Laboratory procedures governing how the valve is arranged, parameters to test for, and procedures on how to collect data are outlined. Lastly, experimental results are displayed and discussed.

6.1 Data Acquisition

Several sensors were used to measure important value parameters. A schematic of the location of each pressure sensor and orifices is shown in Figure 43.Note that unlike the model, the load for the experimental setup is controlled with a variable orifice. A SSI P51-1000-A-B-I36-4.5V-P pressure transducer was mounted to the output of the pump to measure the input pressure of the valve. This pressure sensor has a range of 0-1000psia with a <1ms response time. An OMEGA PX4201-3KGV pressure transducer was used on the output of the high speed valve. This transducer was used because of its fast 0.2ms response time. A necessity when one cycle of the valve is expected to only last 20milliseconds. This pressure sensor has a range of 0-3000psig. Another OMEGA pressure sensor is used in conjunction with an orifice on the input to estimate the input flow.

A Honeywell FS-1500 force sensor with a range of 0-1.5kg is used to measure the torque of the valve plate motor. The motor is mounted on a bearing and allowed to rotate. A screw protruding from the motor mount acts as a moment arm on the force sensor, allowing the input torque of the valve plate motor to be calculated. This can be seen in Figure 51. Finally, an infrared LED and an infrared phototransistor are mounted on the shaft of a hydraulic motor to measure the number of revolutions, and thus the flow rate. The hydraulic motor is a Danfoss OMM8 with a 8.2cm^3 displacement. This arrangement can be seen in Figure 52.

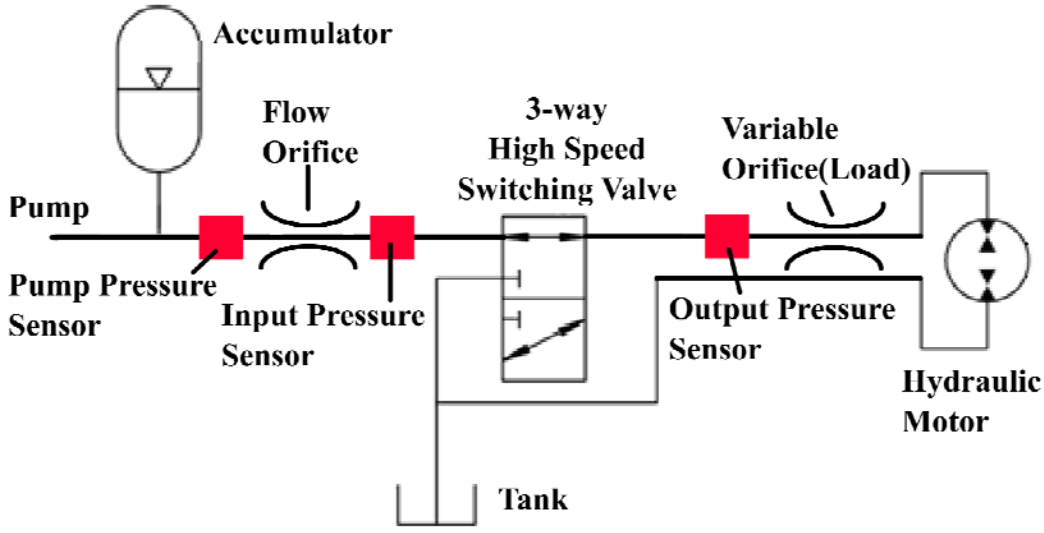

Figure 43: Schematic of experimental setup showing location of sensors, orifices, and other hydraulic components

The accompanying circuitry to control these sensors is shown in Figure 44 with the circuit diagram shown in Figure 45. At the top right are two instrumentation amplifiers, with circuit diagram in Figure 46, to boost the signal of the OMEGA pressure transducer and the force sensor from milliVolts to Volts. At the bottom right is a PWM signal generator which is used to control the Pololu 17Amp DC motor controller on the bottom left. This motor controller controls the speed of the valve plate. In the top left is an EasyDriver 3.1 stepper motor controller to control the stepper motor which controls the duty ratio.

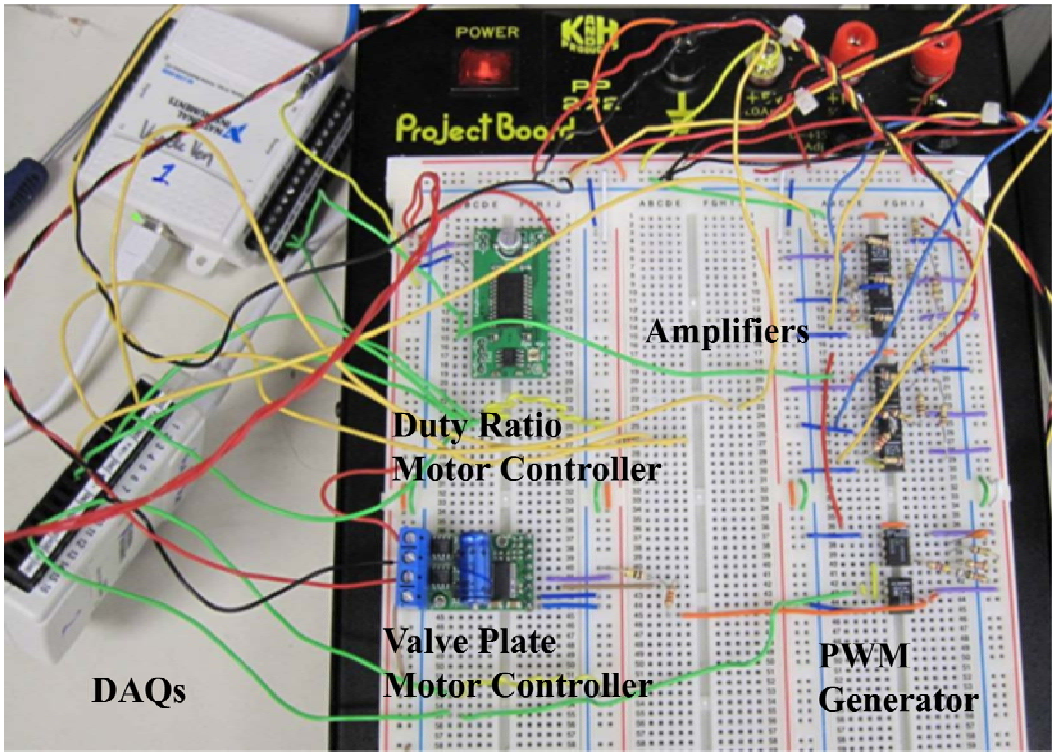

Figure 44: Sensor and motor circuitry

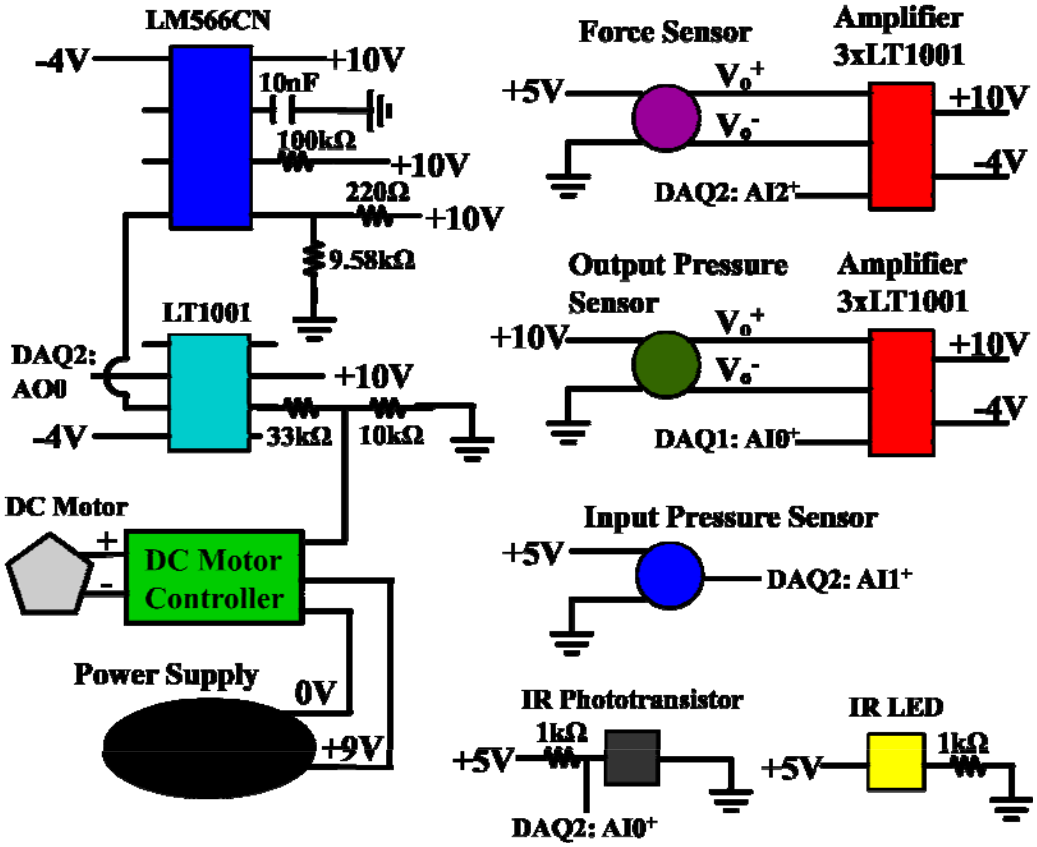

Figure 45: Circuit diagram showing sensor and motor wiring

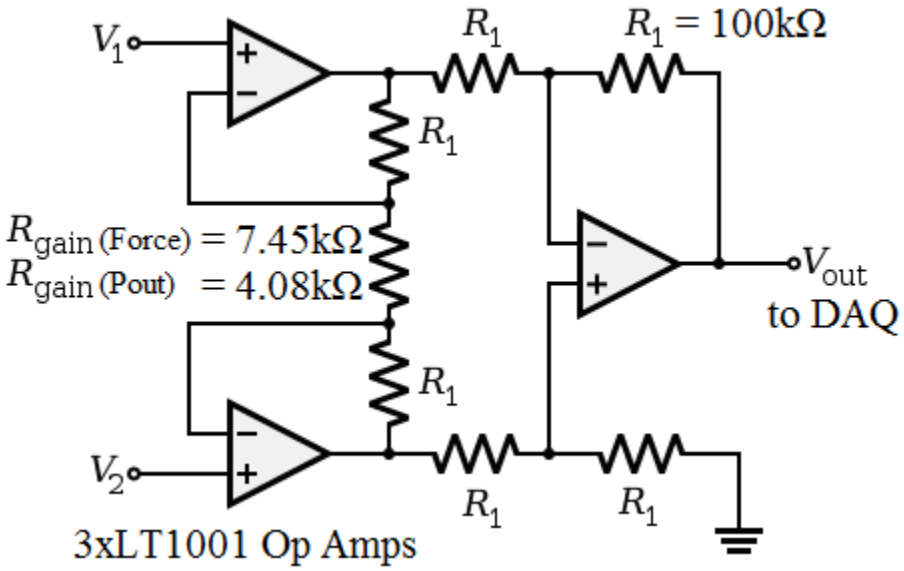

Figure 46: Amplifier circuit from Figure 45 , composed of 3 LT1001 Op Amps

LabView was used to record data from the sensors and control the valve. Two NI USB-6008 data acquisition boards were used as analog to digital converters. These boards have a maximum sampling rate of 10,000 samples per second. This is a total sampling rate, so two inputs could only be read at 5,000kS/s. For this reason, one DAQ was solely used to

record the high speed output pressure ripple at 10kS/s. The second DAQ board was used to record the pump pressure, the force sensor, and the motor encoder signals at 3.33kS/s. This DAQ also output the voltage reference which controlled the valve plate motor speed. The LabView front panel and block diagram used to record the sensor measurements are shown in Figure 47 and Figure 48. This setup was simple and effective.

Two notes on signal noise. First, the motor control circuits need to be isolated from the other circuitry. High levels of electrical noise were added to the signal even if only the motor ground was connected to the circuitry ground. Secondly, the DAQs were connected by USB to a Dell XPS M1530 laptop computer running Windows Vista. Surprisingly, large levels of noise were generated when the laptop's power cord was plugged in. With the amplification from the instrumentation amplifiers, this noise could be over +/- 1V. To alleviate this problem all data was recorded with the laptop running off of battery power.

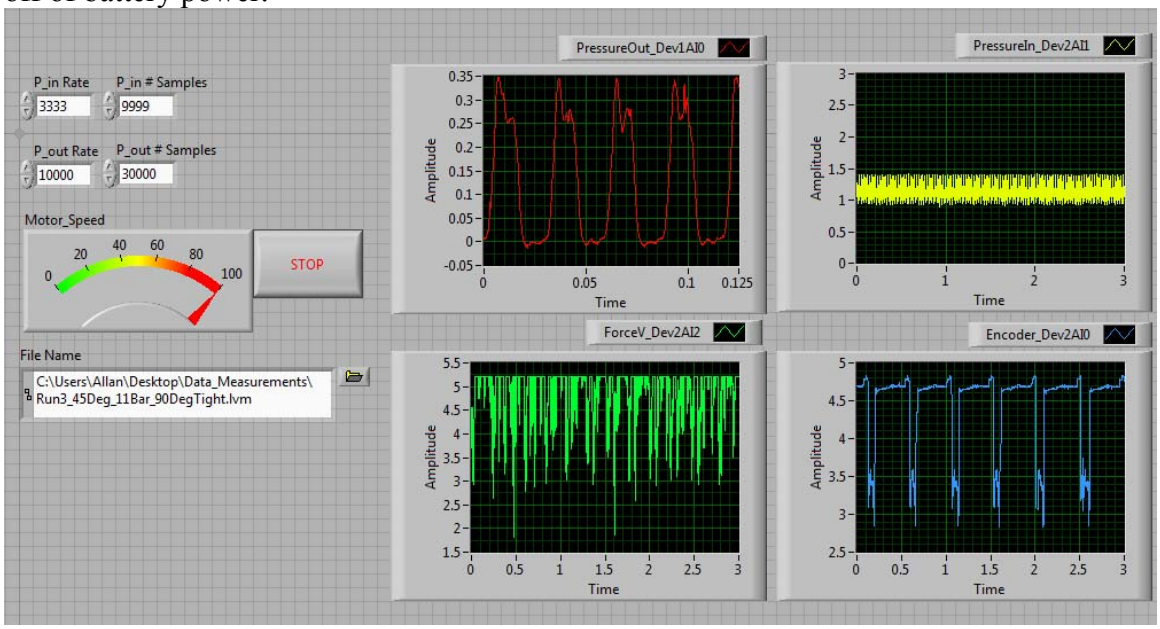

Figure 47: LabView front panel for recording data measurements

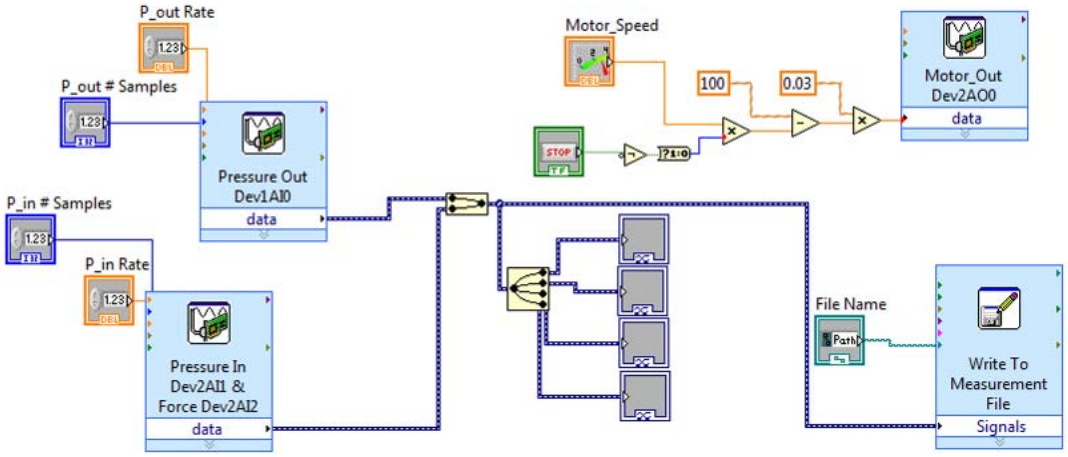

Figure 48: LabView block diagram for recording data measurements

6.2 Laboratory Procedures

Before testing can begin, the high speed valve must be assembled into what will be known as the standard configuration. To do this:

1. Assemble the Tier 1 sub-valve, thrust bearing and valve plate.
2. Wrap half of this assembly in cloth and place in the vise. Using a micrometer measure the axial distance across the assembly in 4 different spots. This is the zero clearance distance.
3. Place a 0.001inch shim between the thrust bearing and the Tier 1 sub-valve and repeat the above process until the axial distance changes. The difference between the zero clearance distance and the new distance is the clearance. Add or subtract shims until 0.001inch clearance is reached.
4. Repeat this process with the valve plate, thrust bearing, and Tier 2 sub-valve.
5. Attach O-rings, thrust bearings, and shaft seals
6. Place the disc springs, two in series, over each tie rod.
7. Tighten down tie rods by first hand tightening the nuts and then applying a 70° turn. This will apply a net 2000N clamping force to the valve.
8. Attach supply and tank hoses to the Tier 1 section.
9. Verify that the tank-side check valve is in the proper direction.
10. Attach tank-line to check valve port.
11. Connect sensors: pressure sensors, motor encoder, thermocouple, force transducer and motors to valve, DAQ, and power supply.
12. Close and anchor blast shield.
13. Turn valve to full open position. At low pressure, turn on pressure and motors. Bleed air from the system and verify sensor functionality.
14. Check for leaks or excessive vibration. Slowly increase pressure and continue bleeding air from system.

The system is now in the standard configuration with a clearance of 0.001inch between the valve plate and the Tier 1 & 2 sections, a clamping force of 2000N, valve plate speed of 1500rpm, input pressure of 1,000psi, output flow of 2gpm, tank-side check valve inserted, fully open(90 degree phase), and constant temperature of ~40C.

In order to determine how well the high speed valve operates, several test runs needed to be performed. These tests runs were used to verify that the duty ratio is variable, how the torque on the valve plate varies with speed, how the efficiency varies with the clearance between the valve plate and the Tier 1 & 2 sections, and if the tank-side check valve is necessary.

Flow and Pressure vs. Phase and Duty Ratio Test Run

This test run is to determine how the output pressure and flow of the high speed valve vary with the duty ratio. The duty ratio is controlled by the phase angle, α, of the Tier 1 sub-valve. The valve is marked from 0º to 90º in 15º increments, where 0º is zero duty ratio and 90º is 1.0 duty ratio.

- Setup the valve into the standard configuration.
- Record data from sensors for 5 seconds.

- Turn off the valve plate motor and pump.
- Decrement the phase angle by 15 degrees.
- Turn on the valve plate motor and pump
- Record the next set of data.
- Repeat until the 0 duty ratio set is recorded.
- Calculate the output power of the valve.

Torque vs. Angular Velocity Test Run
This test run is to determine how the torque on the valve plate varies with the angular velocity of the valve plate. This will allow the viscous friction torque to be calculated.

- Setup the valve into the standard configuration.
- Set the valve speed to 100% of full speed. Take sensor data for 10 seconds.
- Decrement the valve speed to 90% full speed and record the sensor data.
- Repeat in Decrements of 10% full speed until 10% full motor speed is reached.
- Calculate the Torque vs. Speed and compare to theoretical results.

Check Valve Necessity Test Run
This test is to determine what effect the check valve has on the system. The purpose of the tank-side check valve is to prevent cavitation caused by the motor. It is desired to know if the check valve is necessary, if it works as expected, and if the switching frequency is too high for the check valve to operate effectively.

- Remove the tank-side check valve and insert a plug.
- Setup the valve into the standard configuration.
- Repeat the “Flow vs. Phase” procedure.
- Compare results to those measured with a check valve.

Clearance Variation Test Run
The purpose of the clearance test runs are to determine what affect the clearance between the valve plate and the Tier 1 & 2 sub-valves have on the system. It is expected that with decreasing clearance the required torque will increase due to viscous friction and that leakage losses will decrease causing a greater output flow.

- Change the clearance of the valve to 0.0005 inch and check for any damage or wear.
- Repeat all of the above procedures.
- Change the clearance of the valve to 0.0015 inch.
- Repeat all of the above procedures.
- Calculate measured torques and flow rates

6.3 Experimental Results

Figure 49 to Figure 53 show the laboratory setup and close ups of the various sensors. In Figure 49 the entire laboratory setup is shown, including the high speed valve, hydraulic pump, circuitry board, power supply, DAQs, and the data recording laptop. Figure 50

shows the high speed valve fully assembled except for the phase control stepper motor. Ultimately the phase was manually changed due to large torques and software difficulties. Notice the location of the output pressure sensor. Figure 51 is a close up of the top of the high speed valve. The force sensor which measures torque and the valve plate motor are shown. Figure 52 show a close up of the hydraulic unit with attached IR emitters and sensors. These are used to measure the valve's output flow by counting the revolutions of the hydraulic motor and making use of knowledge of the motor's displacement which is 8.2cm^3. Figure 53 shows the markings for the different phase angles of the Tier 1 sub-valve. These phase angles determine the duty ratio of the valve.

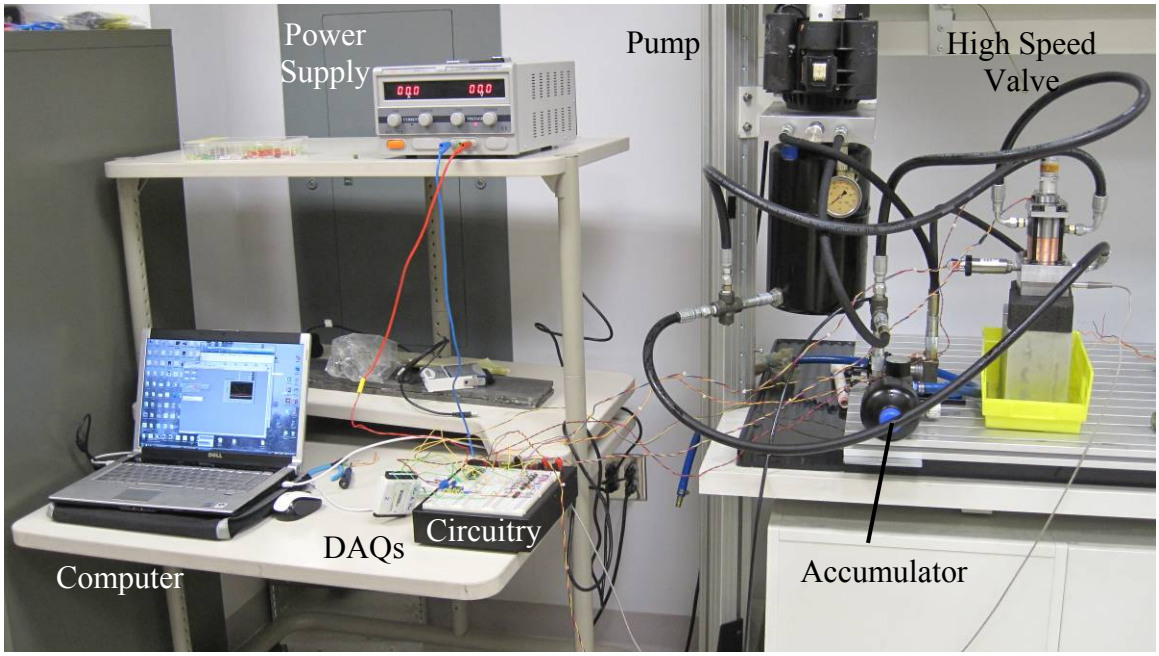

Figure 49: Laboratory setup

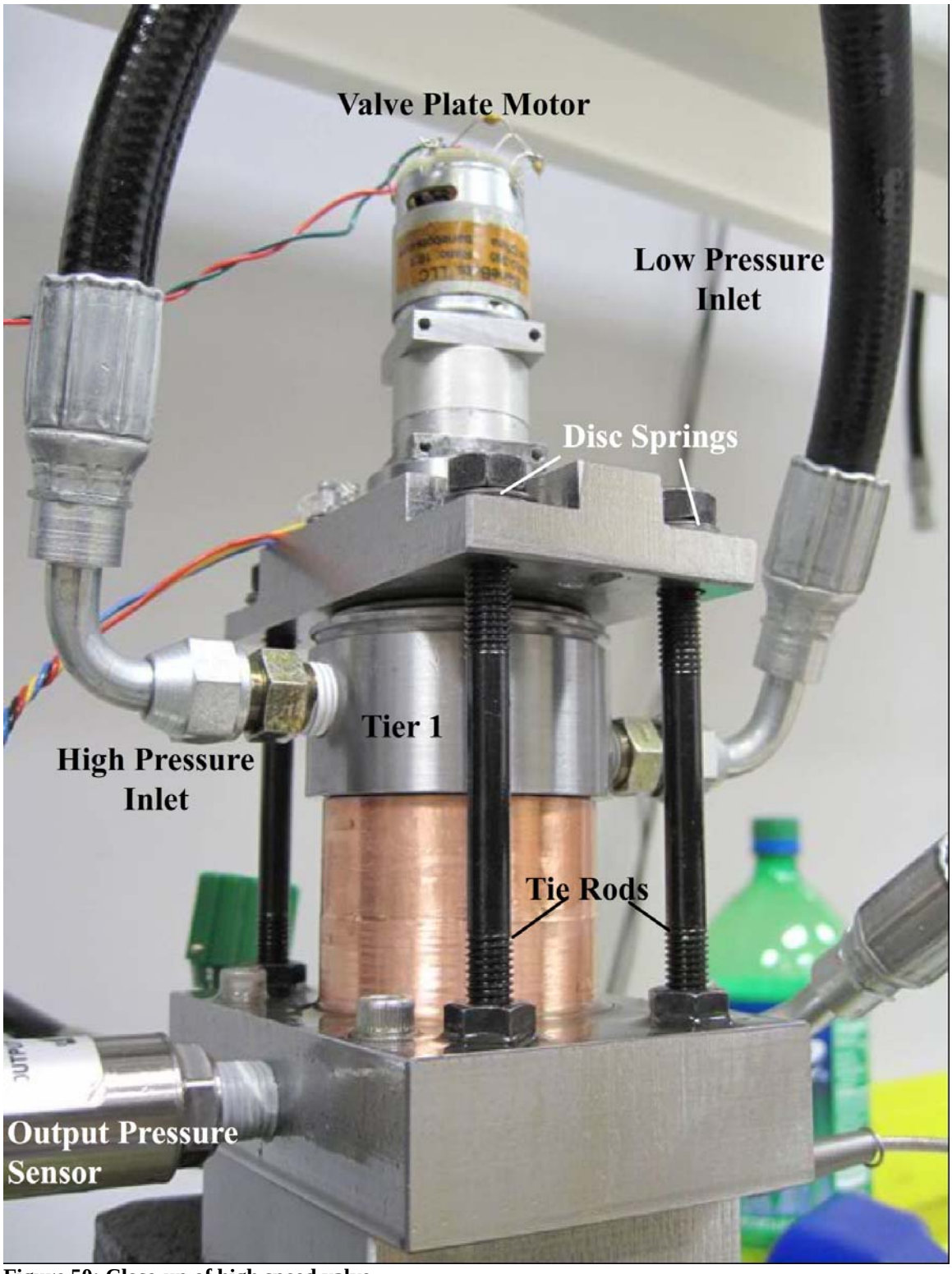

Figure 50: Close-up of high speed valve

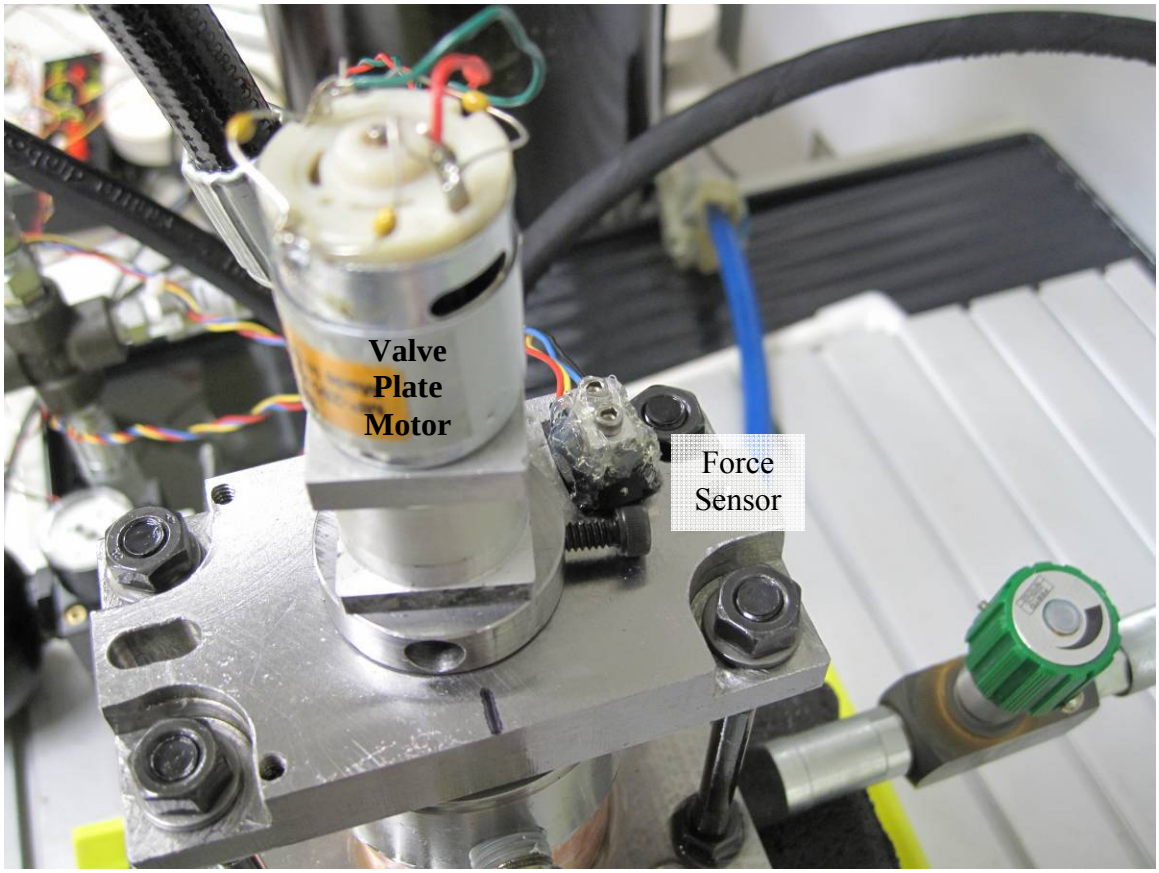

Figure 51: Close up showing force sensor and valve plate motor

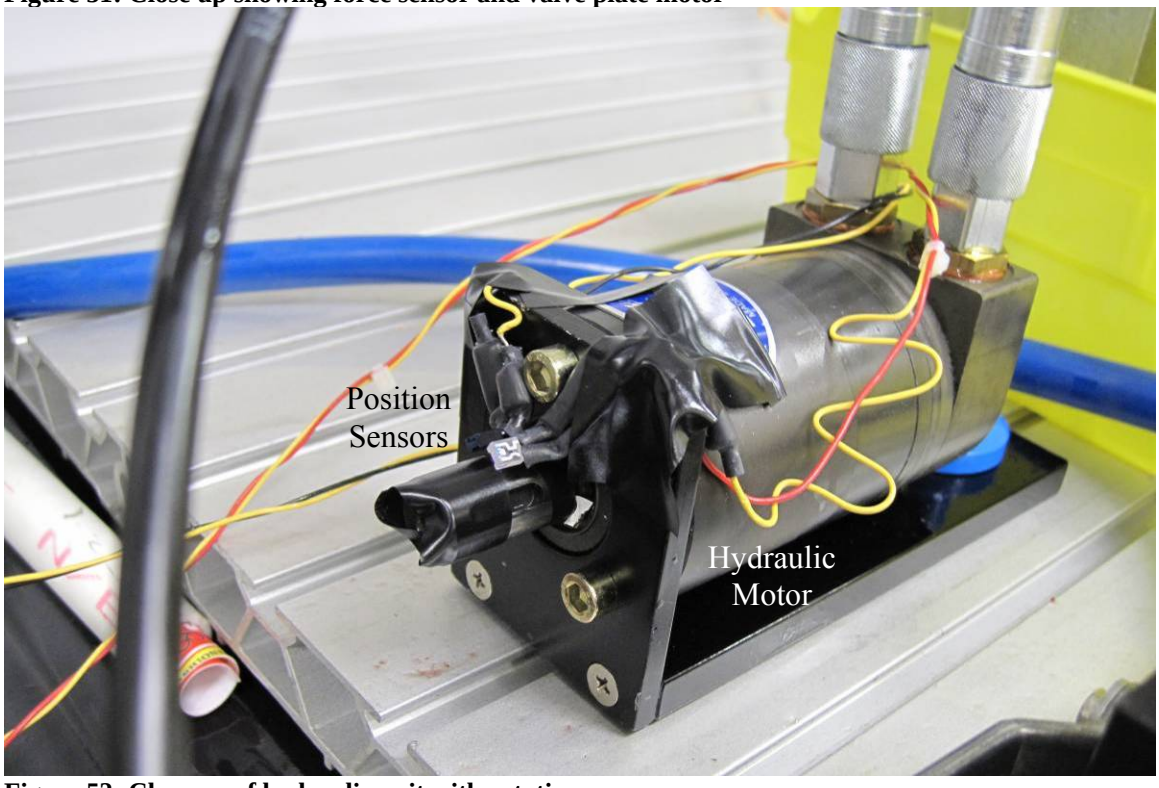

Figure 52: Close up of hydraulic unit with rotation sensors

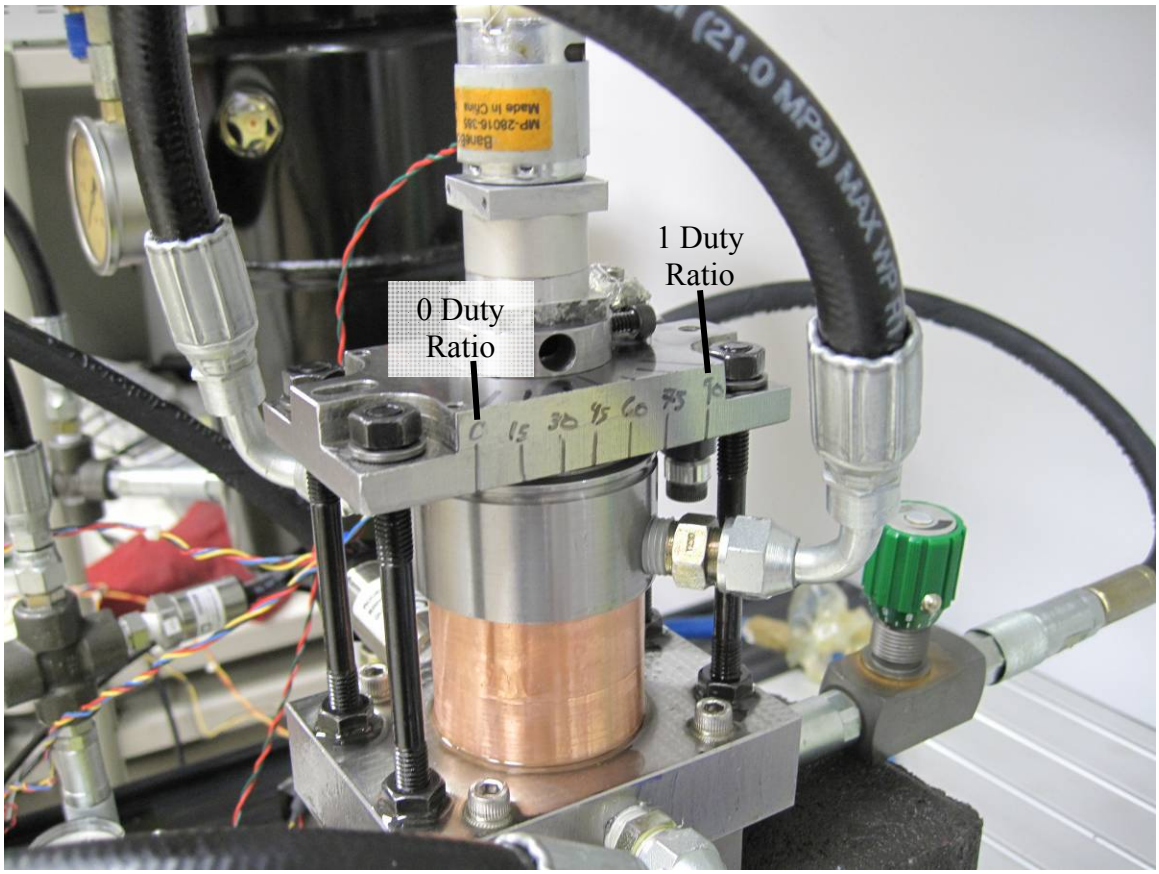

Figure 53: Close up of valve with phase angle marked. At 0° phase the duty ratio is zero. At 90° phase, as shown, the duty ratio is 1.

Figure 54 & Figure 55 show the output pressure of the high speed valve for various duty ratios. These plots were generated with 0.0015inch clearance, 2000N clamping force, a moment arm of 1.17 inch, and with the tank side check valve in place. Notice that the pulse width of the pressure pulse increases with increased duty ratio. A compilation of these results for this test run is shown in Figure 56. The data is scaled as follows to highlight trends rather than absolute magnitudes. The output pressure is divided by the input pressure which ideally would match the duty ratio. The torque on the valve plate is scaled to the maximum torque. The output flow and the angular velocity of the valve plate are scaled to their respective values at 1.0 duty ratio.

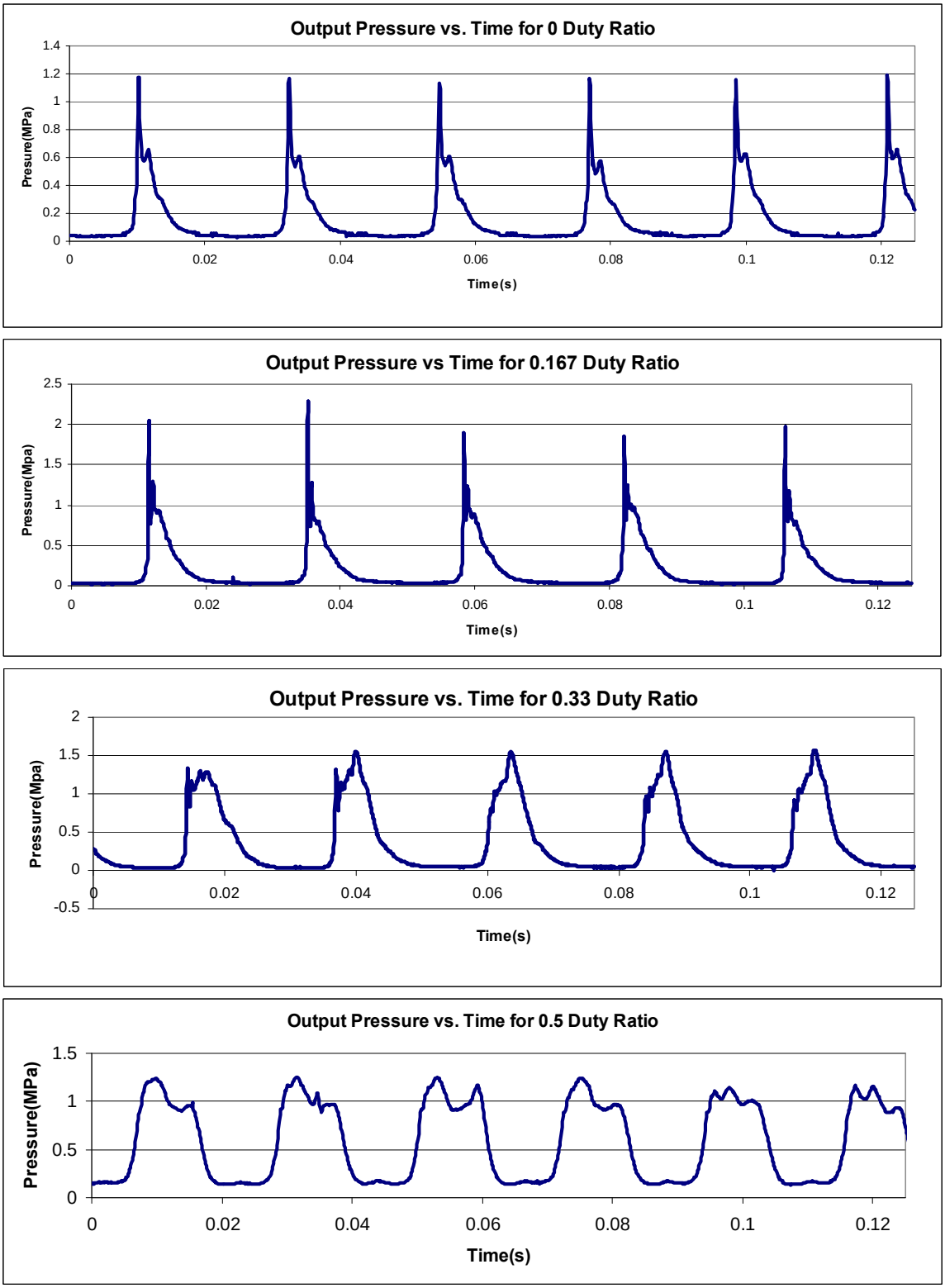

Figure 54: Output pressure for selected duty ratios, 0.0015inch clearance, 2000N clamping force, and tank-side check valve installed.

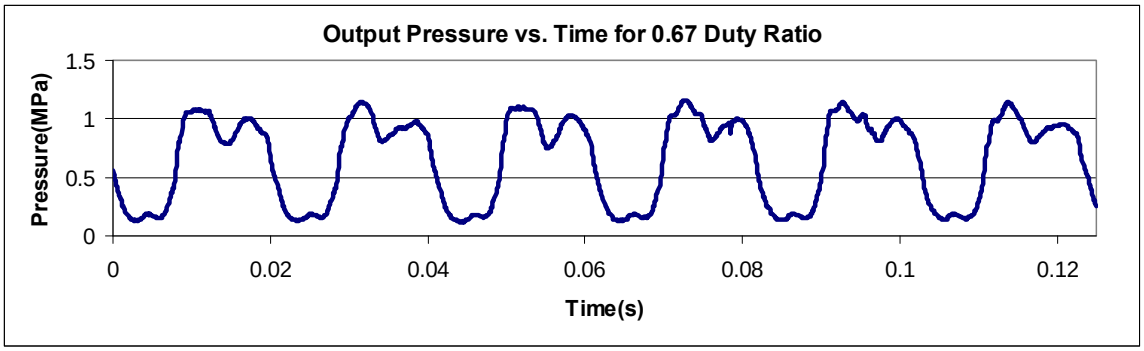

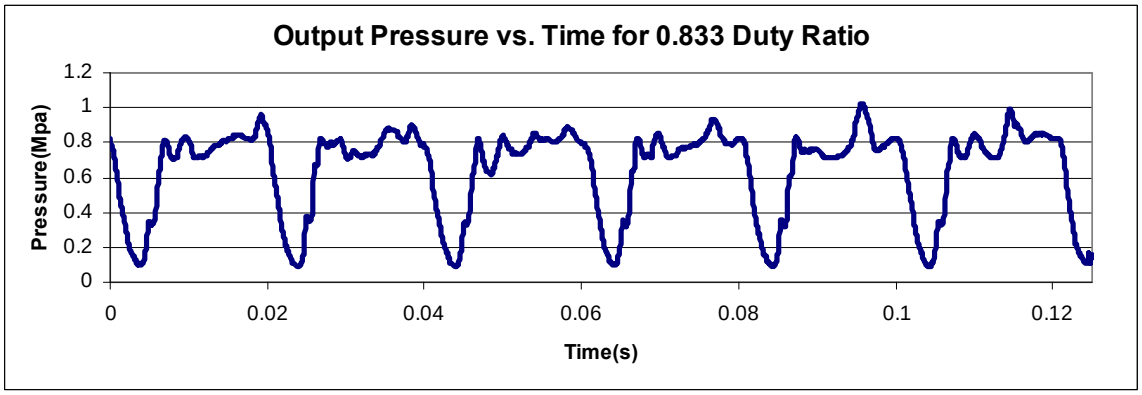

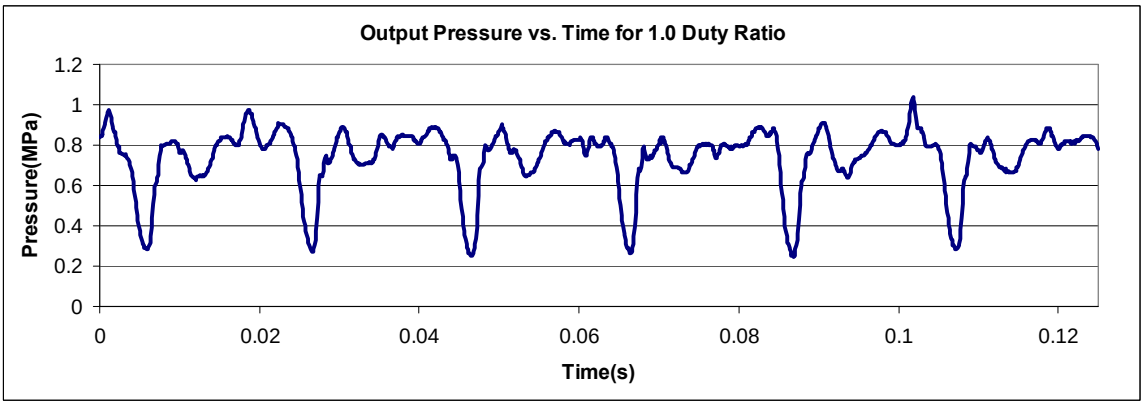

Figure 55: Output pressure for selected duty ratios, 0.0015inch clearance, 2000N clamping force, and tank-side check valve, continued.

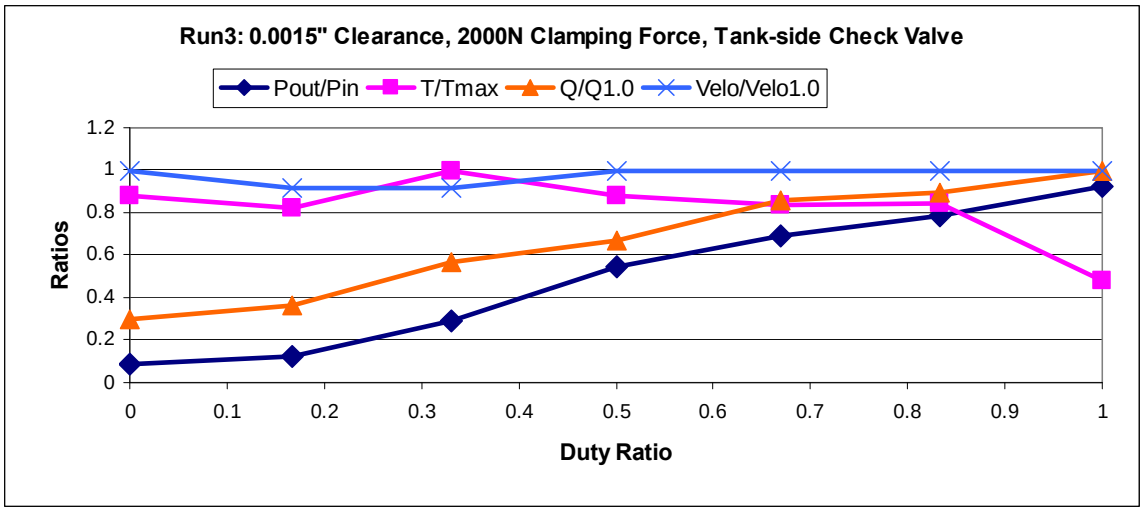

Figure 56: Compilation of results for 0.0015inch clearance, 2000N clamping force, and tank-side check valve

The measured efficiency (total and hydraulic only) vs. duty ratio for selected clearances is shown in Figure 57. Notice that the clearance had little effect on the efficiency, but viscous and rolling friction accounted for roughly half of the power loss.

Figure 58 is a compilation of results showing scaled pressure, flow, torque, and angular velocity of the valve plate for various speed settings. First, notice that the valve plate reaches a maximum velocity for the 60% speed setting and greater. Also, the output flow and pressure vary little with a change in angular velocity, but the torque varies greatly. At low speeds the measured torque is beyond the range of the sensor which is over double the torque at higher speeds.

Figure 59 shows how the torque on the valve plate varies with clearance. The torques at lower angular velocities are omitted because they were outside the range of the sensor. Notice that the torque increases as the clearance decreases. Figure 60 shows the maximum switching frequency that was achieved with the high speed valve. This frequency is calculated by counting the number of pressure pulses per second. Figure 61 shows the output pressure of the high speed valve when there is no tank-side check valve for 0.5 duty ratio, with 0.0015inch clearance, and 2000N clamping force. Additional results can be seen in Appendix B: More Experimental Results.

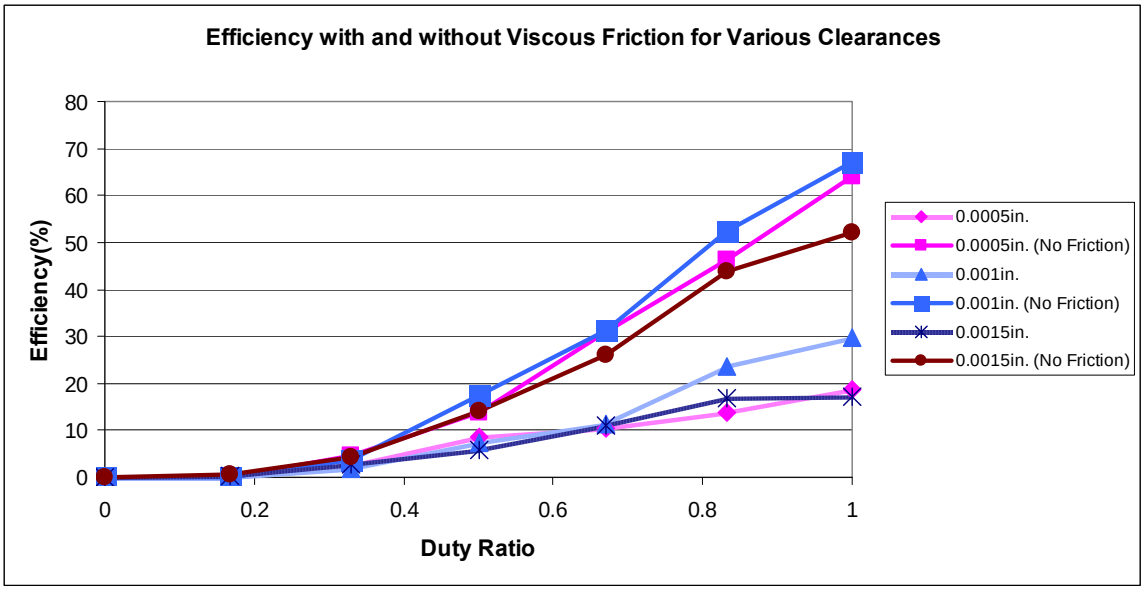

Figure 57: Measured efficiency vs. duty ratio for various clearances

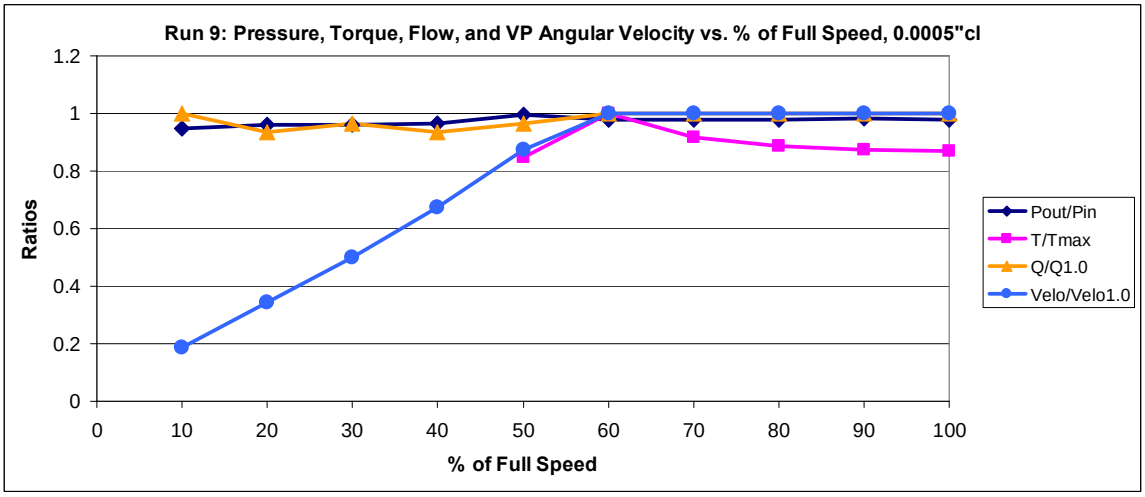

Figure 58: Scaled pressure, flow, torque, and angular velocity for 0.0005inch clearance, 1.0 duty ratio, no tank-side check valve.

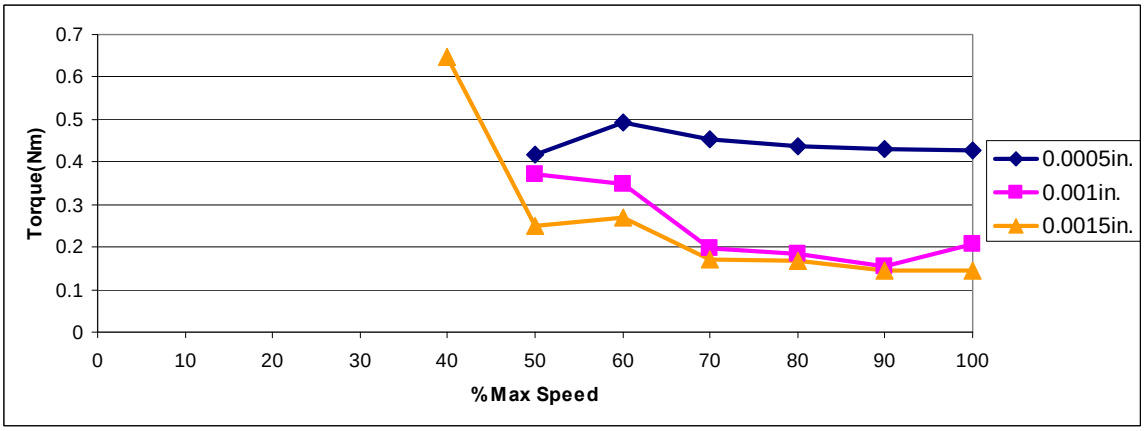

Figure 59: Torque vs. angular velocity for various clearances, no tank-side check valve

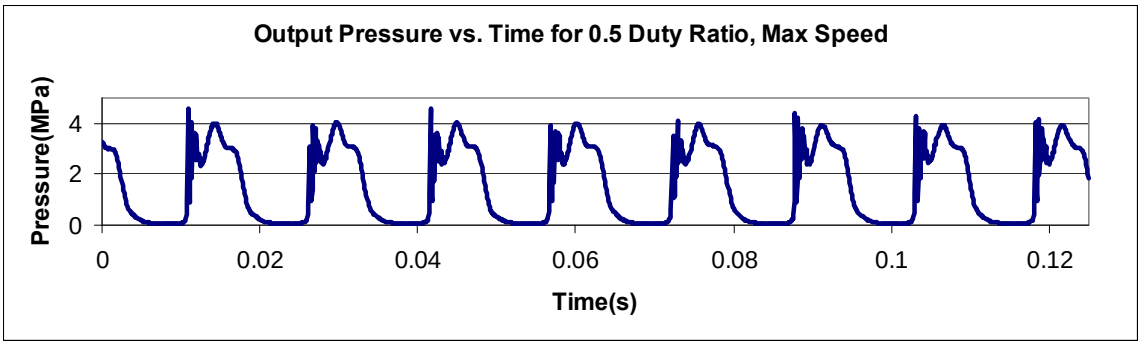

Figure 60: Output pressure vs. time for 0.5 duty ratio, 0.0005inch clearance and maximum angular velocity

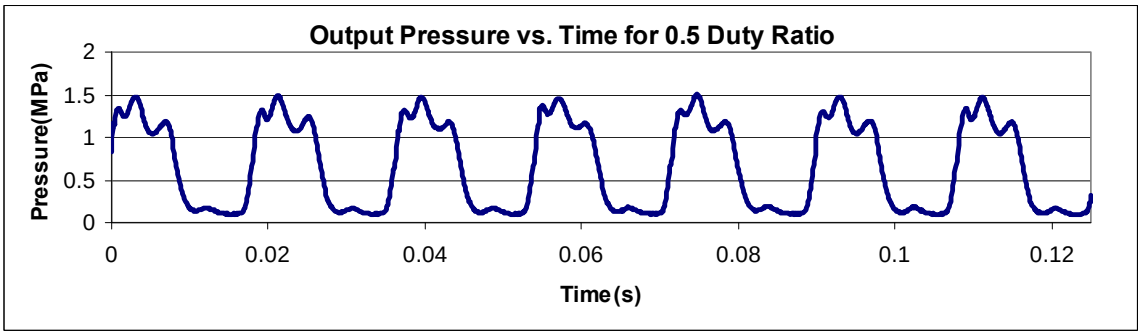

Figure 61: Output pressure for 0.5 duty ratio, 0.0015inch clearance, 2000N clamping force, no tank-side check valve

6.4 Experimental Results Discussion

Looking at Figure 54 , Figure 55, and Figure 56 the first thing to notice is that as the duty ratio is increased the flow and pressure also increase in a somewhat linear manner. Therefore, the primary purpose of the valve, to create a virtually variable displacement pump/motor with switch-mode control has been achieved.

Looking at the zero duty ratio plot, first subplot of Figure 54, pressure spikes can still be seen suggesting that the valve is experiencing unforeseen leakage from pressure to the output port. Also, in this configuration it was impossible to bring the system over 2MPa, again suggesting that there are significant unforeseen leakage losses. Taking apart the valve and looking axially at the valve plate and the sub-valves, a small gap can be seen in the position when the valve is supposed to be completely blocked. Because the valve is not fully blocked, there exists a leakage path from pressure to tank whenever the high speed valve switches. This could account for the unforeseen leakage losses.

To estimate how much of the flow is leaking from the high pressure inlet to the low pressure inlet, the hydraulic motor was first directly connected between the pump and tank and the flow rate was measured. Next the hydraulic motor was reconnected to the valve with no load and 1.0 duty ratio and the flow rate was measured. Finally, a check valve was placed on the low pressure inlet line such that flow could only be pulled from tank and not return to tank. Remember, the model assumes that the hydraulic motor has enough inertia to pull fluid from tank, so any change in flow would indicate that there were leakage losses. Without the check valve in place the flow through the valve is

approximately half of the flow of the motor directly connected to the pump. When the check valve is in place, the flow through the valve is the same as the maximum possible flow. This signifies that nearly half of the flow from the pump is immediately lost as leakage when it enters the valve with 0.0015inch clearances. Performing this same procedure for other clearance values resulted in a 25% leakage loss for 0.0005inch clearance and a 27% leakage loss for 0.001inch clearance.

Originally these leakage estimates were used in combination with the output flow of the valve to indirectly estimate the input flow, which is needed for efficiency estimates. However, it was not known how much the leakage would vary with pressure and duty ratio. Therefore it was necessary to directly measure the input flow, and lacking a flow meter, an additional pressure sensor ($P_{ump,pressure}$) and a variable orifice were added to the inlet of the high speed valve. Using the orifice equation, the orifice parameters could be calculated from the pressure drop across the orifice and the flow rate when directly connected to the hydraulic motor. Fitting a trend line to this data revealed that a negative flow rate is expected for a zero pressure drop across the orifice. This offset of the trend line is assumed to be the leakage loss of the hydraulic motor. Thus, this offset will be added to all measurements of the output flow in order to attain a more accurate estimate of the flow. Further tests need to be conducted to verify this assumption.

Comparing the measured efficiency in Figure 57 to the calculated efficiency shown in Figure 62 for various clearances and neglecting friction losses shows that the model prediction does not agree. In the model, it is assumed that when the valve switches to low pressure the high pressure inlet port is completely blocked, besides leakage, and the pump charges the accumulator. However, in the actual system there is still an input flow to the valve even at 0 duty ratio. In fact the input pressure and flow actually increase as the duty ratio decreases. This is surprising because the pump is expected to have a constant output power for various duty ratios. The result of this is that the efficiency actually increases pseudo linearly instead of logarithmically.

The maximum calculated hydraulic efficiency is around 90% for 0.0005inch clearance, while the maximum measured hydraulic efficiency is about 70% for 0.001inch clearance. This discrepancy is likely from the increased leakage described above or possibly from increased compressibility losses due to increased air entrainment. The total efficiency is also much lower than predicted. The model predicted the friction losses to be the least significant of the power losses, while the actual friction losses account for over half of the power losses. Including the friction losses, the maximum total efficiency is 38% for a clearance of 0.001inch and 25% for 0.0005inch & 0.0015inch clearances at 1.0 duty ratio.

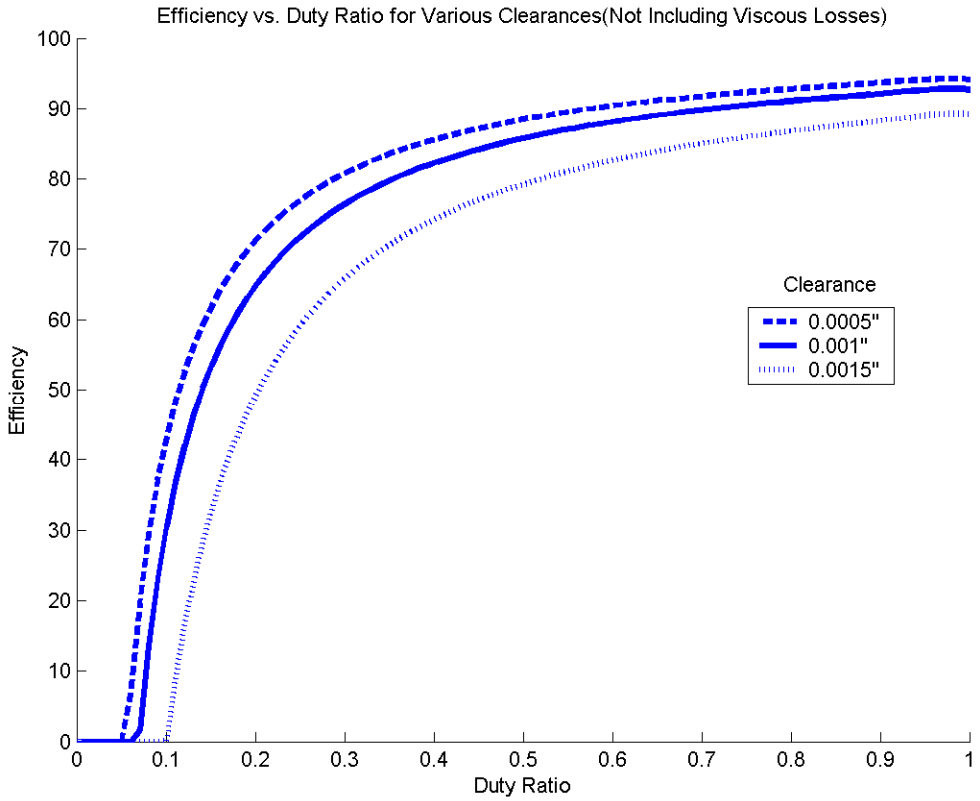

Figure 62: Calculated efficiency vs. duty ratio for selected clearances (Not including viscous losses)

Figure 58 shows the scaled results for a typical speed test run. The angular velocity of the valve plate increases linearly until it reaches a maximum value at what should only be 50% of maximum speed. The angular velocity then remains steady up to 100% of maximum angular velocity. This would appear to be the fault of the motor speed controller. It is expected that as the angular velocity of the valve plate increases, the viscous friction will cause a larger torque. This however is not the case. In most tests the torque at low speeds is above the range of the sensor. Even when fitting a longer moment arm the torque at low speeds is still beyond the range of the sensor. This appears to be due to the valve plate motor. At lower speeds the motor has large vibrations and uneven speeds. As the speed is increased, the motor appears to dynamically balance and runs smoother. This vibration torque appears to generate a torque far larger than the effects of viscous friction. Figure 59 shows the torque vs. angular speed for selected clearances. However, since these torque values only come within range of the sensor once the valve plate has reached a maximum speed, no conclusions can be drawn. Note that a smaller clearance generates a larger torque on the valve plate because of increased viscous friction, which is expected.

It should also be noted that these measured torque values are far larger than anticipated. For Run 3 described above, the torque power loss is greater than or a significant portion of the input power, as shown in Figure 63. The excess torque was so much in fact, that the valve plate motor had to be replaced with a larger gear reduction motor of the same

series. This excess torque could be caused by a misalignment of the valve plate that would result in an increased frictional torque of the internal thrust bearings. A small increase in the friction of the thrust bearings, when multiplied by hundreds of pounds of normal clamping force, would result in large torque requirements.

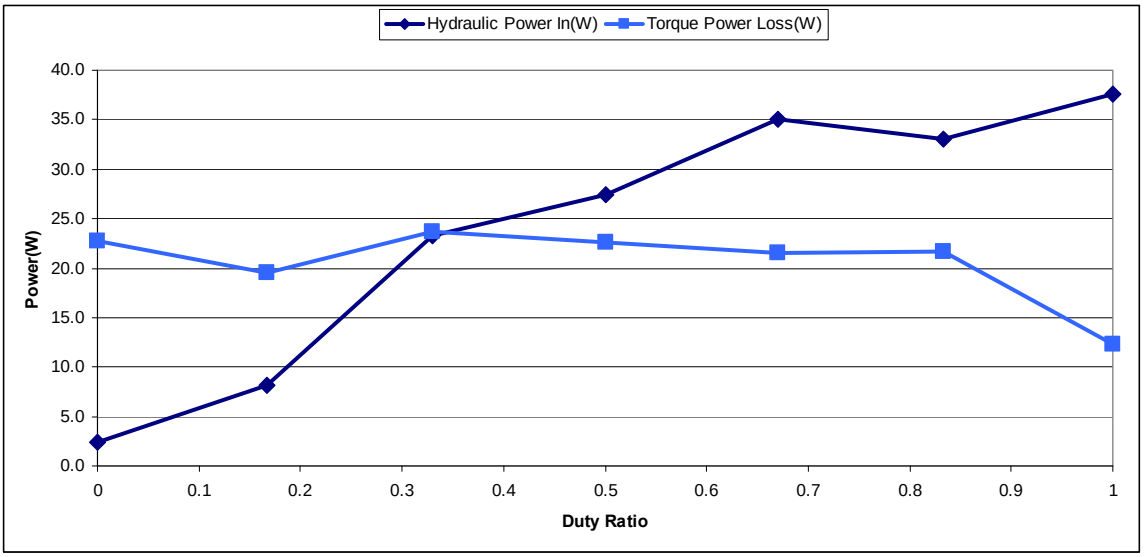

Figure 63: Hydraulic power in and torque power loss vs. duty ratio for 0.0015inch clearance

Figure 60 shows the pressure pulses of the high speed valve at its fastest angular velocity. This generated a 64Hz switching frequency, which is less than the desired 100Hz. Unfortunately this is as fast as the new valve plate motor could go, so a more powerful motor will be needed to reach the desired switching frequency. Finally, Figure 61 shows the output pressure of the valve for when there is no tank-side check valve. There appears to be no change from previous tests runs which included the tank-side check valve. Also note that the laboratory setup did not utilize a flywheel on the hydraulic unit. Thus the assumption that the hydraulic unit would always be pulling flow is not valid. Therefore the check valve may still be necessary to prevent cavitation during normal operation.

The high speed valve is a partial success. The output pressure and flow are controlled by the duty ratio as designed. However larger leakage losses and much larger required torques keep the high speed valve from performing admirably. These issues must be resolved in future iterations of the valve.

Chapter 7: Conclusion

There has been a need for a high speed valve to allow switch-mode control of fixed displacement pump/motors, effectively creating a virtually variable displacement pump/motor. To serve this need, high speed valves have been in development for several decades and typically consist of an oscillating spool or a continuously rotating spool. Oscillating spools have high power requirements due to large accelerations and continuously rotating spools have only recently begun to have fast enough switching frequencies for switch-mode control. Thus, this project set out to design a high speed hydraulic valve with variable duty ratio, suitable for switch-mode control of hydraulic circuits.

Several concepts were brainstormed and analyzed for feasibility. Many concepts relied on unique geometric structures to produce the variable duty ratio. However, in the end it was decided to use a network of simple sub-valves that rotate at a relative angle to each other. This angle determines the duty ratio, while the angular velocity determines the switching frequency. By utilizing a disc style architecture, several advantages are gained.

Once the form of the high speed valve was decided on, the valve was modeled and analyzed. Of particular interest was the power loss due to throttling, leakage, compressibility of the fluid, and viscous friction. These four losses determine the efficiency and performance of the valve. Because these losses are also highly coupled, and optimization routine was used to find what parameters generate the least power loss.

Once the high speed valve was optimized it was shown that the throttling losses contributed the most to the overall power loss, followed by leakage, and compressibility losses. Viscous friction losses were calculated to contribute the least to the total power loss. It was shown that at mid to high duty ratios the high speed valve could theoretically operate at high efficiencies.

After the critical valve geometry was sized by the optimization, the other features of the valve were designed for a first generation prototype. This included the selection of thrust bearings, O-rings for seals, hydraulic connectors, disc springs to apply a clamping force, and choice of motors for actuation. The resultant design is compact, operates over a wide range of duty ratios, and is quiet.

A first generation prototype was then successfully manufactured. Several sensors were used to measure key parameters. Two pressure transducers across an orifice to estimate the input flow and input pressure. One pressure transducer at the outlet of the valve is used to measure the output pressure. Photo-detectors setup as an encoder on an external hydraulic motor are used to measure the output flow. Lastly, a force transducer is used to measure the torque on the valve plate. With data collected from these sensors the functionality of the valve was shown. The output pressure and flow of the valve matches the duty ratio well. The efficiency however, is much worse and is primarily caused by larger leakage flows and much higher than expected torque requirements. In order to move forward with the high speed valve, it will be necessary to isolate the valve plate

from the large clamping forces that hold the valve together, so that a minimal torque is required.

Despite the success of the first prototype there are several aspects of the high speed valve that require further investigation. Many of the complex dynamic interactions of the high speed valve are assumed to be negligible, so only simple orifice and leakage equations were used. However, these complex interactions may have a significant effect on the performance of the high speed valve. To determine what these interactions might be, a computational fluid dynamics (CFD) model of the valve would be insightful. This would help to determine how the complex fluid dynamics affect pressure distributions and flow directions within the valve. As in [19], a CFD analysis would also show if any vortex regions form which would increase the necessary torque requirements. With the increased knowledge from the CFD analysis, the high speed valve could be designed for improved efficiency and performance. Finally, the CFD analysis would pinpoint any stagnation points in the high speed valve in which debris would accumulate and later cause damage to the valve.

If the high speed valve ever intends to become a commercial product, the size, complexity, noise, and maintenance of the valve should be considered in further detail. A majority of the size of the valve is simply to accommodate porting and hydraulic connections. By spacing the inlet ports farther apart, fixing the Tier 1 section while allowing the Tier 2 section to change phase, and utilizing a hydrodynamic thrust bearing, the Tier 1 section of the valve can be reduced in size significantly. As shown in Figure 64, the new Tier 1 section has the tank supply inlet positioned radially and the two high pressure inlet ports placed axially. This configuration is smaller, has fewer parts, and allows for faster control since a smaller mass needs to be rotated to adjust the duty ratio. Conversely, the Tier 1 section could remain fixed while the Tier 2 section would change phase, allowing a further reduction to the mass which needs to be rotated. Using hydrodynamic thrust bearings would also decrease the wear on the valve, though a method to hydrodynamically balance the valve plate axially will need to be developed to reduce the required supporting forces and power loss. Axial balancing would also allow for the valve plate to be magnetically suspended.

High noise and vibration levels are always an issue for switch-mode hydraulic systems so the use of Herschel-Quincke(HQ) tubes could be used to reduce the vibrations within the system[27]. HQ tubes are simply tubes that split and then recombine the fluid flow. By adjusting the length of the HQ tubes the vibrations within the flow can become out of phase and cancel. Because of the added volume introduced by HQ tubes they would increase compressibility losses if placed on the outlet of the valve. However they could be placed on the inlet lines to reduce the back-ripple produced by the valve, which would aid in protecting the rest of the system from high frequency vibrations.

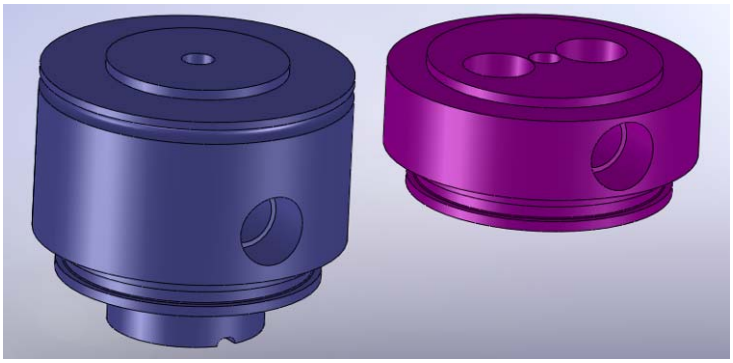

Figure 64: Current prototype Tier 1 and new proposed Tier 1 design

Other parts of the system, such as the accumulator, check valves, and pump/motors deserve to be examined as well. The accumulator needs to be sized and given the correct amount of precharge to properly reduce pressure fluctuations at the inlet of the high speed valve. Though currently the check valves help to mitigate extreme pressure fluctuations, the high speed valve has not been tested at top speeds, so the development of fast acting check valves may still be necessary. Finally, because the flow is pulsed, it is unclear if certain archetypes of pump/motors have advantages over others. A new design of a pump/motor which minimizes compressibility losses and benefits from a pulsed flow input could prove to be a major advantage to switch-mode systems.

Lastly, control systems for the high speed valve, such as those discussed in [23-25], need to be further investigated. Beyond single valve control, multi-valve control is a difficult problem and an area of intense research. If one high speed valve were to be used for each wheel in a hybrid hydraulic vehicle, then fast, precise control would be necessary. Any difference in speed at each wheel could cause skidding or the vehicle to go off course. If this control problem is solved, then independent speed and torque control of each wheel could be achieved.

In conclusion many aspects of the high speed hydraulic valve were a success, but to bring this concept to the next level will require much more research and development. Particularly in making the valve more compact, more efficiency, having a larger operating bandwidth, and developing control systems.

References

[1] Mohan, N., Robbins, W. P., and Undeland, T. M., 1995, *Power Electronics: Converters, Applications and Design*, Wiley and Sons, New York.

[2] Van de Ven, J. D., Olson, M. O., and Li, P. Y., 2008, "Development of a Hydro-Mechanical Hydraulic Hybrid Drive Train with Independent Wheel Torque Control for an Urban Passenger Vehicle," *International Fluid Power Exposition*, Las Vegas, NV, pp. 1-11.

[3] Cao, J., Gu, L., Wang, F., and Qui, M., 2005, "Switchmode Hydraulic Power Supply Theory," *ASME International Mechanical Engineering Congress and Exposition*, Orlando, FL, pp. 85-91.

[4] Khan, S. H., Cai, M., Grattan, K. T. V., Kajan, K., Honeywood, M., and Mills, S., 2005, "Design and Investigations of High-Speed, Large Force and Long Lifetime Electromagnetic Actuators by Finite Element Modeling," *Journal of Physics: Conference Series* ***15***, pp. 300-305.

[5] Jeong, H. S., and Kim, H. E, 2002 " Experimental Based Analysis of the Pressure Control Characteristics of an Oil Hydraulic Three-Way On/Off Solenoid Valve Controlled by PWM Signal," *Transactions of the ASME Vol* ***124,*** pp. 196-205.

[6] Jinghong, Y., Zhaoneng, C., and Yuanzhang, L., 1994, "The Variation of Oil Effective Bulk Modulus with Pressure in Hydraulic Systems," *Journal of Dynamic Systems, Measurement, and Control*, **116**, pp. 146-150.

[7] Mesenich, G., "Pulse Modulated Hydraulic Valve," United States Patent 4979542, Dec. 25, 1990.

[8] Batdorff, M. A., Lumkes, J. H., "Fast Acting Fluid Control Valve"United States Patent 2007/0289649 A1, Dec. 20, 2007.

[9] Giaardo, M., "High-Speed Solenoid Valve for a Fluid Under Pressure, E.G. for Pneumatic Circuits," United States Patent 5048564, Sept. 17, 1991

[10] Jacobs, J. N., "High Speed Gate Valve," United States Patent 5362028, Nov. 8, 1994.

[11] Tomlinson, S. P., and Burrows, C. R., 1992, "Achieving a Variable Flow Supply by Controlled Unloading of a Fixed-Displacement Pump," *Journal of Dynamic Systems, Measurement, and Control*, **114**, pp. 166-171.

[12] Cui, P., Burton, R. T., and Ukrainetz, P. R., 1991, "Development of a High Speed on/Off Valve," *SAE Technical Paper Series*(911815), pp. 21-25.

[13] Ibiary, Y. E., 1978, "Coming: Smart Hydraulic Valves," *Machine Design*, pp. 99-103.

[14] Ota, K., "High Speed Flow Control Valve," United States Patent 5148833, Sept. 22, 1992.

[15] Yokota, S., and Akutu, K., 1991, "A Fast-Acting Electro-Hydraulic Digital Transducer," *JSME International Journal*, **34**(4), pp. 489-495.

[17] Li, P. Y., Li, C. Y., and Chase, T. R., 2005, "Software Enabled Variable Displacement Pumps," *ASME International Mechanical Engineering Congress and Exposition*, **12**, Orlando, FL, pp. 63-72.

[18] Rannow, M. B., Tu, H. C., Li, P. Y., and Chase, T. R., 2006, "Software Enabled Variable Displacement Pumps - Experimental Studies," *ASME International Mechanical Engineering Congress and Exposition*, Chicago, IL.

[19] Tu, H. C., Rannow, M., Van de Ven, J., Wang, M., Li, P., and Chase, T., 2007, "High Speed Rotary Pulse Width Modulated on/Off Valve," *Proceedings of the ASME International Mechanical Engineering Congress*, Seattle, WA, pp. 42559.

[20] Cyphelly, I., and Langen, H. J., 1980, "Ein Neues Energiesparendes Konzept Der Volumenstromdosierung Mit Konstantpumpen," *Aachener Fluidtechnisches Kolloquium*, pp. 42-61.

[21] Lu, X. F., Burton, R. T., Schoenau, G. J., and Zeng, X. R., 1991, "Feasibility Study of a Digital Variable Flow Divider," *SAE Technical Paper Series*(911816), pp. 27-34.

[22] Royston, T., and Singh, R., 1993, "Development of a Pulse-Width Modulated Pneumatic Rotary Valve for Actuator Position Control," *Journal of Dynamic Systems, Measurement, and Control*, **115**, pp. 495-505.

[23] Muto, T., Yamada, H., and Suematsu, Y., 1990, "Pwm-Digital Control of a Hydraulic Actuator Utilizing Two-Way Solenoid Valves," *Journal of Fluid Control*, **20**(2), pp. 24-41.

[24] Ahn, K., Yokota, S., 2005, "Intelligent Switching Control of Pneumatic Actuator Using On/Off Solenoid Valves," *Mechatronics, 15 683-702,* pp. 683-702.

[25] Bobrow, J. E., Lum, K., 1995, "Adaptive, High Bandwidth Control of a Hydraulic Actuator," *Proceedings of the American Control Conference,* Seattle, WA, pp. 71-75.

[26] Artemis Intelligent Power. "Artemis Digital Displacement Pump". 1 Jan 2005. Web. 29 May 2009. <http://www.artemisip.com/index.htm>
[27] Hallez, R. F., 2001, "Investigations of the Herschel-Quincke Tube Concept as a Noise Control Device for Turbofan Engines," *Master's Thesis for Virginia Polytechnic Institute*, Blacksburg, Virginia.
[28] Phaneuf, C., "Electric Motor Integration with a Rotary On/Off Valve," *The Cooper Union for the Advancement of Science and Art*, New York, NY.
[29] Norton, R. L., Machine Design - an Integrated Approach, New Jersey: Pearson Prentice Hall, 2006.
[30] Cundiff, J. S., Fluid Power Circuits and Controls. New York: CRC Press, 2002
[31] Merritt, Herbert. Hydraulic Control Systems. New York: John Wiley & Sons, 1967.
[32] Poclain Hydraulics. "P90 Variable Displacement Pump". 6 Feb. 2009. Web. 29 May 2009. <http://www.poclain-hydraulics.com/portals/0/technical%20catalogs/A18586C.pdf>
[33] O'Connor, James J., ed, Boyd, John, Avallone, Eugene A., ed . Standard Handbook of Lubrication Engineering. New York: McGraw-Hill, 1968
[34] Hamrock, Bernard J., Schmid, Steven R., and Jacobson, Bo O. Fundamentals of Fluid Film Lubrication. 2nd ed. New York : Marcel Dekker, c2004
[35] Oberg, Erik; Jones, Franklin D.; Horton, Holbrook L.; Ryffel, Henry H. Machinery's Handbook (27th Edition). New York: Industrial Press, c2004.
[36] Fuller, Dudley D. Theory and Practice of Lubrication for Engineers. 2nd ed. New York: Wiley, c1984.

Appendices

Appendix A covers the design and analysis of a hydrodynamic thrust bearing which would be used to support the valve plate.

Appendix B shows more of the experimental test results.

Appendix C is a bill of materials for the high speed valve. Cost of components and their suppliers are listed.

Appendix D shows the drawings for all the custom components of the high speed valve.

Appendix E lists the primary Matlab files used to simulate the energy losses of the high speed valve.

Appendix A: Hydrodynamic Thrust Bearing

One advantage of the disc style valve is that the internal clearances of the valve can be determined by fluid forces instead of manufacturing tolerances and thermal expansion as in spool type valves. The clearances can be maintained with either a hydrostatic or hydrodynamic bearing. Hydrodynamic bearings will be investigated because they do not require external pumping. Several types of hydrodynamic bearings exist based on the form that the thrust pad assumes. These include parallel step, fixed inclined step, pivoted incline step, and curved step morphologies. This section will develop the equations to model a hydrodynamic thrust bearing in which to estimate the viscous forces and leakage losses generated.

A hydrodynamic thrust bearing uses viscous forces to wedge fluid between two surfaces, generating an increase in pressure which is used to support a load. A parallel step morphology was chosen to be analyzed because of its simple design, ease of manufacturability relative to the other geometries, and it's ability to handle higher loads. The variables used for this calculation are: R_1 is the inner radius of the thrust bearing, R_2 is the outer radius of the thrust bearing, L is the radial pad length, B is the circumferential pad length, h_1 is the inlet film thickness, h_2 is the outlet film thickness, s_h is the step height, n_s is the proportional distance of the step to the inlet, and U is the plate velocity. After a literature search three methods for determining the dynamic properties of a hydrodynamic step thrust bearing were found: The Raimondi method [33], the Hamrock method [34], and the Machinery's Handbook [35] method

The Raimondi Method involves first finding the dimensionless bearing characteristic number, K_f. "Once this is done all the operating characteristics of the bearing become fixed and the performance readily calculated" [33].

$$K_f = \frac{\mu \cdot U}{m^2 \cdot P \cdot B}, \qquad \text{Equation 35}$$

P = Load per unit area = W/(B*L)
W = Load per pad
μ = Absolute Viscosity
m = Slope of pad surface = (h1-h2)/B

By assuming a square pad(L/B = 1), the inner radius R_1, the number of pads j, and the proportion of the circumference that the pads occupy k, we can calculate:

$$R_2 = -R_1\left(\frac{\pi \cdot k}{j} + 1\right)\left(\frac{\pi \cdot k}{j} - 1\right) \qquad \text{Equation 36}$$

$$L = R_2 - R_1 \qquad \text{Equation 37}$$

$$B = \pi\left(R_1 + R_2\right)k / j \qquad \text{Equation 38}$$

$$U = \omega\left(R_1 + R_2\right)/2 \qquad \text{Equation 39}$$

Choosing the optimum characteristic bearing number for a square pad $K_f = 7.5$ and rearranging Equation 35 the effective slope m for a step thrust bearing can be calculated. For the given characteristic bearing number and the use of a few charts the other performance characteristics of a square pad thrust bearing are given as:

$$h_2 = 7.3 \cdot B \cdot m / 10$$ Equation 40

$$h_1 = m \cdot B + h_2$$ Equation 41

$$f = 7.5 / m$$ Equation 42

$$Q = 0.69 \cdot B \cdot L \cdot U \cdot m$$ Equation 43

$$Q_s = 0.36 \cdot Q$$ Equation 44

$$\Delta T_{emp} = \frac{12.8P}{J\gamma_w c_p}$$ Equation 45

$$\mathrm{P}_{loss} = fWU$$ Equation 46

Where f is the friction coefficient, Q is the flow rate of lubricant drawn into the bearing region, Q_s is the side leakage of the thrust pad, ΔT_{emp} is the temperature rise of the fluid, J is the mechanical equivalent of heat, γ_w is the weight density of the oil, c_p is the specific heat of the oil, and P_{loss} is the power loss of one thrust pad. If the outcome is not desirable, such as a large temperature increase, the chosen geometric values can be iterated until a satisfactory solution is derived.

The Hamrock method creates a set of dimensionless parameters to define the system. It should be noted that unlike the Raimondi method, the Hamrock method does not account for side leakage. First the step height s_h, the inner radius R_1 of the thrust pad, the outer radius R_2 of the thrust pad, and the number of pads j are chosen. From these:

$$B = \frac{(R_1 + R_2)}{2}\left(\frac{2\pi}{j} - \frac{\pi}{36}\right)$$ Equation 47

where the $\pi/36$ is to allow for supply channels. The geometric values that create the largest maximum pressure are:

$$H_o = \frac{h_2}{s_h} = 1.155$$ Equation 48

$$n_s = 0.7182$$ Equation 49

Once these parameters are established, the dimensionless parameters can be calculated.

$$W_z = \frac{3n_s(1-n_s)}{(1-n_s)(H_o+1)^3 + n_s H_o^3} = \frac{P_m}{2}$$ Equation 50

$$F_b = -W_z - \frac{H_o + 1 - n_s}{H_o(1+H_o)} = -Hp$$ Equation 51

$$Q = \frac{-P_m(H_o+1)^3}{6n_s} + H_o + 1$$ Equation 52

Where W_z is the dimensionless load, P_m is the dimensionless maximum pressure, F_b is the dimensionless shear force, Hp is the dimensionless power loss, and Q is the dimensionless flow rate that is drawn into the thrust region. From these values the flow rate q, temperature increase ΔT_{emp}, load per thrust pad w_z, and the power loss P_{loss} can be determined. If the results are unsatisfactory, such as insufficient support load, the starting conditions can be iterated until an acceptable solution is reached.

$$q = Q \cdot U \cdot L \cdot j \cdot s_h / 2$$ Equation 53

$$\Delta T_{emp} = \frac{2 \cdot U \cdot B \cdot Hp \cdot \mu}{\rho \cdot c_p \cdot s_h^2 \cdot Q} \qquad \text{Equation 54}$$

$$w_z = \frac{W_z \cdot B^2 \cdot L \cdot U \cdot \mu}{s_h^2} \qquad \text{Equation 55}$$

$$\mathrm{P}_{loss} = Hp \cdot B \cdot L \cdot U^2 \cdot \mu \cdot j / s_h \qquad \text{Equation 56}$$

Finally, the method described in the Machinery's Handbook combines aspects of the above two methods along with some general rules of thumb. For conciseness this method will not be outlined here.

In order to calculate the power loss of the hydrodynamic thrust bearings it was first necessary to calculate the force the thrust bearing would need to support. The thrust bearings support the valve plate, so it was necessary to calculate the forces on the valve plate due to the fluctuating fluid pressures. These forces are dependent upon the angular position of the valve plate and the phase angle and are shown in Figure 65. The thrust bearings must be designed to operate under the peak forces which are about 1500N.

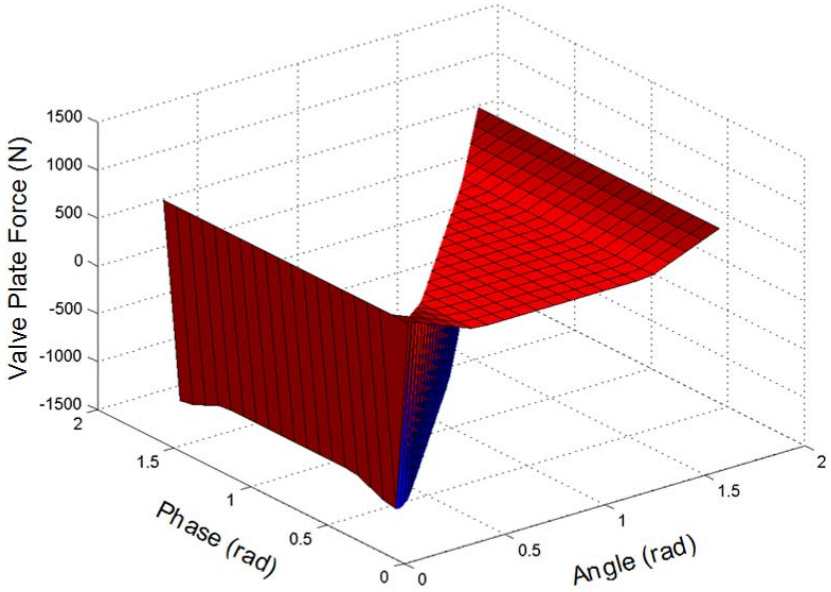

Figure 65: Forces on valve plate for various angles and phases for one half cycle

A comparison of the three methods for a 2000N load, square pads, and an inner diameter of 1cm is given in

Table 6. Remember that the Hamrock method does not account for side leakage, but the load carrying capacity of a square pad with side leakage is only 44% that of a pad without side leakage [36]. Accounting for this allows all three methods to agree reasonably well with each other. In the table, N is the number of thrust pads, h_2 is the outlet film thickness, s_h is the step height, P_{loss} is the power loss of the thrust bearing, ΔT_m is the temperature rise of the thrust bearing, *width* and *length* are the dimensions of the thrust

pad, and q is the flow rate through the thrust bearing. The important values to look at are the power loss and temperature change.

Table 6: Comparison of thrust bearing method results

Method	N	h_2[cm]	s_h[cm]	P_{loss}[W]	ΔT_m[C]	width[cm]	length[cm]	q[m^3/s]
MH	5	0.0012	0.00087	40.5	16	1.628	1.4937	1.60E-06
Hamrock	4	0.002	0.0017	19.6	8.61	1.5	1.8544	1.44E-06
Raimondi	4	0.0012	0.0016	33.6	15.7	1.69	1.69	7.77E-06

The above results were calculated for a smaller valve geometry than previous sections and constitute a 15%-20% drop in efficiency, a considerable energy sink. Also note that another thrust bearing would be needed on the reverse side of the valve plate, although with proper hydrostatic balancing this thrust bearing would not need to support a large load. A comparable ball thrust bearing would require less than half of the power. In order to facilitate manufacture and to remain at a higher efficiency it was decided to replace the hydrodynamic thrust bearings with ball thrust bearings.

Appendix B: More Experimental Results

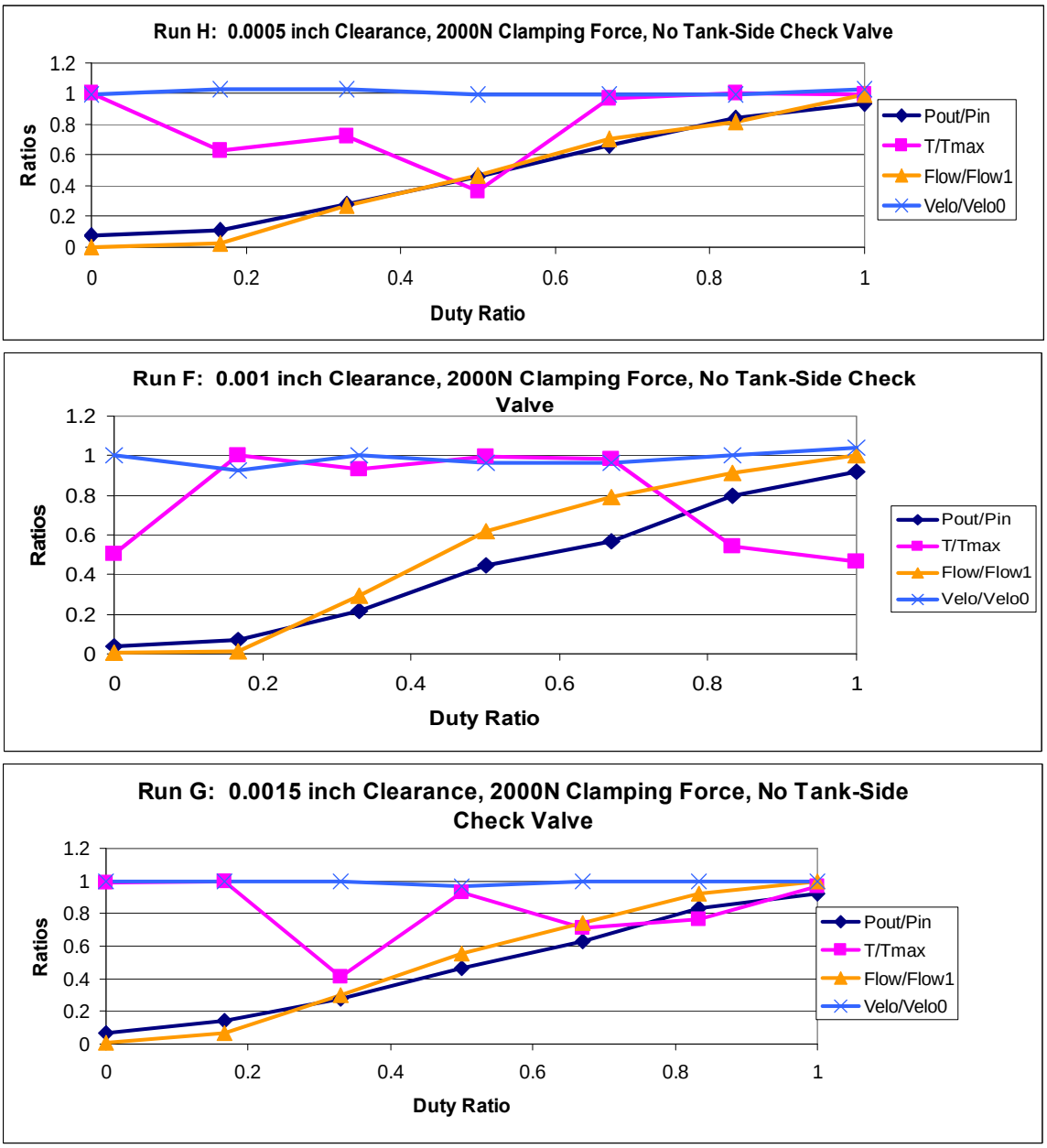

Figure 66: Compilation of results for three selected test runs

Notice that the output pressure and flow increase linearly with increased duty ratio. The torque is expected to decrease with increased duty ratio. This is because the pressure is felt on the back side of the valve plate for longer periods of time, lessening the force on the thrust bearings. However the torque shows no particular pattern in relation to duty ratio. This could be because the torque arm tends to bounce on the force sensor, resulting in noisy and/or offset results.

Appendix C: Bill of Materials

Part	Company	Part #	Description/Notes	Qty.	Cost	Total
Force Sensor	Digi-Key	480-2618-ND	Honeywell force sensor, measures torque	1	$48.68	$48.68
Pressure Sensor, Input	Digi-Key	734-1049-ND	Input pressure sensor	1	$68.63	$68.63
Check Valve	Inserta	ICT-B-04-N15	Check valves to remedy pressure extremes	2	$44.00	$88.00
Insertion Tool	Inserta	IMT-C-04	Check valve insertion tool	1	$28.25	$28.25
Tier 1 Sub-Valve	L&M Machine	AAK-007	Tier 1 sub-valve, Tank & Ps inputs	1	$443.00	$443.00
Tier 2 Sub-Valve	L&M Machine	AAK-009	Tier 2, exit sub-valve	1	$308.00	$308.00
Valve Plate	L&M Machine	AAK-003	The 3rd disc, its rotation causes pulses	1	$242.00	$242.00
Motor Mount, Freq	Made in house	AAK-0013	Mount for valve plate motor	1	$0.00	$0.00
Motor Mount, Phase	Made in house		Mount for the motor that controls phase	1	$0.00	$0.00
Motor Plate	Made in house	AAK-005	Attaches to pump/motor. Holds check valves	1	$0.00	$0.00
Outer Sleeve	Made in house		Outer sleeve of the valve	1	$0.00	$0.00
Thrust Plate	Made in house	AAK-0011	Attaches to tie rods, lets Tier 1 rotate	1	$0.00	$0.00
Ball Bearing	McMaster	5972K158	Valve plate motor bearing	1	$13.80	$13.80
Bearing Washers	McMaster	5909K78	Washers for needle thrust bearing	2	$1.68	$3.36
Bore O-ring	McMaster	9262K205	Bore O-Rings (100 Pack)	1	$8.13	$8.13
Bushings	McMaster	6381K406	Valve plate shaft bushings	2	$3.72	$7.44
Coupling	McMaster	6208K53	Coupling, 1/8in & 3/16in Bore, 1/2inx3/4in	1	$21.26	$21.26
Disc Springs	McMaster	96475K236	Springs to keep valve together (12 Pack)	8	$8.89	$71.12
Dowel Pins	McMaster	91585A912	Position locating pins (100 Pack)	1	$6.41	$6.41
Face Seal O-ring	McMaster	9262K107	O-rings on motor side(100 Pack)	1	$7.75	$7.75
Needle Thrust Bearing	McMaster	5909K18	Thrust bearing for Tier 1 to thrust plate	1	$4.85	$4.85
Nut	McMaster	90685A045	M8x1.25 Nut(100 Pack)	1	$8.81	$8.81
Phase Belt	McMaster	4198T27	O-ring, 1/8inx2-7/8in ID (10 Pack)	1	$8.25	$8.25
Pipe-Pipe Adaptor	McMaster	50925K131	1/4 male NPT to 1/4 male NPT	4	$1.29	$5.16
Plug	McMaster	4513K322	1/4 NPT plug	2	$0.75	$1.50
Shaft	McMaster	1327K39	Valve plate shaft. 1/8in diam, 12in long	1	$6.16	$6.16
Shaft Seal	McMaster	13125K63	Valve plate shaft seal	1	$12.75	$12.75
Shims, 0.0005in	McMaster	9502K26	6inx50x0.0005in shim stock	1	$38.65	$38.65
Shims, 0.005in	McMaster	3088A238	1-1/4inx1-3/4inx0.005in shims(10 Pack)	1	$5.45	$5.45
Tie Rod	McMaster	93275A034	Threaded rods, M8x1.25x110mm	4	$2.75	$11.00
Bushing	MSCDirect	35401470	For phase motor shaft 3/16inx5/16inx3/16in	1	$11.60	$11.60
Pipe Cross	MSCDirect	01212661	1/4 NPT female cross	2	$22.26	$44.52
Shims, 0.001in	MSCDirect	05408984	1.255inx1.75inx0.001in shims(10 Pack)	1	$23.78	$23.78
Ball Thrust Bearings	Nachi	51106	Supports valve plate (pg 315)	2	$36.45	$72.90
Pressure Sensor, Output	OMEGA	PX4201-3KGV	Output pressure sensor	1	$0.00	$0.00
Thermocouple	OMEGA	TC-K-NPT-G-72	Measures oil temperature	1	$34.00	$34.00
Lexan	Plastics Unlimited	n/a	1/2inx12inx12in Lexan sheets for blast box	5	$15.03	$75.15
DC Motor Driver	Sparkfun	ROB-09107	Motor driver for valve plate motor	1	$39.95	$39.95
Stepper Motor	Sparkfun	ROB-08420	Motor to control phase (Robo Lab has some)	1	$14.95	$14.95
Stepper Motor Driver	Sparkfun	ROB-08368	Easy Driver v3, motor driver for phase control	1	$14.95	$14.95
Adaptor	Tompkins	2404-06-04	-04 Pipe(male) to -06 JIC 37(male)	6	$1.78	$10.68
Hose - 4ft	Tompkins	6M3K, 6FJ-6FJ90	Hydraulic hose w/ JIC 37 Flare -06. 1 elbow	4	$47.80	$191.20
DC Motor	Trossen Robotics	MP-28016-385	DC motor to drive valve plate	1	$29.68	$29.68
					Total	$2,031.77

Appendix D: Drawings

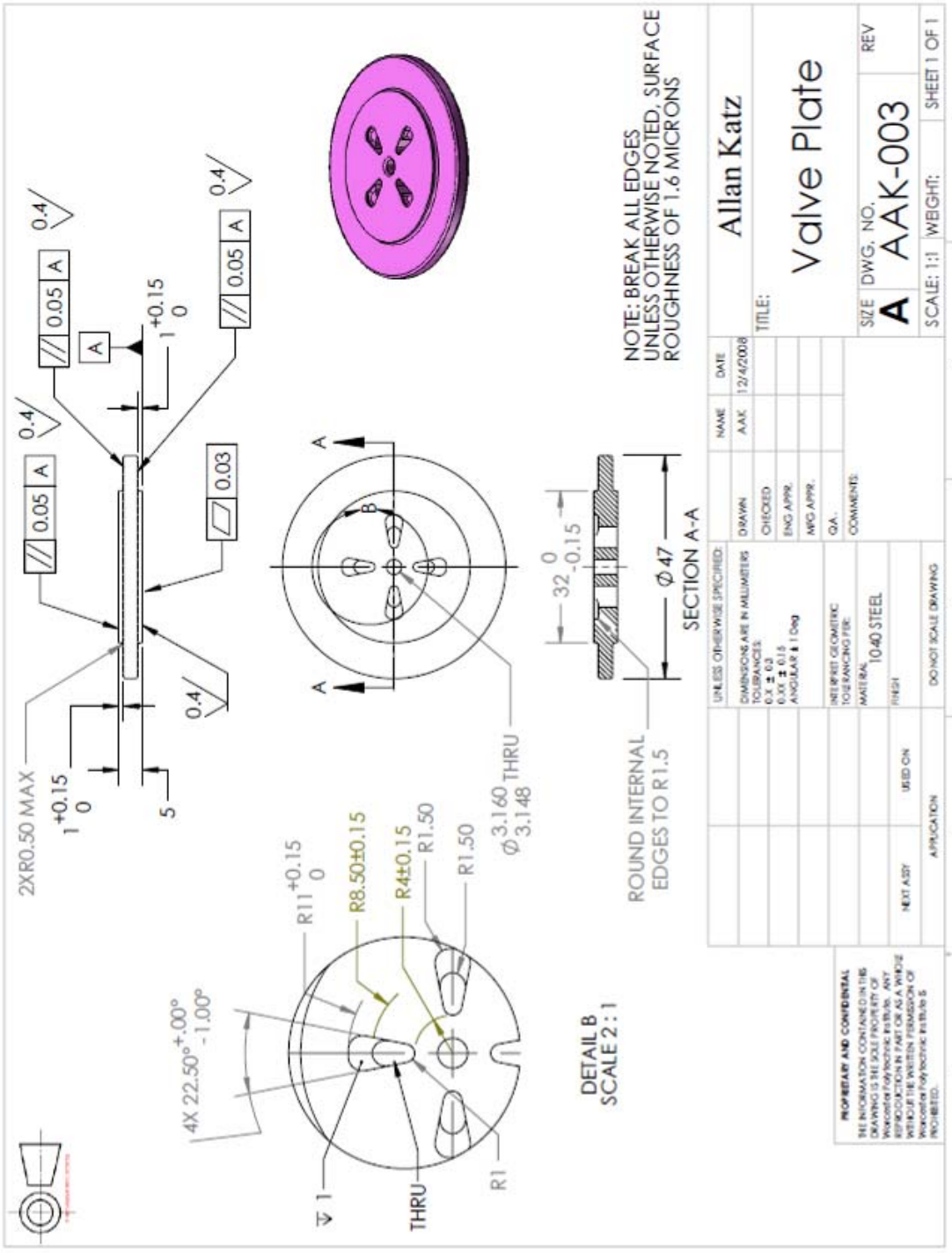

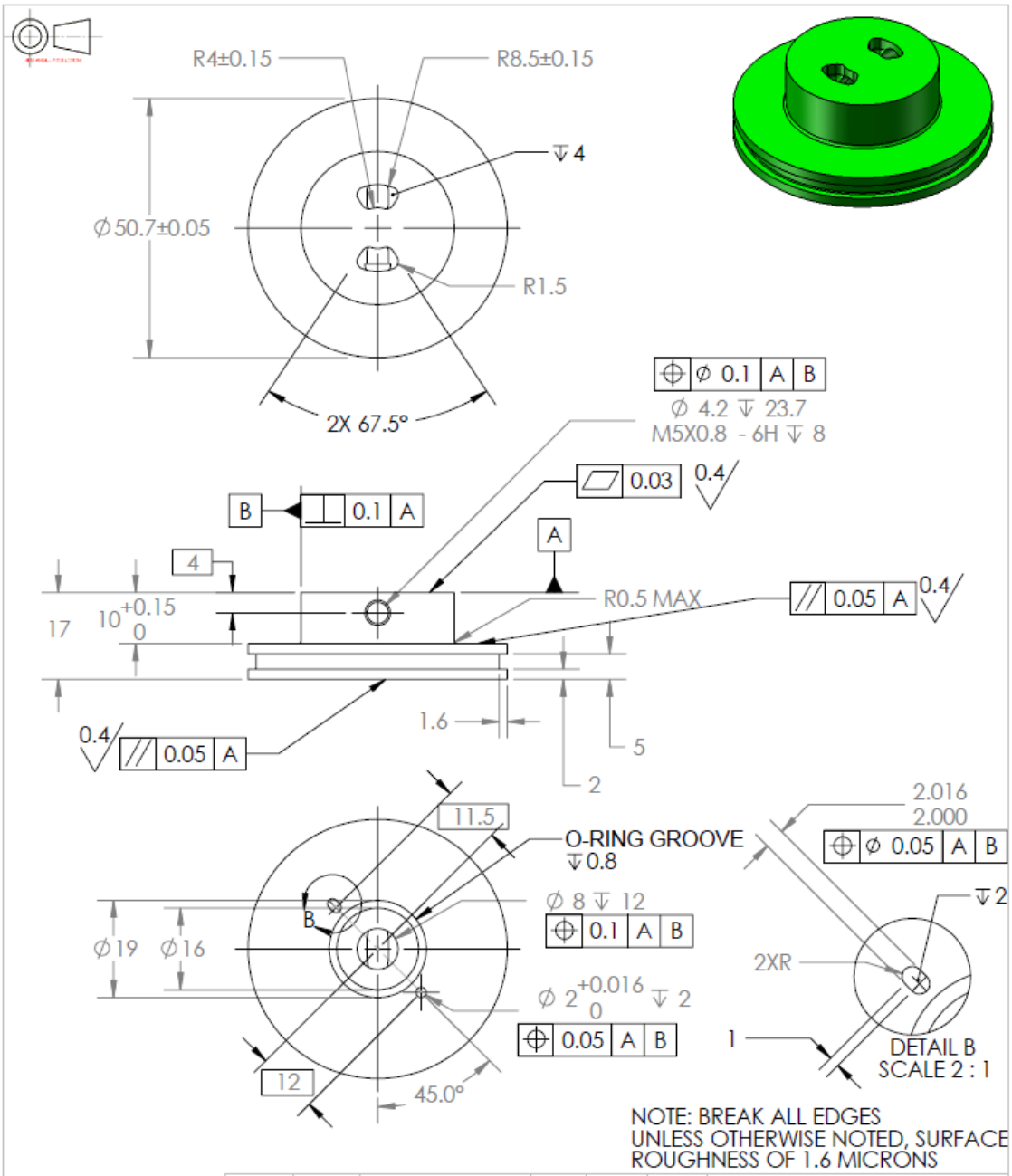
R4±0.15
R8.5±0.15
⌀50.7±0.05
R1.5
2X 67.5°
⌀ 0.1 A B
⌀ 4.2 ↧ 23.7
M5X0.8 - 6H ↧ 8
0.03
0.4
B 0.1 A
A
4
17
10 +0.15 0
R0.5 MAX
0.05 A
0.4
0.4
0.05 A
1.6
5
2
11.5
O-RING GROOVE
↧0.8
⌀19
⌀16
B
⌀ 8 ↧ 12
0.1 A B
⌀ 2 +0.016 0 ↧ 2
0.05 A B
12
45.0°
2.016
2.000
⌀ 0.05 A B
↧2
2XR
1
DETAIL B
SCALE 2 : 1
NOTE: BREAK ALL EDGES
UNLESS OTHERWISE NOTED, SURFACE
ROUGHNESS OF 1.6 MICRONS
DIMENSIONS ARE IN MILLIMETERS
TOLERANCES:
x ± 0.3
X.X ± 0.3
X.XX ± 0.15
ANGULAR ± 1 Deg
MATERIAL
1040 STEEL
FINISH
NEXT ASSY
USED ON
APPLICATION
DO NOT SCALE DRAWING
NAME
DATE
DRAWN
AAK
12/4/08
CHECKED
ENG APPR.
MFG APPR.
Q.A.
COMMENTS:
Allan Katz
Motor Cap
SIZE
A
DWG. NO.
AAK-009
REV.
SCALE:1:1
WEIGHT:
SHEET 1 OF 1
PROPRIETARY AND CONFIDENTIAL
THE INFORMATION CONTAINED IN THIS DRAWING IS THE SOLE PROPERTY OF Worcester Polytechnic Institute. ANY REPRODUCTION IN PART OR AS A WHOLE WITHOUT THE WRITTEN PERMISSION OF Worcester Polytechnic Institute IS PROHIBITED.

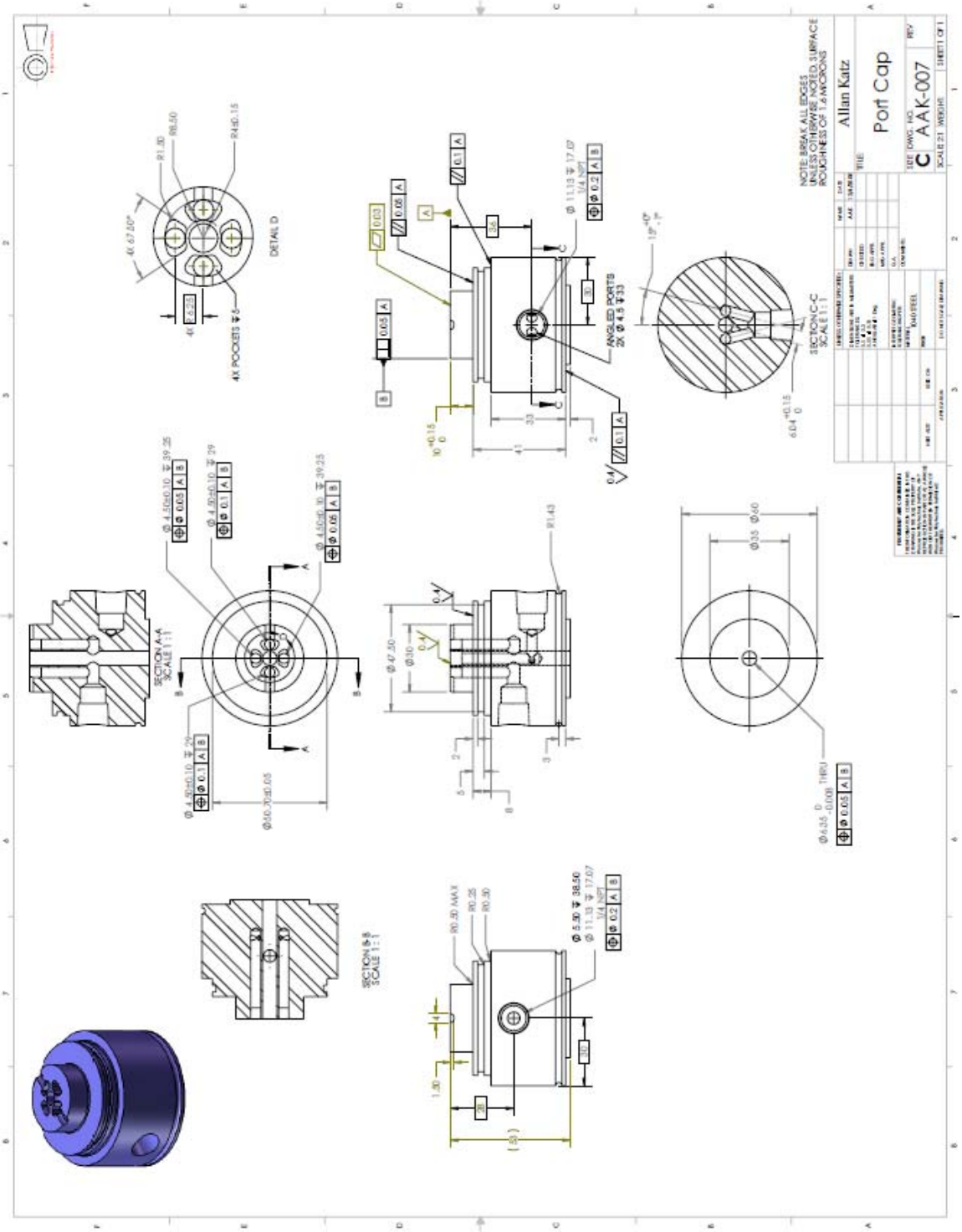
Port Cap
Allan Katz
AAK-007
SECTION A-A
SCALE 1:1
SECTION B-B
SCALE 1:1
SECTION C-C
SCALE 1:1
DETAIL D
4X POCKETS
ANGLED PORTS
2X Ø 4.5
NOTE: BREAK ALL EDGES
UNLESS OTHERWISE NOTED, SURFACE
ROUGHNESS OF 1.6 MICRONS

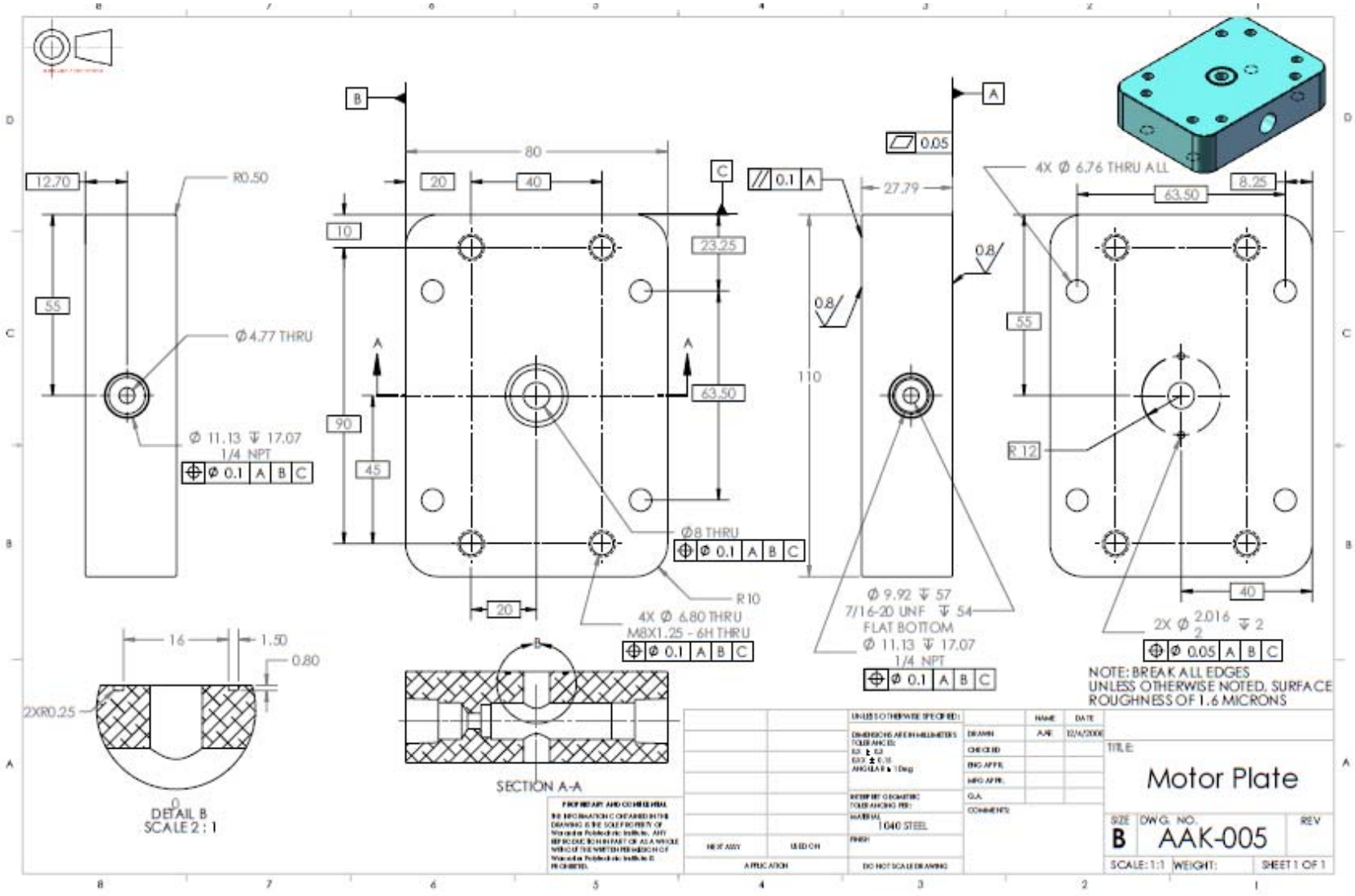
12.70
R0.50
55
Ø4.77 THRU
Ø 11.13 ↧ 17.07
1/4 NPT
⌖ Ø 0.1 A B C
80
20
40
10
23.25
63.50
90
45
Ø8 THRU
⌖ Ø 0.1 A B C
R10
4X Ø 6.80 THRU
M8X1.25 - 6H THRU
⌖ Ø 0.1 A B C
20
0.05
0.1 A
27.79
0.8
110
Ø 9.92 ↧ 57
7/16-20 UNF ↧ 54
FLAT BOTTOM
Ø 11.13 ↧ 17.07
1/4 NPT
⌖ Ø 0.1 A B C
4X Ø 6.76 THRU ALL
63.50
8.25
55
R12
40
2X Ø 2.016 ↧ 2
⌖ Ø 0.05 A B C
NOTE: BREAK ALL EDGES
UNLESS OTHERWISE NOTED, SURFACE
ROUGHNESS OF 1.6 MICRONS
16
1.50
0.80
2XR0.25
DETAIL B
SCALE 2 : 1
SECTION A-A
UNLESS OTHERWISE SPECIFIED:
NAME
DATE
DRAWN
AAK
10/6/2008
CHECKED
ENG APPR.
MFG APPR.
Q.A.
COMMENTS
1040 STEEL
NEXT ASSY
USED ON
APPLICATION
DO NOT SCALE DRAWING
TITLE:
Motor Plate
SIZE
B
DWG. NO.
AAK-005
REV
SCALE: 1:1
WEIGHT:
SHEET 1 OF 1

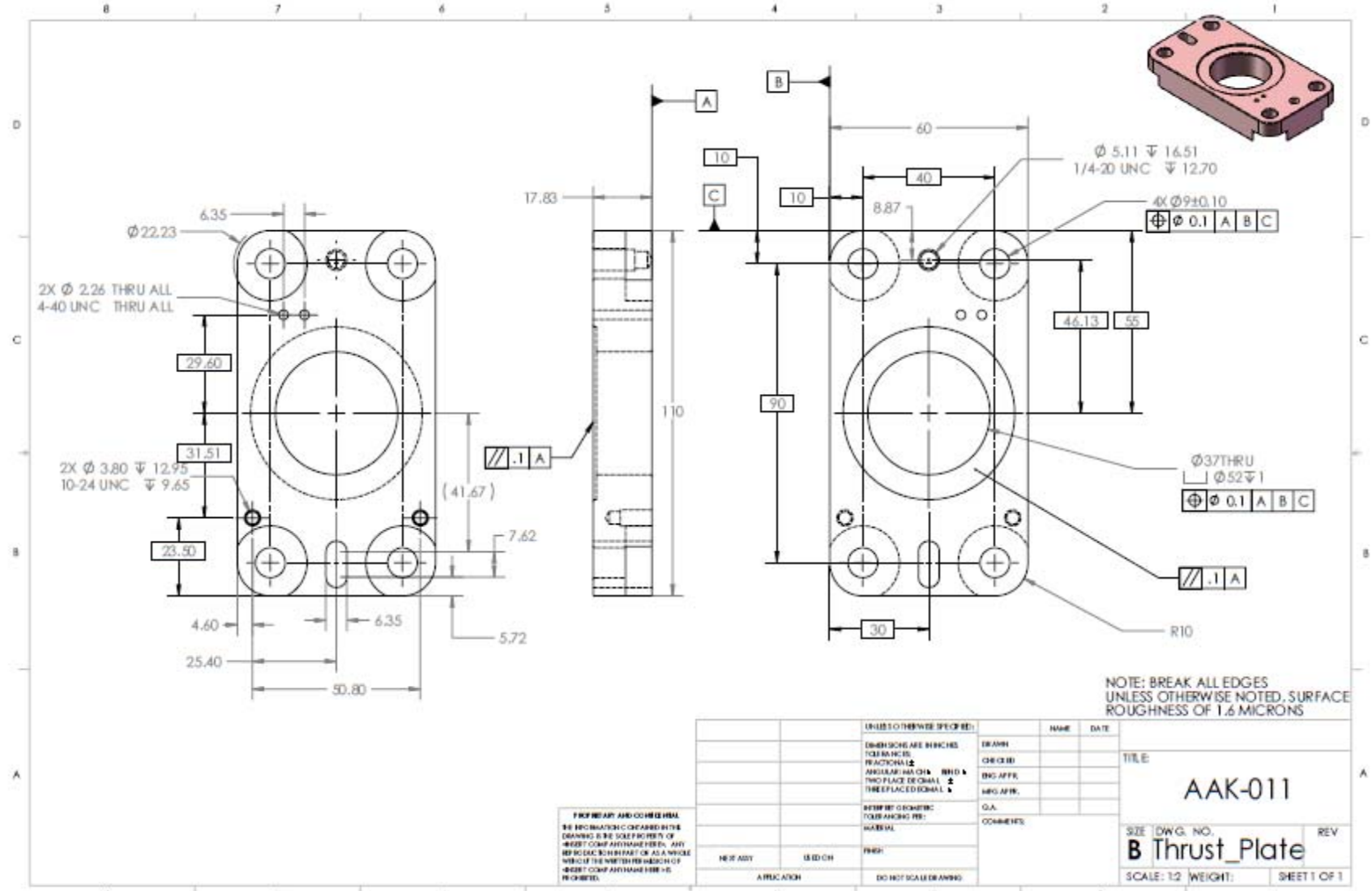
Ø22.23
6.35
2X Ø 2.26 THRU ALL
4-40 UNC THRU ALL
29.60
31.51
2X Ø 3.80 ↧ 12.95
10-24 UNC ↧ 9.65
23.50
(41.67)
7.62
4.60
6.35
5.72
25.40
50.80
17.83
110
.1 A
A
B
C
10
10
60
40
8.87
Ø 5.11 ↧ 16.51
1/4-20 UNC ↧ 12.70
4X Ø9±0.10
Ø 0.1 A B C
46.13
55
90
Ø37THRU
Ø52↧1
Ø 0.1 A B C
.1 A
30
R10
NOTE: BREAK ALL EDGES
UNLESS OTHERWISE NOTED, SURFACE
ROUGHNESS OF 1.6 MICRONS
UNLESS OTHERWISE SPECIFIED:
DIMENSIONS ARE IN INCHES
TOLERANCES:
FRACTIONAL ±
ANGULAR: MACH ± BEND ±
TWO PLACE DECIMAL ±
THREE PLACE DECIMAL ±
INTERPRET GEOMETRIC TOLERANCING PER:
MATERIAL
FINISH
NEXT ASSY
USED ON
APPLICATION
DO NOT SCALE DRAWING
NAME
DATE
DRAWN
CHECKED
ENG APPR.
MFG APPR.
Q.A.
COMMENTS:
TITLE:
AAK-011
SIZE
DWG. NO.
REV
B Thrust_Plate
SCALE: 1:2
WEIGHT:
SHEET 1 OF 1

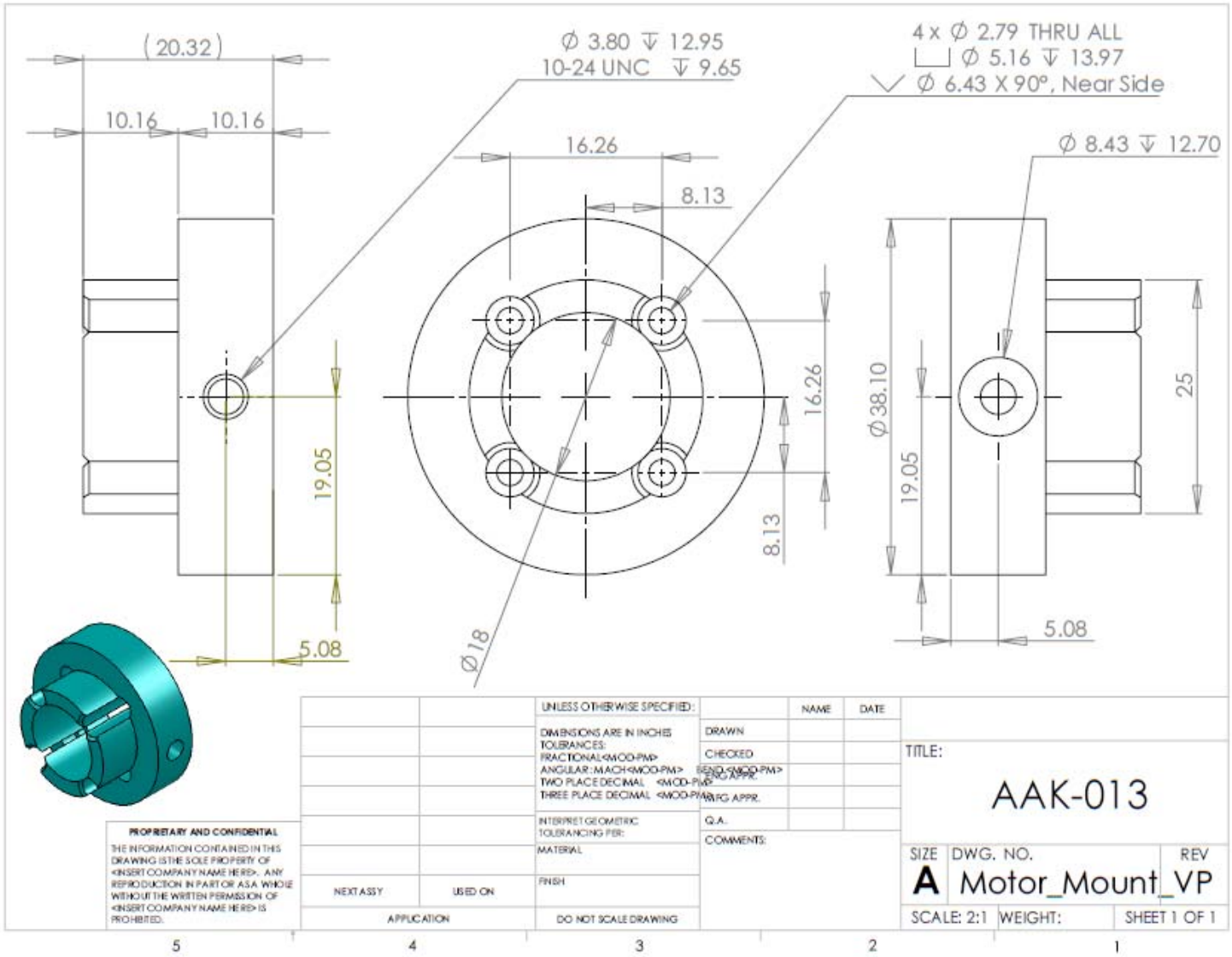
(20.32)
10.16
10.16
Ø 3.80 ↧ 12.95
10-24 UNC ↧ 9.65
4 x Ø 2.79 THRU ALL
⌴ Ø 5.16 ↧ 13.97
Ø 6.43 X 90°, Near Side
16.26
8.13
Ø 8.43 ↧ 12.70
19.05
16.26
8.13
Ø38.10
19.05
25
5.08
Ø18
5.08
UNLESS OTHERWISE SPECIFIED:
DIMENSIONS ARE IN INCHES
TOLERANCES:
FRACTIONAL <MOD-PM>
ANGULAR: MACH <MOD-PM> BEND <MOD-PM>
TWO PLACE DECIMAL <MOD-PM>
THREE PLACE DECIMAL <MOD-PM>
INTERPRET GEOMETRIC TOLERANCING PER:
MATERIAL
FINISH
NEXT ASSY
USED ON
APPLICATION
DO NOT SCALE DRAWING
NAME
DATE
DRAWN
CHECKED
ENG APPR.
MFG APPR.
Q.A.
COMMENTS:
PROPRIETARY AND CONFIDENTIAL
THE INFORMATION CONTAINED IN THIS DRAWING IS THE SOLE PROPERTY OF <INSERT COMPANY NAME HERE>. ANY REPRODUCTION IN PART OR AS A WHOLE WITHOUT THE WRITTEN PERMISSION OF <INSERT COMPANY NAME HERE> IS PROHIBITED.
TITLE:
AAK-013
SIZE
A
DWG. NO.
Motor_Mount_VP
REV
SCALE: 2:1
WEIGHT:
SHEET 1 OF 1
5
4
3
2
1

Appendix E: Matlab Files

```
%*******************************start*********************************
%*********************************************************************
%Disc_Throt_Loss.m
%Allan Katz
%Created October 24th, 2008
%This file calculates the throttling energy loss for the high speed
%on/off valve for all phase values. This includes throttling from
%transitions across the check valves, and the fully open throttling
%losses.
function EThrotLoss = Disc_Throt_Loss(Dim)

warning off MATLAB:divideByZero;

%Declare Global Variables
global N;global rho;global Amax;global thetaTr;global D;global thetaL
%*********************************************************************
%Parameters which are passed to this function from outside
Di = Dim(1);              %Inner Diameter of Orifice[m]
Do = Dim(2);              %Outer Diameter of Slot[m]
thetaTr = Dim(3);         %Transition Angle[rad]
N = Dim(4);               %Number of cycles/rev
Q = Dim(5);               %Full Flow[m^3/s]
Ps = Dim(6);              %Supply Pressure[Pa]
Ptank = Dim(7);           %Tank Pressure[Pa](1atm)
Pc = Dim(8);              %Pressure Drop Across Check Valve[Pa](20 psi)
Popen = Dim(9);           %Fully Open Pressure Drop[Pa]
A = Dim(10);              %Area of Slots
rho = Dim(11);            %Density[kg/m^3]
Cd = Dim(12);             %Orifice Coefficient
ph = Dim(13);             %Phase

% % Hard set parameters for when not optimizing.
% Di = 0.005;                   %Inner Diameter of Orifice[m]
% Do = 0.03;                    %Outer Diameter of Slot[m]
% thetaTr = 22.5*pi/180;        %Transition Angle[rad]
% N = 2;                        %Number of cycles/rev
% Q = 5e-4;                     %Full Flow[m^3/s]
% Ps = 7.777*10^6;              %Supply Pressure[Pa]
% Ptank = 101000;               %Tank Pressure[Pa](1atm)
% Pc = 137895;           %Pressure Drop Across Check Valve[Pa](20 psi)
% A = (Do^2-Di^2)*thetaTr*N/8;  %Area of slots
% rho = 850;                    %Density[kg/m^3]
% Cd = 0.61;                    %Orifice Coefficient
% ph = 45*pi/180                %Phase
% Popen = rho/2*(Q/(Cd*A))^2    %Fully Open Pressure Drop[Pa]

n = 1000;                     %Number of Points
dPT = zeros(1,n);             %Pressure Drop Across Valve
Qv = zeros(1,n);              %Flow thru valve
AEff = zeros(1,n);            %Effective Area
thetaL = pi/N - thetaTr;      %Long Slot Angle
theta = linspace(0,2*pi/N,n); %Angle of Valve Plate
x = linspace(0,2*pi/N,n);     %For Plotting, x-axis
D = (Do^2 - Di^2)*N/8;        %Shortcut variable
```

```
Amax = A;                          %Maximum Orifice Area
FullyOpendP = 2*Popen;             %Pressure drop across 2 orifices

%*********************************************************************
%Equations: Calculate the orifice area and then the pressure drop.
%Adjust for case when check valve opens
%*********************************************************************
for i = 1:n                            %Theta Loop
    %Effective Orifice Area
    AEff(i) =
(A1(theta(i))^2+A2(theta(i),ph)^2)/(A1(theta(i))^2*A2(theta(i),ph)^2);
    if(AEff(i) == Inf || AEff(i) == NaN)
%If Pathway for one valveport closed, use pathway for other valve port
%This can be used because of the symmetry of the valve
        theta(i) = mod(theta(i)+pi/N,2*pi/N);
    end
    if(theta(i)<pi/N)
        %If in first half of cycle, Inlet Pressure is Tank
        Pi = Ptank;
    else
        %Else Inlet Pressure is Supply Pressure
        Pi = Ps;
    end

    %Pressure Drop Across Sub-Valves
    dPT(i) = rho/2*Q^2/Cd^2*((A1(theta(i)))^2 +
(A2(theta(i),ph))^2)/(A1(theta(i))*A2(theta(i),ph))^2;
    Qv(i) = Q;          %Full flow thru valve

    %If Pressure Drop is to Great, Check Valve Opens
    %Pressure Drop becomes constant and Flow becomes Variable
    if(dPT(i) > (Pi + Pc - Ptank))
        dPT(i) = Pi + Pc - Ptank;
        Qv(i)=
(2*Cd^2*(dPT(i))*(A1(theta(i))*A2(theta(i),ph))^2/(rho*((A1(theta(i)))^
2+(A2(theta(i),ph))^2)))^(1/2);
    end
    A1track(i) = A1(theta(i));              %Track A1 Orifice
    A2track(i) = A2(theta(i),ph);           %Track A2 Orifice
    Ploss(i) = dPT(i)*Qv(i)+Pc*(Q-Qv(i));   %Power Loss[W]
    if isnan(Ploss(i))
        Ploss(i) = Pc*Q;                    %Allows for Integration
    end
end                                         %End Theta Loop
%*********************************************************************
%Throttling Energy Loss per Rev. To integrate with respect to time
%divide by angular velocity. This gives energy/cycle. Muliply by N to
%give energy per rev
EThrotLoss = trapz(x, Ploss)/(2*pi*50)*N*N;
AvgPloss = sum(Ploss)/n;                    %Average Power Loss per Rev
%
% %Plot Everything
% figure(1)
% subplot(3,1,1)
% plot(x, dPT)
% title('0.25 Duty Ratio')
% xlabel('Angle(rad)');
```

```
% ylabel('Pressure Drop(Pa)');
% % title('Pressure drop vs. angle')
%
% subplot(3,1,2)
% plot(x, Qv)
% xlabel('Angle(rad)');
% ylabel('Flow thru valve (m^3/s)');
% % title('Flow vs. Angle');
%
% subplot(3,1,3)
% plot(x, Ploss)
% xlabel('Angle(rad)');
% ylabel('Power Loss(W)');
% % pause(0.01);
% % title('Power loss vs. Angle');
% %
% %
% figure(2)
% %Plot Areas
% subplot(2,1,1)
% plot(x, A1track)
% title('A1');
% subplot(2,1,2)
% plot(x, A2track)
% title('A2');

%**************************************************************************
%***************SUB FUNCTION FOR ORIFICE AREA 1*********************
%**************************************************************************
function Area1 = A1(theta)
global N; global thetaTr; global D; global Amax; global thetaL
%Keep theta in range, pi/N allowed because of symmetry
theta = mod(theta,pi/N);

if (theta>=0 && theta <= thetaTr)
    Area1 = D*theta;                    %Opening orifice area
elseif (theta>thetaTr && theta<thetaL)
    Area1 = Amax;                       %Constant orifice area
elseif (theta>=thetaL && theta<=(thetaL+thetaTr))
    Area1 = D*(thetaL+thetaTr - theta); %Closing orifice area
else
    disp('OMGWTFBBQ A1 is FUdgEd!')     %default
end
%**************************************************************************
%***************SUB FUNCTION FOR ORIFICE AREA 2*********************
%**************************************************************************
function Area2 = A2(theta,phase)
global N; global thetaTr; global D; global Amax; global thetaL

%Keep theta within range
theta = mod(theta,2*pi/N);
if (theta>=0 && theta <= phase)
    Area2 = 0;                      %Area is not over output slot yet
elseif (theta>phase && theta<(phase + thetaTr))
    Area2 = D*(theta-phase);        %Opening orifice area
elseif (theta>=(phase+thetaTr) && theta<=(phase+thetaL))
    Area2 = Amax;                   %Constant orifice area
```

```
elseif (theta>(phase+thetaL) && theta<(phase+thetaL+thetaTr))
    Area2 = D*(phase+thetaL+thetaTr - theta);   %Closing orifice area
elseif (theta>= (phase+thetaL+thetaTr) && theta<=2*pi/N)
    Area2 = 0;                      %Passed output slot again
else
    disp('OMGWTFBBQ A2 is FUdgEd!') %default
end
%*********************************************************************
%*********************************end*********************************



%***************************start*************************************
%*********************************************************************
%File Disc_Opt.m
%Allan Katz
%Created October 24th, 2008
%Calculates the efficiency of the phase controlled on/off disc valve.
%Takes into account losses from viscous friction, throttling, bulk
%modulus, and leakage losses. This function is optimized by the Opt2.m
%file. All totals are based on One revolution = N cycles

function Loss = Disc_Opt(v)

warning off MATLAB:divideByZero;
% %*******Driving Parameters(For when using Opt2.m)******************
% Di = v(1)/100             %Slot Inner Diameter [m]
% Do = v(2)/100             %Slot Outer Diameter [m]
% thetaTr = v(3)*pi/180     %Amount of radians spent in transition[rad]
% N = round(v(4))           %Number of valve sections, cycles/rev
% Q = v(5)                  %Flow Rate [m^3/s]
% Ps = v(6)*10^6            %Supply Pressure [Pa]
% Rrim = v(7)/100           %Radial Dist. Do to outer edge of disc [m]
% cb = v(8)/1000            %Radial Clearance(Disc and Bore)[m]
% cff = v(9)/1000           %Clearance Valve Section Front Face[m]
% thvp = v(10)/100          %Valve Plate Thickness[m]
% thpp = v(11)/100          %Rotating Port Plate Slot Depths[m]
% cfb = v(12)/1000          %Clearance Valve Section Back Face[m]

%*******System variables(For when not using Opt.m)*******
Di = 0.01;                  %Inner Diameter of Slot [m]
Do = 0.0352;                %Outer Diameter of Slot[m]
thetaTr = 22.5*pi/180;      %Transition Angle; Angle of Slot [rad]
N = 2;                      %Number of cycles per revolution
Q = 6.3*10^(-4);              %Inlet Flow [m^3/s](2gpm)
Ps = 16*10^6;               %Supply Pressure [Pa]
Rrim = 0.007084;            %Radial Dist. Do to outer edge of disc[m]
cb = 0.001;                 %Radial Clearance(Bore)[m]
cff = 2.54*10^-5;           %Clearance(Front Face)[m]
thvp = 0.005;               %Valve-Plate Thickness[m]
thpp = 0.004;               %Sub-Valve Thickness[m]
cfb = 2.54*10^-5;           %Clearance(Back Face)[m]

%************************System Properties**************************
T = 60;                             %Temperature of Fluid[C]
% mu = -5.479*10^-4*T + 0.06062;    %Viscosity for DTE 25
```

```
mu = -0.001875*T + 0.2;            %Viscosity for DTE 28
% mu = 0.0387;                     %DTE 25 @ 40C  [Pa-s]
% mu = 0.005825                    %DTE 25 @ 100C [Pa-s]
% mu = 0.125                       %DTE 28 @ 40C  [Pa-s]
% mu = 0.0125                      %DTE 28 @ 100C [Pa-s]
Cd = 0.61;                         %Orifice Coefficient
rho = 850;                         %Density [kg/m^3]
Pcheck = 137895;                   %Check Valve P-Drop[Pa] = 20psi
Ptank = 101325;                    %Tank Pressure = 1atm [Pa]
%For 100 Hertz: 2 Pulses/cycle and 2 cycles/rev[rad/s]
wn = 2*pi*50/N;                    %Angular velocty[rad/s]
Dhole = 0.0079;                    %Exit hole diameter[m](5/16in)
Duty = 0.25;                       %Duty Ratio
Phase = Duty*pi/N;                 %Phase Angle of Tier2[rad]
Ri = Di/2;                         %Slot Inner Radius[m]
Ro = Do/2;                         %Slot Outer Radius[m]
Rbore = Ro + Rrim;                 %Radius to outer edge of disc[m]
Dbore = 2*Rbore;                   %Bore Diameter
De = Do + 0.009;                   %Balancing slot outer diameter
Re = De/2;                         %Balancing slot radius[m]
thvpe = 0.001;                     %Depth of balancing slot[m]

%*************************CALCULATED PARAMETERS*********************
A = (Do^2-Di^2)*thetaTr*N/8;           %Area of Slot
vmax = Q/A;                            %Maximum Fluid Velocity [m/s]
Popen = rho/2*(Q/(Cd*A))^2;            %Fully Open Pressure Drop[Pa]
if(Popen > 17236)
    disp('Fully Open Pressure Drop is Greater than 2.5psi');
    PopenPSI = Popen*0.00014503774;    %Convert to psi
    disp(PopenPSI);
end

Etot = 2*pi.*Q.*(Ps-Ptank)./(wn).*Duty; %Total Energy/rev at duty ratio
thetaL = pi/N-thetaTr;                 %Valve passage angle[rad]
%Create array to pass variables to Disc_Throt_Loss.m
Dim = [Di, Do, thetaTr, N, Q, Ps, Ptank, Pcheck, Popen, A, rho, Cd,
Phase];

%*********************************************************************
%*************************Transitional Losses*************************
%*********************************************************************
%Energy loss from transitions and throttling
%2N pressure pulses/rev, 2 transitions/pulse = 4N trans/rev
%Call Disc_Throt_Loss, returns throttling energy loss/rev
ETRFunc = Disc_Throt_Loss(Dim);

%*********************************************************************
%*************************Bulk Modulus Losses*************************
%*********************************************************************
%Calculate Effective Bulk Modulus
Esteel = 190*10^9;                     %Elastic Modulus of 1040 Steel
bulkSteel = Esteel/2.5;                %Bulk Mod of Rigid Container
bulkOil = 1.8*10^9;                    %Bulk Modulus[Pa]
AirPer = 0.02;                         %Percent Air
gammaAir = 1.4;                        %Gamma air?
bulkAir = gammaAir*Ps;                 %Bulk Modulus of Air
%Bulk moduli are like resistors in parallel
```

```
invBulkOil = (1-AirPer)/bulkOil + AirPer/bulkAir+1/bulkSteel;
effBulk = 1/invBulkOil;                 %Effective Bulk Modulus

%Calculate Inlet Volume
Vvp = A*thvp;                            %Valve plate slot volume
%Volume of balancing slot sections
Vvpextra = (De^2-Do^2)*thetaTr*N/8*thvpe;
Vpp = (Do^2 - Di^2)*N/8*thetaL*thpp;     %Tier2 slot volume
%Volume of Tier2 Passageways
VppPort = pi*(0.0075)^2*0.02/4 + N*pi*(0.004)^2*(Do/2)/4;
%Total volume that alternates pressure(2*N pulses/rev)
Vtot = 2*N*(Vvp + Vpp + Vvpextra + VppPort);
%Change in volume from bulk modulus effects
Vbulk = Vtot/effBulk*(Ps-Ptank);
Ebulk = Vbulk*(Ps-Ptank)                 %Energy loss from bulk modulus

%*********************************************************************
%**************************Friction Losses****************************
%*********************************************************************
%Viscous Friction Torque(bore area of vp)
Tfbore = pi*Dbore^3*thvp*mu*wn/(4*cb);

%Viscous Face Torque Ri to Ro(Front)
Tvpfrontslot = N*mu*wn*thetaTr/(2*cff)*(Ro^4-Ri^4);
%Viscous Face Torque Ri to Ro(Back)
Tvpbackslot = mu*wn*pi/(4*cfb)*(Ro^4-Ri^4);

%Viscous Face Torque Ro to Rbore(Front)
Tvpfouter = 2*(pi*mu*wn/(2*cff)*(Rbore^4-Ro^4));
%Viscous Face Torque Ro to Rbore(Front)
Tvpbouter = 2*(pi*mu*wn/(2*cfb)*(Rbore^4-Ro^4));

%Total Viscous Friction Losses
EflossTot = 2*pi*(Tfbore+Tvpfrontslot+Tvpbackslot+Tvpfouter+Tvpbouter)
%Power Loss,Slot Area
PflossSlots = 2*pi*(Tvpfrontslot + Tvpbackslot)*25;
PflossBoreness = 2*pi*(Tfbore)*25              %Power Loss, Bore Area
PflossOuter = 2*pi*(Tvpfouter+Tvpbouter)*25    %Power Loss, Outer Area
%*********************************************************************
%**************************Leakage Losses*****************************
%*********************************************************************
h = cff/2;              %Shortcut Variable, half front face clearance
hb = cfb/2;             %Shortcut Variable, half back face clearance
dP = Ps - Ptank;        %Shortcut Variable, Pressure Differential
b = Ro-Ri;              %Shortcut Variable, slot radial lengths
%Transition angle from orifice to plate flow, front and back
thetaQTr = 2*h^2/(3*Cd*mu*(Ro+Ri))*(rho/2*dP)^(1/2);
thetaQTrb = 2*hb^2/(3*Cd*mu*(Ro+Ri))*(rho/2*dP)^(1/2);

Qori = 2*Cd*h*(Ro-Ri)*(2/rho*dP)^(1/2);       %Flow thru orifice, front
Qorib = 2*Cd*hb*(Ro-Ri)*(2/rho*dP)^(1/2);     %Flow thru orifice, back

%Circumferential Volume Leakage*************************************
VLcircumf = 4*N^2/wn*(2*Qori*thetaQTr +
8*b*h^3*dP/(3*(Ro+Ri)*mu)*log(thetaTr/thetaQTr) +
4*b*h^3*dP/(3*(Ro+Ri)*mu*thetaTr)*(thetaL-thetaTr));
```

```
%The back circumferential leakage is dependent upon the phase, check
%what regime the leakage flow is in. Mid-range duty ratio regime:
if(Phase>=thetaTr && Phase <= thetaL)
    %Volume of circumferential leakage
    VLcircumb = 4*N^2/wn*(2*Qorib*thetaQTrb + (Ro-
Ri)*cfb^3*dP/(6*(Ro+Ri)*mu)*log((Phase*(pi/N-Phase))/(thetaQTrb)^2));

%Extremity duty ratio regime
elseif ((Phase>=0 && Phase<=thetaTr) || (Phase>=thetaL && Phase<=pi/N))
    if(Phase>=thetaL && Phase<=pi/N)
%If high duty range, convert to low range
        Phase2 = pi/N – Phase;
    else
        Phase2 = Phase;           %If within low range, keep as is.
    end
    %Volume of circumferential leakage
    VLcircumb = 4*N^2/wn*(2*Qorib*thetaQTrb+(Ro-
Ri)*cfb^3*dP/(6*(Ro+Ri)*mu)*log((Phase2*thetaL)/(thetaQTrb)^2+(pi/N-
Phase2-thetaL)/thetaL));
end
ELcircum = (VLcircumf + VLcircumb)*dP   %Circumferential Energy Loss

%Radial Leakage(Front)
Qradfront = N*thetaL*cff^3*dP*(Rbore + Re)/(24*mu*(Rbore-Re));
%Radial Leakage(Back)
Qradback = N*cfb^3*dP*(Rbore + Ro)/(24*mu*(Rbore-
Ro))*(thetaL*Duty+thetaTr*(1-Duty));

ELradfront = 2*pi*dP/wn*Qradfront;  %Energy Loss from Radial
Leakage(Front)
ELradback = 2*pi*dP/wn*Qradback;    %Energy Loss from Radial
Leakage(Back)
ELrad = (ELradfront+ELradback)

PLrad = ELrad*25;               %Power loss from radial leakage
PLcircum = ELcircum*25;         %Power loss from circumferential
leakage

ELeakTot = ELcircum + ELrad;    %Total Leakage Energy Losses
%*****************************************************************
%*****************************Total Losses**************************
%*****************************************************************
ElossTot =  ETRFunc + Ebulk + EflossTot + ELeakTot;  %Total Energy Loss
PercentThrot = ETRFunc/ElossTot*100;   %Percent losses from throttling
PercentBulk = Ebulk/ElossTot*100;      %Percent losses from compress.
PercentFloss = EflossTot/ElossTot*100; %Percent losses from friction
PercentLeak = ELeakTot/ElossTot*100;   %Percent losses from leakage

Efficiency = (1-ElossTot/Etot)*100;    %Efficiency
%Inefficiency used in optimization (ie, minimize this)
Loss = 100-Efficiency;
%*****************************************************************
%*********************************end*****************************


%****************************start*********************************
```

```
%*********************************************************************
%File Opt2.m
%Allan Katz
%Created October 24th, 2008
%Minimizes Energy Loss using the given starting conditions, v, with
%lower,lb, and upper, ub, bounds
%Di = the slot inner diameter, Do = slot outer diameter, thetaTr =
%transition angle, N = # of cycles per rev, Q = Flow rate, Ps = Supply
%Pressure, Rrim = radial distance from Do to bore, cb = bore radial
%clearance, cff = valve port front face clearance, thvp = valve plate
%thickness, thpp = rotating port plate slot depths, cfb = valve plate
back face clearance. Note: If Di upper limit is to close in value to Do
lower limit, then the code will optimize so throttling losses will be
mostly from the check valve and is inaccurate.
%Values which give optimum performance will be stored in "q".

clc, close all, clear all
% v =[1,    2,   3,       4,    5,           6,     7,       8,
9,       10,   11,    12]

% v =[Di,   Do,    thetaTr, N,    Q,           Ps,    Rrim,    cb,
cff,     thvp, thpp,  cfb]

lb = [0.2,  2,     2.00,    2,    1.00*10^-4,  1.0,   0.5,     0.0254,
0.0254,  0.5,  0.4,   0.0254];%lower bound

v =  [0.5,  4.0,   15.0,    2,    1.26*10^-4,  6.9,   1.0,     0.03,
0.03,    0.75, 0.75,  0.03]; %starting guess

ub = [1,    10,    22.5,    2,    6.30*10^-4,  35.0,  4.0,     1.00,
0.05,    1.0,  1.0,   0.05];%upper bound

[q fval] = fmincon(@Disc_Opt,v,[],[],[],[],lb,ub); %Optimize Disc_Opt.m
q
%*********************************************************************
%*********************************end*********************************
```